Catalysis and Kinetics of Hydrogenation of Nitrobenzene to *p*-Aminophenol

A Thesis Submitted to the

University of Pune

For the Degree of

Doctor of Philosophy in Chemistry

By

Manisha J. Vaidya

Homogenous Catalysis Division
National Chemical Laboratory
Pune 411 008. India

August 2002

Form – A

Certified that the work incorporated in the thesis entitled, "**Catalysis and Kinetics of Hydrogenation of Nitrobenzene to *p*-Aminophenol**" submitted by **Manisha J. Vaidya** was carried out under my supervision. Such material as has been obtained from other sources has been duly acknowledged in the thesis.

August 2002 (**R. V. Chaudhari**)

Pune Research Guide

Dedicated

To

My Parents

Acknowledgement

I would like to acknowledge my research guide, Dr. R. V. Chaudhari for his valuable support and guidance to my research. He has been a constant source of inspiration to me during my stay at NCL. His enthusiastic attitude, innovative ideas and scientific knowledge have inspired me profoundly. It has been an intellectually stimulating and rewarding experience to work with him. I truly feel privileged to have joined his research group.

I would like to gratefully acknowledge Dr. R. Jaganathan for his valuable help in reaction engineering and modeling related studies.

I also take this opportunity to thank, Dr. R. M. Deshpande, Dr. C. V. Rode Dr. S. P. Gupte, Dr. A. A. Kelkar, Dr. S. K. Sabapathy, Dr. G. S. Grover, Dr. V. V. Ranade, Dr. S. S. Joshi, Dr. V. M. Bhandari, Dr. V. H. Rane and Dr. Divekar for their cooperation during the research years in NCL. It has been a pleasure and a privilege to work with such a talented, perceptive and meticulous group of scientists. The acknowledgement would be incomplete without thanking Mr. Raheja, who managed the administrative work nicely during this tenure. I also thank Mr. Bhalerao for his help throughout my stay at NCL.

I would like to thank all my friends and colleagues-Pradnya, Anamika, Nitasha, Charu, savita, Shubhangi, Manjusha, Santosh, Mahesh, Ankush, Vivek, Gunjal, Mahajan, Suju, Sunil Tonde, Sunil Shinde, Abhishek, Shashi, Yogesh, Rajesh, Tushar, Anand, Makrand, Shekhar, Debu, Bibhas, Nandu, Amit, Umesh, Vikas, Prashant, Kausik and Nakul for their help in my day-to-day research life. Special thanks are due to Mr. Borkar, Mr. David, Mr. Kadam, Mr. Narwade, Mr. Wanjale and Mr. Dure for their help in maintenance of reactor and related instrumentation.

I express my sincere thanks to the Council of Scientific and Industrial Research, New Delhi for awarding me the Senior Research Fellowship and to the Director, National Chemical Laboratory, Pune, Dr. Paul Ratnasamy for allowing me to pursue my research work and use the necessary infrastructure.

Finally, I wish to express my sincere thanks to my brothers and sister, parents-in-law, whose constant support made my research a much easier job. Needless to say that it was because of the efforts of my parents and especially my father today I stand where I am.

No thanks can be enough to acknowledge the encouragement and support of my husband Shrikant without whose support, the completion of this thesis would have been a difficult task for me. Needless to mention that the thesis is much much better for his efforts.

August 2002 **Manisha J.Vaidya**

Pune

List of contents

List of Tables

List of Schemes

List of Figures

Abstract of the Thesis

The developments in the area of catalysis have revolutionized the modern chemical industry. A particular area where the catalysis has contributed significantly is in the replacement of conventional reagent based processes by new catalytic processes that allow efficient utilization of raw materials and energy and produce minimal or no waste. In view of the growing environmental concerns, the need for alternative greener routes to several existing products has become extremely important. The future of these emerging green catalytic processes will eventually depend on their economic viability and process efficiency. Therefore, the studies relevant to catalysis and other fundamental aspects like kinetics of these reactions assume significant importance. This thesis presents studies on the preparation of *p*-aminophenol by catalytic hydrogenation routes and fundamental issues related to the catalysis and kinetics of these processes. *p*-Aminophenol (PAP) is an important intermediate used for the preparation of paracetamol, as a developer in photography and in dye industry. The conventional method for *p*-aminophenol uses iron-acid reduction of nitrobenzene or *p*-nitrophenol as a key step, which produces an equivalent amount of Fe/FeO sludge waste. There is an urgent need to develop a cleaner alternative to the conventional process. The studies presented in this thesis clearly indicate that, the catalytic hydrogenation using transition metal based catalysts is an alternative to the iron-acid reduction routes.

The following specific problems were chosen for the present work:

- Catalyst screening and optimization of process parameters for hydrogenation of nitrobenzene to *p*-aminophenol: Activity and selectivity studies.

- Kinetic modeling of catalytic hydrogenation of nitrobenzene to *p*-aminophenol in a batch slurry reactor using Pt/C catalyst.
- Investigation of adsorption of nitrobenzene, aniline and hydrogen from slurries of activated carbon and 3%Pt/C catalyst at different temperatures to determine the adsorption equilibrium constants.
- To investigate catalytic hydrogenation of *p*-nitrophenol to *p*-aminophenol in a stirred slurry reactor: Activity-selectivity studies and kinetic modeling.

The thesis has been presented in five chapters, the synopsis of which is presented here.

The first chapter presents a comprehensive literature review on the preparation of *p*-aminophenol. Several methods have been reported for the preparation of *p*-aminophenol but the most significant ones are: (1) hydrogenation of nitrobenzene in the presence of an acid to *p*-aminophenol and, (2) direct hydrogenation of *p*-nitrophenol to *p*-aminophenol. The reduction is often accomplished by using Fe/HCl as the reducing agent but this route produces large amounts of Fe/FeO sludge waste. It has been reported widely in patents that transition metal based heterogeneous catalysts and in particular platinum containing catalysts efficiently catalyze the direct hydrogenation of nitrobenzene to *p*-aminophenol in the presence of acids. But there has been no detailed report on the catalysis and kinetics of this industrially important reaction. The catalytic hydrogenation of *p*-nitrophenol to *p*-aminophenol has also been reported in the literature using several supported metal catalysts including Pd, Pt and Ni. A detailed literature review on these catalytic reactions has been presented in this chapter and the scope of the present thesis outlined.

In chapter 2, an experimental study on the catalytic hydrogenation of nitrobenzene in aqueous acid medium to *p*-aminophenol has been reported. The formation of aniline is the major competing reaction. The activity of various heterogeneous transition metal catalysts like Pt, Pd, Ru, Rh and Ni was investigated. It was observed that Pt/C has higher activity for the hydrogenation of nitrobenzene in aqueous acidic medium to *p*-aminophenol. The effect of various reaction parameters such as catalyst loading, reaction temperature, hydrogen pressure and amount of sulfuric acid was also studied on selectivity to *p*-aminophenol. Complete conversion of nitrobenzene was achieved in almost all the reactions. It was observed that under optimized reaction conditions p-aminophenol could be obtained in selectivity as high as 75%. The possibility of using various solid acids like acidic zeolites, clays and acid treated alumina, and silica etc. as alternatives to the corrosive mineral acids was also investigated. It was observed that montmorillonite and sulfonated polystyrene resin efficiently catalyzed the rearrangement of intermediate β-phenylhydroxylamine to *p*-aminophenol. In the second part, the kinetics of hydrogenation of nitrobenzene to *p*-aminophenol using 3% Pt/C catalyst has been presented. The experiments were carried out in a mechanically agitated autoclave over a temperature range of 323–353 K using water as a solvent. The effect of catalyst loading, hydrogen pressure and nitrobenzene loading on the initial rate of hydrogenation was investigated. The analysis of initial rates showed that the data were in kinetic regime. The initial rates were calculated from the amount of *p*-aminophenol and aniline formed and the rate parameters evaluated by simulating a batch reactor model.

In chapter 3, results on adsorption of nitrobenzene, aniline and hydrogen on activated carbon and Pt/C catalyst have been presented. Adsorption from the liquid

phase is an important step in liquid-solid as well as gas-liquid-solid catalytic reactions. The nature of adsorption isotherm and the mechanism of adsorption play important roles in the activity of the catalysts. The adsorption isotherms were determined for individual components and for mixtures of nitrobenzene and aniline from their methanol solution. The adsorption equilibrium constants were calculated at different temperatures. It was observed that adsorption capacity of nitrobenzene was higher than that of aniline from its methanol solution on activated carbon as well as on 3% Pt/C catalyst. The dynamics of the adsorption processes was also investigated. Adsorption of hydrogen was investigated from its aqueous solution at different temperatures.

Chapter 4 presented a study on catalytic hydrogenation of *p*-nitrophenol to *p*-aminophenol. This is an alternative route for the preparation of *p*-aminophenol. Various supported metal catalysts like Pt, Pd, Rh, Ru and Ni have been screened for their activity and selectivity for hydrogenation of *p*-nitrophenol to *p*-aminophenol. The effect of various reaction parameters like temperature, hydrogen pressure, solvent, speed of agitation, catalyst loading and metal content was investigated. Further, the kinetics of hydrogenation of *p*-nitrophenol to *p*-aminophenol was also investigated using 1% Pt/C catalyst. The initial rate data collected at different sets of conditions were fitted to different rate equations to find a suitable rate equation.

In chapter 5, a summary of the conclusions and future scope in the synthesis of *p*-aminophenol by catalytic hydrogenation route has been given. The key issues in improvement of processes for the synthesis of *p*-aminophenol by catalytic hydrogenation route are also discussed.

Thus, the present thesis reports investigations on the fundamental aspects related to catalysis and kinetics of catalytic hydrogenation reactions relevant to *p*-

aminophenol manufacture. The results indicate that the catalytic hydrogenation route is an important alternative to the conventional synthesis of *p*-aminophenol, which generates large amounts of waste. The information may be useful in understanding the influence of catalyst and reaction parameters and also the design and selection of a suitable reactor for such a process.

* * * * *

Chapter One

Introduction and Literature Survey

1.1 Introduction

In recent years, stringent environmental regulations and competition in chemical industry has resulted in increased demands for the development of environmentally acceptable and sustainable manufacturing processes. This aspect, often referred to as *Green Chemistry*, has redefined the traditional concepts of process efficiency, which in the past were focused essentially on the product yield. *Green Chemistry*, however, evaluates performance of a chemical process based on its ability to eliminate waste products and use of hazardous and/or toxic substances. New discoveries in the area of catalysis have improved several important reaction classes e.g. hydrogenation, oxidation, alkylation, reductive amination, acylation, hydroxylation, isomerization, carbonylation etc., which are routinely used in the chemical industry [1]. The environmentally benign catalytic processes have replaced several waste generating conventional counterparts. The new advances in the area of catalysis and reaction engineering provide important tools for the development of *Green Chemistry* [2].

The reduction of organic molecules via catalytic hydrogenation is an ideal example of how catalysis has revolutionized the chemical manufacturing practices. The reduction of organic compounds is a key step in the synthesis of several chemicals. Conventionally, the reduction has been carried out using stoichiometric amounts of reducing agents such as sodium borohydride, lithium aluminum hydride, hydrazine hydrate or iron-acid. The major disadvantages of these conventional reduction processes are: (a) use of stoichiometric amounts of reducing agents posing serious waste disposal problems due to generation of large quantities of undesired inorganic salts, (b) difficulties in the separation of products from the reaction mixture and it's effect on reducing the product yield, (c) non-reusability of reagents,

and (d) corrosion problems (e.g. in case of iron-acid reagents). Replacement of conventional reduction methods by the catalytic hydrogenation is perhaps one of the most significant achievements of modern catalysis. Table 1-1 summarizes a few important examples of industrially relevant catalytic hydrogenation processes. Hydrogenation of nitro compounds to amines has wide ranging applications in the synthesis of several key intermediate and fine chemicals. The conventional process for reduction of nitro compounds (commonly known as Béchamp process) employed stoichiometric amounts of Fe-acid as the reducing agent producing almost equivalent amount of Fe-FeO sludge as a byproduct [19]. Apart from the serious waste disposal problems, the Béchamp process also suffered from the difficulties in the separation of desired products from the reaction mass and use of corrosive reagents like acids. The catalytic hydrogenation using supported metal catalysts (gas-liquid-solid multiphase catalytic reactions) has emerged as a cleaner alternative to the conventional Béchamp process with better selectivity and yields [3,4]. Although, these novel catalytic reactions have been employed in several instances, there is still a wide scope for their extension to several other products. However, the success of such extension will depend on proper choice of the catalyst and availability of information relevant to fundamental issues like catalysis, kinetics, mass-transfer effects, adsorption characteristics etc. Such information will not only help in the design of optimized catalysts to achieve maximum yield of the desired products with minimum side reactions, but will also be a key factor in the development of efficient catalytic processes. Several examples of catalytic hydrogenation studies have been published previously [4b-6] from catalysis and reaction engineering viewpoint, but systems involving complex multiphase catalysis (gas-liquid-liquid-solid reactions) demand further detailed investigations. One such

example is the hydrogenation of nitrobenzene to *p*-aminophenol in a four-phase catalytic reaction system. The primary objective of this work was to investigate catalysis, kinetics and adsorption properties of multiphase catalytic hydrogenation reactions. For this purpose, hydrogenation of nitrobenzene and *p*-nitrophenol to *p*-aminophenol were chosen as the model reaction systems. These reactions are also important in the manufacture of *p*-aminophenol, an intermediate for a drug paracetamol. This chapter presents a comprehensive literature review on the preparation of *p*-aminophenol via catalytic hydrogenation routes, catalysts used and kinetic studies.

Table 1-1: Examples of heterogeneously catalyzed liquid phase hydrogenation reactions.

Sr.	***Substrate***	***Catalyst***	***Product***	***Application***	***Reference***
1	*2,4-Dinitrotoluene*	*Pd/Al_2O_3*	*Toluenediamine*	*Intermediate for TDI (fine chemicals)*	*[3]*
2	*Chloronitrobenzenes*	*PtS/C*	*Chloroanilines*	*Pharmaceuticals & dyes*	*[4]*
3	*o-Nitroanisole*	*Pd/C*	*o-Anisidine*	*Dyes & fine chemicals*	*[5]*
4	*Butynediol*	*$Pd\text{-}Zn/CaCO_3$*	*cis-Butenediol*	*Intermediate for vitamin-A & endosulfan*	*[6]*
5	*p-Isobutylacetophenone*	*Pd/C, Ni/HY*	*p-Isobutylphenylethanol*	*Intermediate for Ibuprofen*	*[7]*
6	*Glucose*	*Raney Ni*	*Sorbitol*	*Pharmaceuticals*	*[8]*
7	*Adiponitrile*	*Raney Ni*	*Hexamethylenediamine*	*Intermediate for Nylon6,6*	*[9]*
8	*1,5,9-Cyclododecatriene*	*Pd/Al_2O_3*	*Cyclododecene*	*Intermediate for 121-laurolactum*	*[10]*
9	*Cinnamaldehyde*	*Pt-Co/C or Pt-Ru/C*	*Cinnamyl alcohol*	*Fine chemicals, perfumery*	*[11]*
10	*3-Hydroxypropanal*	*Ni/ support*	*1,3-Propanediol*	*Fine chemicals*	*[12]*
11	*2,8-Dichloroadenosine*	*$Pd/BaSO_4$*	*Adenosine,*	*Pharmaceutical Neuro-regulatory drug*	*[13]*
12	*Reductive amination of 4-chloroacetylcatechol*	*Pd/support*	*Adrenaline*	*Pharmaceuticals*	*[14]*
13	*4-Aminoacetylphenol*	*Pd/support*	*Octopamine*	*Pharmaceuticals*	*[15]*
14	*Soyabin oil*	*Ni /Support*	*Saturated oil*	*Fat industry*	*[16]*
15	*Phenylacetylene*	*Pd/C, Al_2O_3*	*Styrene*	*Raw material for polystyrene*	*[17]*
16	*Acetophenone*	*Ru/Al_2O_3*	*1-Phenylethanol*	*Pharmaceuticals, intermediate for styrene*	*[18]*

1.2 *p*-Aminophenol as an important intermediate

p-Aminophenol is a commercially important chemical intermediate used in the manufacture of several analgesic and antipyretic drugs such as paracetamol, acetanilide, phenacetin etc. (Figure 1-1). Apart from pharmaceuticals, *p*-aminophenol is also used in the manufacture of various industrial dyes. It is a strong reducing agent and is also marketed as a photographic developer under the trade names of *Activol, Azol, Certinal, Citol, Paranol, Rodinol, Unal and Ursol-P*, either alone or in combination with hydroquinone [21]. The oxalate salt of *p*-aminophenol, marketed under a trade name of *Kodelon*, is used as a corrosion inhibitor in paints and anticorrosion-lubricating agent in two-cycle engine fuels. It is also used as a wood stain, imparting rose like color to timber, and as a dyeing agent for fur and feathers [21].

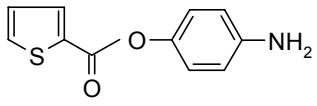

2-Thiophene carbonyl ester
(Analgesic and Antipyretic)

[20a]

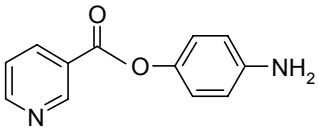

3-Pyridene carbonyl ester
(Analgesic)

[20a]

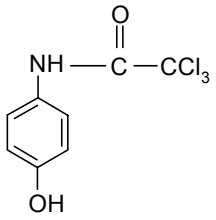

Trichloroacetanilide
(Antipyretic and Analgesic)

[20b]

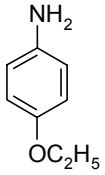

p-Phenitidin
(Analgesic)

[21]

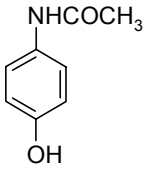

Paracetamol
(Analgesic & Antipyretic)

[21]

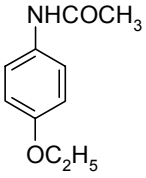

Phenacetin
(Analgesic and Antipyertic)

[21]

Figure 1-1: Drug formulations using *p*-aminophenol as an intermediate

1.3 Synthesis of *p*-aminophenol

Because of its industrial importance, synthesis of *p*-aminophenol has attracted considerable interest. Industrially, *p*-aminophenol is manufactured by the hydrogenation of nitrobenzene and *p*-nitrophenol. Several other methods e.g. chlorophenol amination [22], hydroquinone amination [23], electrolytic reduction of nitrobenzene and *p*-nitrophenol [24] etc. have also been reported, though these are not industrially practiced. Most of the information available on these reactions is patented and there are very few published papers dealing with scientific issues related to catalysis and kinetics of these reactions. The available literature on this subject is summarized in Table 1-2 and discussed in the following sections.

1.3.1 Hydrogenation of nitrobenzene

A major process for the manufacture of *p*-aminophenol is via hydrogenation of nitrobenzene in the presence of a mineral acid such as sulfuric acid (Scheme 1-1).

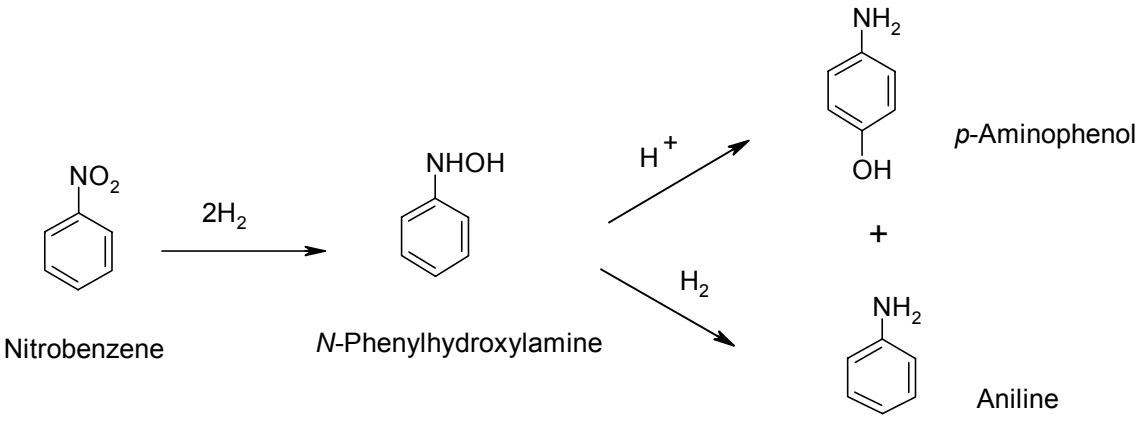

Scheme 1-1: Synthesis of *p*-aminophenol by reduction of nitrobenzene in aqueous acid medium.

Table 1-2: Summary of the literature on the synthesis of *p*-aminophenol.

Substrate	***Catalyst***	***Reaction conditions***	***Remarks***	***Reference***
NBN	*Zn-NH_4Cl,*	*T=323 K; P_{H2} = 1atm; solvent: water*	*conv: 50 %; sel: 64 %* *Rearrangement in separate vessel using H_2SO_4*	*[27]*
NBN	*Al flakes/H_2SO_4*	*T= 353 k; P_{H2} = 1 atm; water*	*conv:100 %; sel: 75 %*	*[28]*
NBN	*PtO_2,/H_2SO_4*	*T=373 K ; P_{H2} = 34 atm; water*	*isolated yield of PAP: 57%*	*[30]*
NBN	*PtO_2,/HCl*	*T= 373 K; P_{H2}= 34 atm; water*	*conv:90 %; sel:67.5%*	
NBN	*MoS /H_2SO_4*	*T= 423 K; P_{H2} = 34 atm; water.*	*isolated yield of PAP 53%*	
NBN	*0.3% Pt/C, H_2SO_4*	*T= 388 K; P_{H2} = 34 atm; water*	*conv:100 % ; sel: 83 %* *Octadecyl trimethyl ammonium chloride (surfactant)*	*[36]*
NBN	*1% Pt/C, H_2SO_4*	*T= 358 K; P_{H2} = 1 atm; water*	*conv:100%; sel: 79%* *non ionic surfactant added*	*[35]*
NBN	*MoS, H_2SO_4*	*T= 428 K; P_{H2} = 20.4 atm; water*	*conv:100%; sel: 78%*	*[34]*
	Pt-S/C, H_2SO_4	*T= 408 K; P_{H2} = 14 atm; water*	*conv:93.26%; sel: 78%*	*[34]*
NBN	*Pt/ γ-Al_2O_3, H_2SO_4*	*T= 360K; P_{H2}= 1 atm; water*	*sel: 85%,* *dodecyl trimethyl ammonium chloride (surfactant)*	*[47]*
NBN	*1%Pt/C,*	*T= 359 K; water*	*conv: 41%; sel: 82%* *RSO_3H, R= alkyl, alkylphenyl acids aded*	*[53]*
NBN	*1% Pt/C, H_2SO_4*	*T= 353 K; P=1 atm*	*dimethylalkylamine sulfate , sel= 73 %*	*[38]*
NBN	*3%Pt/C, H_2SO_4*	*T=358 K; P_{H2}= 5 atm, water*	*conv.: 57.1%, sel:80%; dimethylalkylamine oxide (surfactant)*	*[39]*

NBN= Nitrobenzene; T= Temperature; P_{H2} = Hydrogen pressure; PNP= p-Nitrophenol; PAP= p-Aminophenol

Substrate	Catalyst	Reaction conditions	Remarks	Reference
NBN	PtO_2/H_2SO_4	T= 298 K; P_{H2}= 1 atm; water	conv.=100%, sel: 56%; DMSO added	[43b]
NBN	5% Rh/C + $RhCl_3$ H_2SO_4	T= 363 K; P_{H2} = 20.4 atm, water	conv: 88%, sel: 85%,	[32]
NBN	3% Pt/C, H_2SO_4	T= 358 K; P_{H2} = 1 atm, water	conv.= 88%, sel=73%; Reaction stopped before complete conv. to recycle organic layer	[41]
NBN	3% Pt/C, H_2SO_4	T= 353 K; P_{H2} = 1 atm, methanol	conv:75 %,, sel:79%; diethyl sulfide added	[48]
NBN	1 % Pt/Pd / C, γ- Al_2O_3	T= 333 K; P_{H2} = 3.4 atm; water	conv:99%,, sel83%,formic acid different acids	[40]
NBN	2%Pt-Ru-C(Pt/Ru=5), H_2SO_4	T= 368 K; P_{H2}= 2 atm, water	sel: 86%, dodecyltrimethyl ammonium bromide	[54]
NBN	Pt.Pd.Rh and Ru	T= 353K; P_{H2}= 3-7 atm	sel, Pt=70%, Pd=20%, Rd= 16% and Ru= 0%.	[33]
NBN	WC (Tungstate carbide)	P_{H2} = 2 atm, EtOH	conv. 99 %,, sel.80 %, without EtOH sel: 58.5%,	[55]
NBN	5% Pt/C, H_2SO_4	T = 373 K; P_{H2}= 1atm; water	conv:80 %,, sel:83%,	[31 b]
NBN	Pt/C,H_2SO_4	T=353 K; water	alkyltrimethylammonium halides	[53]
NBN	Pt/CMK-1	T= 353 K; P_{H2}= 1 atm	Conv. = 67 %; sel. = 84 % in 4 hrs.	[50]
PNP	Fe/Acid	T= 353 K; P_{H2}= 1 atm	Sel= 99.1%	[58 a]
PNP	25% Ni, NaOH;	T= 333 K; P_{H2} = 27-34 atm water	sel: 90%	[65]
PNP	Reduced by thiourea dioxide	T= 313 K; P_{H2}= 1atm, EtOH+ NaOH+ urea.	Sel=87-91%	[66a]

Substrate	***Catalyst***	***Reaction conditions***	***Remarks***	***Reference***
PNP	*1%Pt/C*	*T= 358 K; P_{H2} = 1 atm; water*	*Conv.: 100 %; sel.: 87 %.*	*[67]*
PNP	*Montmorillonite Pd(II)-complex*	*T= 298 K; P_{H2}= 1 atm.*	*sel: 95-98%*	*[68]*
PNP	*Raney Ni*	*T= 313 K; 75 % EtOH in water*	*Reduction by hydrazine hydrate*	*[64]*
PNP	*5%Pd/C, H_2SO_4*	*T=298 K; P_{H2} = 2 atm; water*	*conv: 100 %; sel: 84%*	*[60a]*
PNP	*5% Pd/C, boric acid*	*T=373 K; P_{H2}= 4 atm; water*	*Acetylation to N-acetyl-p-aminophenol Sel. = 87..2*	*[66b]*
PNP	*Pd-La/C*	*T= 413 K; P= 6.5 atm; acetic acid+ acetic anhydride*	*Direct acetylation to N-acetyl-p-aminophenol*	*[60c]*
PNP	*Pd/C*	*T= 433 K; P= 10 atm; acetic acid+ acetic anhydride*	*Direct acetylation to N-acetyl-p-aminophenol Conv. : 100 % sel.: 95 %*	*[60d]*

The preparation of *p*-aminophenol from nitrobenzene involves a two-step reaction carried out in a single reactor. In the first step, nitrobenzene is reduced to phenyl hydroxylamine, which undergoes a Bamberger rearrangement in the presence of an aqueous acid to give *p*-aminophenol [25]. Formation of aniline (via further hydrogenation of phenylhydroxylamine) is a major side reaction. The proposed mechanism for the conversion of phenylhydroxylamine to *p*-aminophenol in the presence of an acid (Bamberger rearrangement) is given in Scheme 1-2 [26].

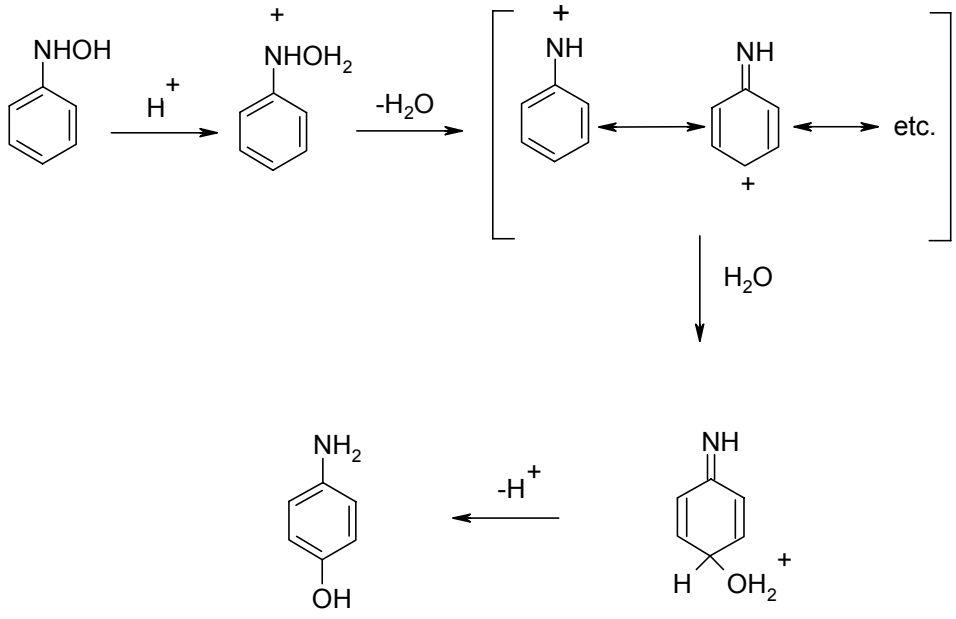

Scheme 1-2: Mechanism for Bamberger rearrangement of phenylhydroxylamine to *p*-aminophenol [26 b].

The intermediate phenylhydroxylamine can be isolated and separately subjected to the rearrangement using acid. Alternatively, both the steps (i.e. reduction and rearrangement) can also be accomplished in a single operation. Bassford [27] reported the preparation of *p*-aminophenol from nitrobenzene using a two-step process. In the first step, nitrobenzene was reduced to

phenylhydroxylamine using Zn/NH_4Cl as the reducing agent in the aqueous phase. After the reaction, zinc hydroxide was removed by filtration and washed with warm water. In the second step, the filtrate and washings were acidified with sulfuric acid and heated to 353 K to convert phenylhydroxylamine to *p*-aminophenol. *p*-Aminophenol thus obtained remained in aqueous solution as its hydrosulfate salt. This solution was cooled and made slightly alkaline by adding aqueous ammonia and further cooled to recover solid *p*-aminophenol in as high as 86% yield. Other reducing agents such as sodium hydrogen sulfide, acid ammonium sulfide etc. can also be used essentially in neutral aqueous solutions of salts such as ammonium chloride, ammonium sulphate, calcium chloride etc. for the conversion of nitrobenzene to phenylhydroxylamine [27]. Bean [28] reported that nitrobenzene could be converted to *p*-aminophenol in good yields (75%) in the presence of aluminum flakes and an aqueous solution of a mineral acid. He also observed that sulfuric acid was more effective than other acids (phosphoric acid and HCl) to get higher yields of *p*-aminophenol. Several other nitro compounds were also converted to corresponding 4-hydroxylamine derivatives using this procedure (Scheme 1-3).

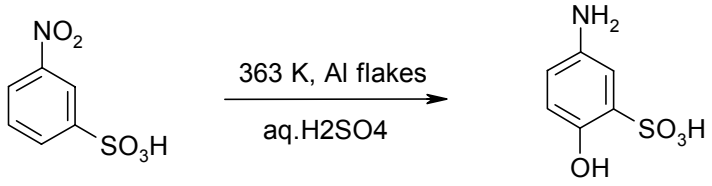

3-nitro-benzenesulfonic acid

5-amino-2-hydroxybenzenesulfonic acid

Scheme continued…

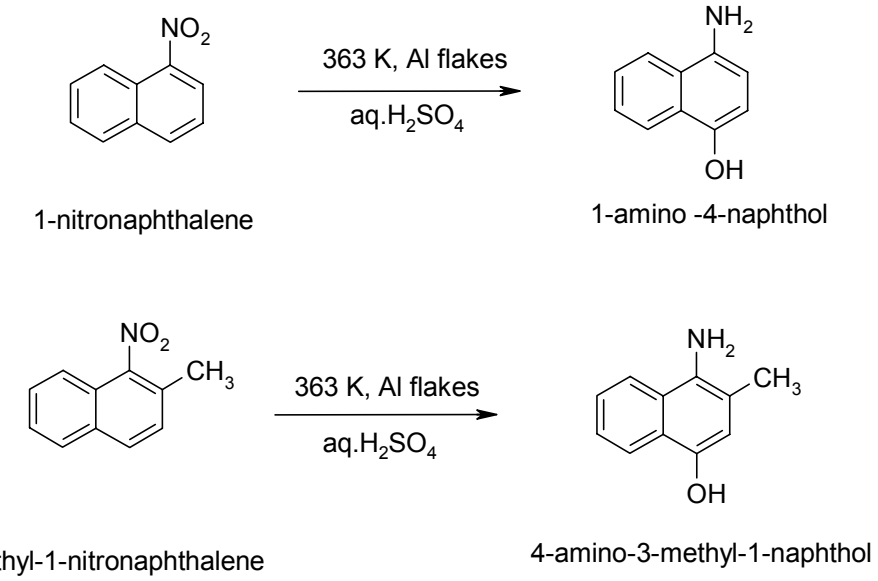

Scheme 1-3: Synthesis of 4-hydroxylamine derivatives by reduction of corresponding nitro substrates [28].

Among several catalysts used for the reduction step, iron-acid catalyst has become the obvious choice because of its lower cost. The various stoichiometric reactions in Fe-HCl mediated reduction of nitro aromatics are given below [29].

$$Fe + 2HCl \longrightarrow FeCl_2 + 2[H] \quad (1\text{-}1)$$

$$FeCl_2 + 2HCl \longrightarrow FeCl_4 + 2[H] \quad (1\text{-}2)$$

The nascent hydrogen produced in the above steps reacts with nitro compound to give amine. The Fe salt produced is converted to Fe-hydroxide sludge. The overall reaction during a nitro reduction is given below:

$$RNO_2 + 3Fe + 4H_2O \xrightarrow[\text{acid}]{353\text{-}363K} RNH_2 + Fe(OH)_2 + Fe(OH)_3 + FeO + [H] \quad (1\text{-}3)$$

$$Fe(OH)_2 + 2Fe(OH)_3 \longrightarrow Fe_3O_4 + 4H_2O \quad (1\text{-}4)$$

The conventional metal-acid reduction produces almost an equivalent amount of metal oxide sludge, which cannot be recycled. This sludge not only poses serious disposal problems but also makes the separation of final product (*p*-aminophenol) from the reaction mass difficult. The problem of waste formation in the conventional reduction process was overcome by Henke and Vaughen [30], who first disclosed the preparation of *p*-aminophenol by catalytic hydrogenation of nitrobenzene in presence of an aqueous mineral acid. In a typical procedure, hydrogenation of nitrobenzene was carried out in a pressure autoclave at 373 K and 3.4 MPa of hydrogen pressure using PtO_2 as a catalyst in 40% aqueous sulfuric acid. The yield of *p*-aminophenol was 57%. Subsequently, several other heterogeneous catalysts e.g. Pd [31], Rh [32], Ru [33], MoS [34], WC [55] etc. were reported for this reaction, but the highest activity was obtained with Pt catalysts [33].

The key issue in the preparation of *p*-aminophenol by catalytic hydrogenation of nitrobenzene was lower yield of *p*-aminophenol, since further hydrogenation of the intermediate phenylhydroxylamine to aniline was the main competing reaction. Formation of other side products such as *o*-aminophenol and 4,4'-diaminodiphenylether has also been reported [21]. Spiegler [35,36] reported that the use of surfactants (quaternary and non-quaternary ammonium compounds) gave enhancement in the yield of *p*-aminophenol during the catalytic hydrogenation of nitrobenzene. Several quaternary ammmonium salts such as dodecyltrimethyl ammonium chloride, octadecyl trimethyl ammonium chloride were found to increase the yield of *p*-aminophenol. Non-quaternary amine compounds e.g. triethylamine sulfate, tributyl amine sulfate were also investigated. It was concluded that rate/yield obtained in the presence of quaternary ammonium compounds was higher

than that with non-quaternary compounds. Brown et al. [37] observed that certain non-ionic surfactants such as polyethers and polyols could be used instead of quaternary ammonium compounds. Use of chloride surfactants resulted in the formation of chloroanilines as impurities. This was overcome by use of sulfate salts [38] or oxide type ammonium salts [39]. The maximum yield of *p*-aminophenol obtained using quaternary ammonium compound (C-cetyl betaine) as surfactants was 98% [36].

The type of the acid used for rearrangement is an important factor in the preparation of *p*-aminophenol by catalytic hydrogenation of nitrobenzene. The key step in this reaction is the Bamberger rearrangement of the intermediate phenylhydroxylamine (Scheme 1-2). Henke [30] reported that sulfuric acid was the most effective acid for rearrangement of phenylhydroxylamine to *p*-aminophenol. For example, use of hydrochloric acid and phosphoric acid gave poor yields of *p*-aminophenol (less than 6-7%) as compared to that obtained using sulfuric acid (57%). Lee et al. [40] investigated the effectiveness of various organic acids in addition to sulfuric acid in the rearrangement step (Table 1-3).

Table 1-3: Effect of organic acid promoters on the selectivity to *p*-aminophenol [40]

Organic acid	***Reaction time***	***Selectivity (%)***	
	(hr)	***p-Aminophenol***	***Aniline***
None	*5*	*67.8*	*18.6*
Methanesulfonic acid	*3*	*70.5*	*17.2*
Acetic acid	*3*	*74.8*	*18.3*
Formic acid	*2.5*	*83.3*	*16.3*
Oxalic acid	*4*	*77.1*	*18.2*
Trichloroacetic acid	*4*	*79.2*	*16.6*

***Reaction conditions**: Nitrobenzene: 12.3 gm; 3% Pt/C: 0.015gm; water: 120 gm; sulfuric acid: 13.5 % w/w; temperature: 353 K; H_2 pressure: 4.2 kg/cm²; organic acid: 0.5 gm.*

Highest enhancement in the activity and selectivity to *p*-aminophenol was observed by the addition of formic acid along with sulfuric acid. It was believed that the addition of organic acid stabilizes phenylhydroxylamine by forming an ion pair with the organic acid and partitioning of the intermediate species into the aqueous solution.

Benner [41] observed that the interruption of hydrogenation step before all the nitrobenzene was consumed helped the catalyst stay in the nitrobenzene layer and the aqueous layer containing *p*-aminophenol, aniline and other minor byproducts could be readily separated from the catalyst-nitrobenzene layer by decantation. The *p*-aminophenol then could be recovered from the aqueous layer and further purified whereas the nitrobenzene (organic) layer containing catalyst could be conveniently recycled.

The intermediate phenylhydroxylamine formed during hydrogenation of nitrobenzene does not appear as a major constituent in the reaction because of fast competing reactions leading to the formation of aniline and *p*-aminophenol. However, the addition of phosphorous acid salts or morpholine to the reaction medium results in the formation of phenylhydroxylamine in presence of platinum catalyst with no further hydrogenation to aniline [42]. This selectivity to arylhydroxylamine was attributed to the modification of the catalyst surface by a poisoning effect of the additive, inhibiting selectively the hydrogenation of aryl hydroxylamine [42].

Rylander [43] observed that the addition of dimethylsulfoxide (DMSO) to the reaction system in the absence of any acid also increased the selectivity to phenylhydroxylamine. The phenylhydroxylamine accumulation was found to be much lower on Pd catalyst as compared to Pt catalyst. It had been observed that

during competitive hydrogenation of nitrobenzene and hydroxylamine over Pt and Pd catalyst, nitrobenzene was reduced preferentially over Pt whereas phenylhydroxylamine over Pd [44]. This selectivity was attributed to the higher adsorption strength of phenylhydroxylamine on Pd catalyst compared to Pt catalyst. Karwa et al. [45] investigated selective hydrogenation of nitrobenzene to phenylhydroxylamine on Pt/C catalyst under a wide range of operating conditions and observed that the addition of DMSO apparently suppressed the reduction of phenylhydroxylamine to aniline leading to increased selectivity of phenylhydroxylamine. It was also noted that the selectivity to phenylhydroxylamine decreased with increase in temperature but remained unaffected by hydrogen pressure. The selectivity to phenylhydroxylamine was also found to be directly proportional to the polarity of the solvent used. Pernoud et al. [46] screened several supported group VIII metals (Ir, Ni, Pd, Rh, Pt) for the selective hydrogenation of nitrobenzene to phenylhydroxylamine, in neutral aqueous medium without any additives and concluded that the selectivity to phenylhydroxylamine close to 90% could be obtained at 80% conversion of nitrobenzene using Pt/SiO_2 catalyst at very low temperature (278 K) and 2 MPa pressure of hydrogen [46].

Although, platinum catalysts are well suited for hydrogenation of nitrobenzene to *p*-aminophenol, they are capable of further hydrogenating *p*-aminophenol to alicyclic compounds which are undesirable byproducts. Moreover, conventional platinum catalysts are easily poisoned and are not reusable without treatment. Greco [34] reported use of powdered MoS/C catalysts, which were less expensive than the commercial noble metal catalysts used for the hydrogenation of nitrobenzene to *p*-aminophenol. The MoS/C catalyst provided complete hydrogenation of nitrobenzene without possibility of over hydrogenation and with

the consequential elimination of usual nitrobenzene recovery step and catalyst treatment. This catalyst could also tolerate high temperatures required for rearrangement of phenylhydroxylamine to *p*-aminophenol. The maximum yield of *p*-aminophenol obtained using MoS/C catalyst was 80 % [34].

Dunn et al. [47] reported that the selectivity to *p*-aminophenol in the catalytic hydrogenation of nitrobenzene could be increased to 83% using Pt/γ-alumina catalyst. Caskey and Chapmann [48] obtained even higher selectivity to *p*-aminophenol by hydrogenating nitrobenzene at low temperatures (273-313 K) using platinum catalyst by the addition of a sulfur compound. The phenylhydroxylamine obtained was isolated and subjected to rearrangement in a separate vessel to get overall selectivity of 90% to *p*-aminophenol.

The selectivity to *p*-aminophenol was also enhanced by the addition of a second metal in combination with noble catalysts. Thus, Gao et al. [49] observed that the selectivity for *p*-aminophenol increased from 23 to 66 % by the addition of 2-mercaptopyrimidine and cobalt to the reaction system during the palladium catalyzed hydrogenation of nitrobenzene. Ahn et al. [50] showed that noble metal supported on carbon molecular sieve, CMK-1 (with regular mesoporous structure having an average pore diameter of 3 nm) had better activity compared to the commercial carbon supported precious metal catalyst in terms of conversion and selectivity. The enhancement in activity in case of CMK-1 supported catalyst was believed to be due to increased metal dispersion and subsequent reduction in the pore diffusion resistance because of mesoporous structure of CMK-1.

Dewal et al. [51] and Juang et al. [33] investigated the effect of temperature, pressure, sulfuric acid and surfactant concentration on the catalytic hydrogenation of nitrobenzene in aqueous medium to *p*-aminophenol using 10% and 5% Pt/C

catalysts respectively. According to Dewal et al. [51], the yield of *p*-aminophenol increased from 31 % to 56 % with increase in quaternary ammonium salt (octadecyl trimethyl ammonium chloride) concentration from 0 to 0.3 % at 363 K. The sulfuric acid concentration was varied from 10-25 % (w/w) and it was observed that optimum selectivity to *p*-aminophenol could be obtained when the concentration of sulfuric acid was 15 % w/w. The yield of *p*-aminophenol increased with hydrogen pressure and temperature. Juang et al. [33] proposed that the rate-determining step for the catalytic hydrogenation of nitrobenzene was adsorption of hydrogen on the metal surface. These authors also observed that platinum catalyst favored formation of *p*-aminophenol whereas palladium catalyst favored the aniline formation.

p-Aminophenol was also prepared in good yields (90% conversion with 55% selectivity) by catalytic transfer hydrogenation of nitrobenzene using 5% Pd/C catalyst and 25 % phosphoric acid as hydrogen donor at 353 K. Unlike the catalytic hydrogenation using hydrogen gas, the addition of surface-active reagents to the reaction system did not further improve the selectivity to *p*-aminophenol in catalytic transfer hydrogenation reaction [52].

The literature summarized in the above section indicates that several attempts to improve the selectivity for *p*-aminophenol have been made and the nature of investigations was mainly performance evaluation of catalyst / promoter systems. For a four-phase catalytic reaction like this, it is equally important to understand the kinetics of the reaction and significance of interphase and intraparticle mass transfer effects, so that the optimum reaction conditions can be determined. Furthermore, there have been no published reports on the kinetics of catalytic hydrogenation of nitrobenzene to *p*-aminophenol.

1.3.2 Hydrogenation of *p*-nitrophenol to *p*-aminophenol

Hydrogenation of *p*-nitrophenol to *p*-aminophenol is an alternative method for the preparation of *p*-aminophenol. The starting material i.e. *p*-nitrophenol is expensive compared to nitrobenzene, which is a drawback of this route. The major routes to *p*-nitrophenol are given below.

1) Chlorination of nitrobenzene to *p*-nitrochlorobenzene, and its subsequent hydrolysis [56]

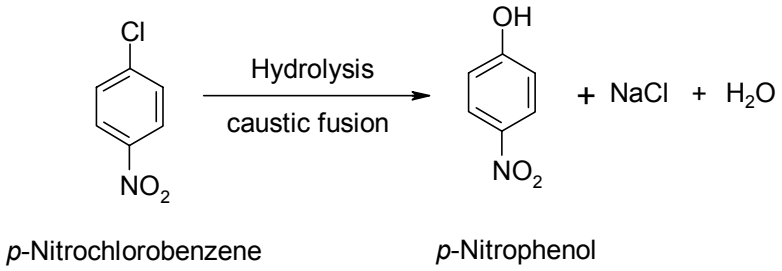

p-Nitrochlorobenzene *p*-Nitrophenol (1-5)

2) Nitration of phenol [57]

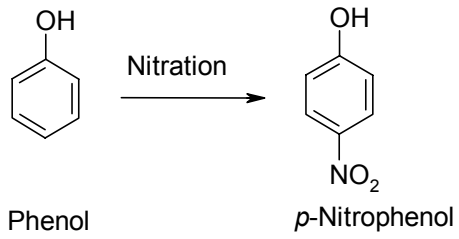

Phenol *p*-Nitrophenol (1-6)

Several methods have been reported for the hydrogenation of *p*-nitrophenol to *p*-aminophenol. Conventional methods for the conversion of *p*-nitrophenol to *p*-aminophenol employ reduction using iron turnings in a weakly acidic solution or suspension (scheme 1-4) as reducing agents similar to those described in earlier section for nitrobenzene reduction [58c].

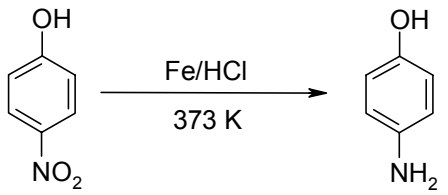

Scheme 1-4: Reduction of *p*-nitrophenol to *p*-aminophenol by iron-acid.

In this conventional method, the *p*-aminophenol formed by reduction of *p*-nitrophenol is converted to the water-soluble sodium aminophenolate by adding sodium hydroxide before Fe-FeO sludge is separated from the reaction mixture. Acidification of the solution precipitates *p*-aminophenol, a procedure performed in the absence of air because the salts are easily susceptible to oxidation in aqueous solutions [21]. Other reagents consisting of Zn, Al, Sn etc. [59] have also been reported for the reduction of *p*-nitrophenol to *p*-aminophenol. The obvious drawback of these reduction processes is the formation of huge amounts of undesirable metal oxide sludge, which poses serious pollution problem. Catalytic hydrogenation of *p*-nitrophenol obviates the problem of sludge formation associated with the conventional reduction method. Several reports describe the preparation of *p*-aminophenol by catalytic hydrogenation of *p*-nitrophenol using supported metal catalysts e.g. Pd/C [60], Pt/C [61], supported Ni [56], and colloidal Rh, Pd and Pt catalysts [63].

Goswami et al. [64] investigated the reduction of *p*-nitrophenol using hydrazine as reducing agent and Raney nickel catalyst in ethanol-water solvent. The effect of various reaction parameters like solvent, hydrazine hydrate and catalyst and promoter concentrations was also investigated. The reaction was reported to be

first order with hydrazine and nitro compound concentration. The apparent hydrogenation rate constant was dependent on the nature of substrate, dielectric constant and ionic strength of solvent and catalyst amount. Sidheshwaran et al. [56] investigated the suitability of nickel catalysts for the hydrogenation of *p*-nitrophenol to *p*-aminophenol and concluded that excellent conversions ranging from 85-93 % could be obtained with nickel catalysts under optimized reaction conditions.

Chandalia et al. [60b] investigated the hydrogenation of *p*-nitrophenol to *p*-aminophenol using 1% Pd/C catalyst in 95% ethanol solvent at 353 K. The effect of agitation frequency, catalyst loading, *p*-nitrophenol concentration, and temperature on the hydrogenation rate and yield of *p*-aminophenol was studied. It was concluded that the mass transfer of hydrogen from gas to bulk liquid phase (G-L) and liquid-phase to catalyst particle (L-S) were the rate controlling steps. Yao et al. [63] investigated the hydrogenation of nitroaromatics (including *p*-nitrophenol) over colloidal Pd, Rh and Pt catalysts. An empirical rate equation was also proposed to predict the hydrogenation rates.

1.3.3 Amination method

Bean et al. [23f] prepared several aminophenols by direct amination of hydroquinone in presence of aqueous ammonia and ammonium salts (phosphates or arsenates). In a typical procedure, the mixture of hydroquinone, diammonium phosphate, aqueous ammonia and water was heated in an autoclave at 473 K for 12 hrs. The resulting solution was filtered and treated with conc. hydrochloric acid to neutralize the mixture. After cooling, *p*-aminophenol crystallized out from the reaction medium. The yield of *p*-aminophenol was 60 % (Scheme 1-5).

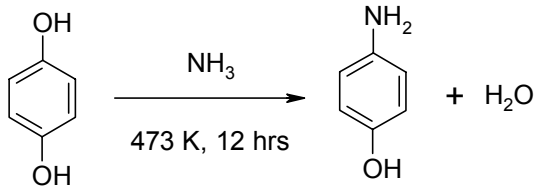

Scheme 1-5: Synthesis of *p*-aminophenol by catalytic amination of hydroquinone

Watabe et al. [23a-d] reported the catalytic amination of hydroquinone in the presence of phenol using a silica supported lanthanum phosphate catalyst. The reactions were carried out at high temperature (513 K) in an autoclave to give 80-95 % conversion of hydroquinone with 52-81% selectivity to *p*-aminophenol. The formation of *p*-phenylenediamine (9-20%)was a major side reaction.

p-Aminophenol was also prepared by amination of *p*-chlorophenol with ammonia in the presence of CuCl and $CaCl_2$ as catalysts (Scheme 1-6). Conversions of *p*-chlorophenol as high as 94.2 % could be achieved with 89.6 % selectivity to *p*-aminophenol [22].

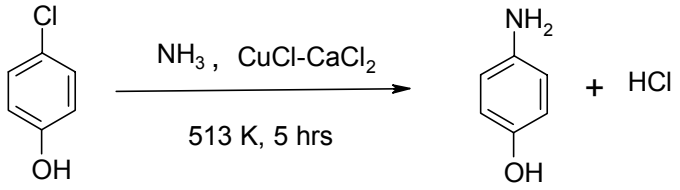

Scheme 1-6: Catalytic amination of *p*-chlorophenol to *p*-aminophenol.

1.3.4 Electrolytic reduction

The electrochemical reduction method has attracted increasing interest because it eliminates the pollution problems associated with the conventional metal-acid

reduction routes. The electrolysis of nitrobenzene, phenylhydroxylamine, or azoxybenzene in deoxygenated acid solutions, using graphite or copper-mercury cathodes at potential differences of –300 to –600 mV and temperatures of 333-363 K, were reported to yield *p*-aminophenol in the range of 65-99 % [24]. Aniline was again obtained as a major by-product. Several parameters e.g. nature of electrode, metal additives, electrolytes, agitation, flow properties through cells affected the selectivity to *p*-aminophenol. Electrolytic oxidation of aniline to *p*-aminophenol by electrochemically activated molecular oxygen via direct electron transfer from cathode, in the presence of iron compounds, was also reported [24h].

1.4 Adsorption from solution

In heterogeneous catalysis, adsorption of reaction species plays a key role in the activity–selectivity behavior of catalyst and catalytic reaction mechanism. In this part, a brief description of the adsorption phenomenon and the relevant literature on adsorption of nitrobenzene, aniline and hydrogen relevant to hydrogenation of nitrobenzene to *p*-aminophenol is presented.

All surfaces contain unsaturated bonds and this bond causes the reactant molecules to get attached to the catalyst surface. The degree of interaction obviously depends on the nature of adsorbate and the adsorbent. Depending on the nature of interaction, adsorption is classified as either physical or chemical (called as physisorption and chemisorption respectively) adsorption. Physisorption is caused by the forces of molecular interaction, which include dipole and dispersive forces and thus, physisorption is a result of the same forces that cause condensation and solidification of fluid phases. On the contrary, chemisorption involves interaction of electrons of the adsorbate and adsorbent resulting in the formation of a chemical

bond. Unfortunately, it is not always easy to determine experimentally whether physi- or chemi-sorption is taking place. Table 1-4 gives a comparison between physical and chemical adsorption.

Table 1-4: Comparison between physisorption and chemisorption [69a]

Property	***Physisorption***	***Chemisorption***
Heat of adsorption	*Low (< 2-3 times latent heat of evaporation)*	*High (> 2-3 times latent heat of evaporation)*
Rate of adsorption	*Rapid, non activated, reversible*	*Activated, may be slow and irreversible*
Rate of desorption	*Activation energy for desorption equals heat of adsorption*	*Activation energy for desorption may be larger than heat of adsorption*
Temperature range over which adsorption occurs	*Close to condensation temperature of the adsorbate*	*Occurs at a wide range of temperatures and at temperatures much above the condensation temperature.*
Specificity	*Non specific*	*Highly specific*
Electrical conductivity	*Electrical conductivity of the catalyst not affected*	*May affect electrical conductivity of catalyst.*

The information presented in Table 1-4 indicates that if the heat of adsorption is very large or if the adsorption has higher activation energy than the latent heat of evaporation, then the adsorption is clearly a chemisorption. Unfortunately, often the heat of adsorption is about 40-50 kJ/mole, it is very difficult to determine whether the adsorption is physical or chemical. Other criteria, which are helpful in distinguishing between these two types of adsorption, are electrical conductivity (which changes appreciably upon adsorption) and IR spectroscopy. Often, the differentiation based on one criterion is not enough and the use of combination of criteria described in Table 1-4 can be useful in deciding the nature of adsorption. Knowledge of the type of adsorption is useful, since only chemisorbed species act as

intermediate in catalytic reactions. For a typical heterogeneous reaction A + B → C, two distinct mechanistic situations can arise as shown below in Figure 1-5.

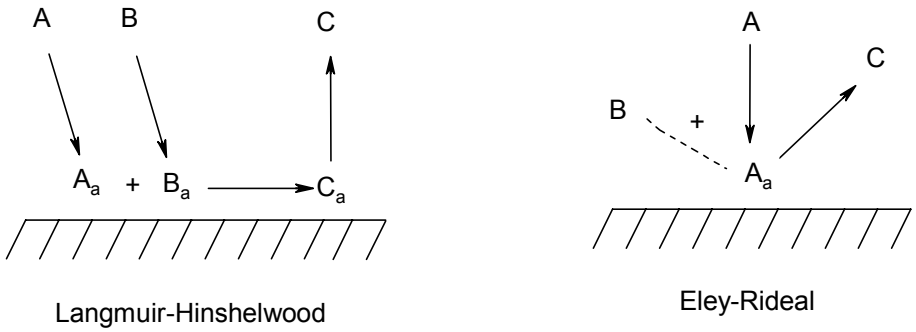

Figure 1-2: Possible mechanisms for a heterogeneous catalytic reaction

The reaction is said to be Langmuir-Hinshelwood type if both the reactants are adsorbed on the catalyst surface and react with each other to give product, whereas it is Eley-Rideal type if one of the reactants is adsorbed on the catalyst surface and reacts with the other reactant from the bulk medium to give the product.

1.4.1 Adsorption isotherms

The amount of material adsorbed on catalyst surface at equilibrium conditions for a specific adsorbate-adsorbent system depends on concentration (pressure for gas phase adsorbate), temperature, surface area of the adsorbent and nature of adsorbate. The relation between the amount adsorbed at equilibrium and the adsorbate pressure or concentration at constant temperature is represented by the adsorption isotherms.

1.4.1.1 Langmuir adsorption isotherm

The Langmuir adsorption isotherm [70] is most widely used relationship for the adsorbed quantity of adsorbate at equilibrium as a function of concentration. The Langmuir isotherm is given by,

$$\theta = \frac{q}{q_m} = \frac{KC_e}{1 + KC_e} \tag{1-7}$$

or

$$\frac{C_e}{q} = \left(\frac{1}{q_m K}\right) + \left(\frac{1}{q_m}\right) C_e \tag{1-8}$$

Where, q_m is the amount necessary to cover the entire surface with one layer of adsorbate (monolayer coverage); θ is fractional surface coverage, K is adsorption equilibrium constant and C_e is equilibrium concentration (pressure in case of gas) of the adsorbate. The values of adsorption equilibrium constant, K, and monolayer adsorption capacity, q_m, can be calculated from the plots of C_e/q vs C_e at different temperatures [69a].

The Langmuir model of adsorption is based on some assumptions: (a) the adsorption is localized, (b) the maximum adsorption is monolayer, (c) all surfaces have same nature, and (d) no interaction exits between the adsorbed species meaning that the heat of adsorption is independent of surface coverage. These assumptions are not always valid in the practical situations and therefore often, the experimental adsorption data cannot be fitted to equations 1-7 or 1-8. In particular, the non-homogeneity of the surfaces and interaction of adsorbed species produces

variation in heat of adsorption with surface coverage. The Freundlich isotherm incorporates the variation of heat of adsorption.

1.4.1.2 Freundlich adsorption isotherm

The Freundlich adsorption isotherm is given by [71a]:

$$q = kC_e^n \tag{1-9}$$

or

$$log\ q = log\ k + n\ log\ C_e \tag{1-10}$$

Where, k is adsorption constant and n (>1) is exponent. This isotherm assumes that the heat of adsorption exponentially decreases with surface coverage, θ. Often, this equation satisfactorily represents data over a wide range of values of θ and for systems that do not follow the Langmuir isotherm. Even for the system, that does follow the Langmuir isotherm over a moderate range of coverage intermediate between extremes of θ=0 and θ=1, the Langmuir isotherm is nearly equivalent to being proportional to a fractional power of concentration. The Freundlich isotherm, by suitable adjustment of the two constants thus can be made to fit the data very well [71b]. The plots of $log\ q$ versus $log\ C_e$ are linear for the systems following Freundlich adsorption isotherm.

1.4.1.3 Heat of adsorption

The heat of adsorption is a significant property for the differentiation of physical and chemical adsorption. For any process to occur spontaneously, the Gibbs free energy, ΔG, must decrease. Adsorption also obeys this rule. According to the second law of thermodynamics,

$$\Delta G = \Delta H - T\Delta S \tag{1-11}$$

The entropy of adsorbate decreases on going from gas phase to the adsorbed phase, therefore ΔS is negative, because the adsorbed state has fewer degrees of freedom (it is more ordered) than the gaseous state. It is generally assumed that the entropy of adsorbent is unaltered by adsorption. Hence, for the majority of adsorption, ΔS is less than zero. Therefore, according to equation 1-11, it is necessary that ΔH be less than zero for ΔG to be less than zero. This means that every adsorption process for which the entropy of adsorbent-adsorbate decreases during the adsorption, the adsorption process will be exothermic (ΔH<0). Heat of adsorption can be calculated from adsorption isotherms using the vant Hoff equation [69 a]:

$$\left(\frac{\partial \ln K}{\partial T}\right) = \frac{\Delta H}{RT^2} \tag{1-12}$$

Where, ΔH is the heat of adsorption. Alternatively, a calorimetric method gives an integral value of the heat of adsorption, which is the average value over the degree of surface coverage considered.

In any solid catalyzed reaction, a number of steps have to occur before the reactants are converted into product, significant of these are: adsorption of reactants on the catalyst surface, reaction between adsorbed species to give product and desorption of product from the catalyst surface to reaction medium, which occur successively. The overall catalytic reaction (in the absence of mass transfer resistances) is controlled by one of the above-mentioned steps or combination of these steps. To understand the catalytic process and its controlling mechanism, it is necessary to understand the adsorption behavior of various reaction species on the

catalyst surface. In view of the importance of the adsorption studies, it was another objective of this work to investigate the liquid phase adsorption characteristics of nitrobenzene, aniline and hydrogen over a wide range of temperature and concentrations on Pt/C catalyst. The intermediate phenylhydroxylamine is very unstable and immediately rearranges to *p*-aminophenol in the presence of acid or gets further hydrogenated to aniline, therefore, the adsorption of phenylhydroxylamine was not investigated.

1.4.2 Adsorption of nitrobenzene, aniline and hydrogen from liquid phase

Adsorption of nitrobenzene and aniline has been investigated in literature in the context of purification of wastewater, since nitrobenzene, aniline and other nitro compounds are major pollutants in waste/sewage water. Knowledge of adsorption equillibria of these organic pollutants/adsorbate and adsorption capacity of the adsorbents is required in the design of purification processes. A representative summary of literature available on the adsorption of nitrobenzene and aniline from solution is presented in Table 1-5.

The adsorption of aniline has been investigated on activated carbon, coal and various clays in the literature [72]. Ardizzone et al. [73] studied the adsorption of aniline from *n*-hexane onto alumina and iron particles. The values of ΔG° calculated using adsorption isotherms fall in the range of typical physisorption processes indicating the occurrence of short-range van der Waals' interactions between adsorbent and adsorbate. Radovic et al. [74] investigated the adsorption of aniline and nitrobenzene on activated carbon from aqueous solutions. Adsorption of aniline was proposed to involve two parallel mechanisms: (a) electrostatic attraction between anilinium cations and negatively charged carbon surface groups, and (b)

dispersive interactions between aniline molecules and graphene layers. On the contrary, in case of nitrobenzene (nondissociating adsorbent) the adsorption primarily results from the dispersive interaction between the nitrobenzene and graphene layers.

Aggarwal et al. [75] investigated the adsorption of nitrobenzene on activated carbon from dilute aqueous solutions and concluded that the adsorption was influenced by the surface area and the nature of the carbon surface. Thus, the presence of carboxylic groups on the carbon surface reduced the adsorption capacity while the presence of quinonic groups enhanced it. Such selectivity behavior was attributed to the probability of interaction of electron clouds of the benzene ring in nitrobenzene with the partial positive charges on the carbon atom from carbonyl group [75]. Zhou et al. [76] investigated adsorption of several organic compounds including nitrobenzene and aniline on the activated carbon. The experimental data were correlated using the Langmuir as well as Redlich-Peterson and Jossens-Myers equations.

The interaction of hydrogen with the heterogeneous catalyst is a key factor in the catalytic hydrogenation reactions. Most of these reactions involve chemisorption of hydrogen on the surface of the solid catalyst. Hydrogen adsorption from vapor phase on various catalysts is well reported in literature [90, 91]. On the contrary, the adsorption of hydrogen on catalysts in the liquid phase is little investigated. Smith et al. [92-94] investigated the adsorption of hydrogen from the liquid phase on Pd/ γ-Al_2O_3 catalysts in a slurry reactor. Separate measurement of adsorption of hydrogen on the heterogeneous catalyst in a slurry of cumene indicated that the adsorption of hydrogen on the catalyst surface was reversible. The adsorption data

were fitted to an empirical correlation. Table 1-6 summarizes the results available on the adsorption of hydrogen on adsorbent from solution.

Thus, there is no comprehensive information available on the adsorption of various reaction species from solution during the hydrogenation of nitrobenzene (i.e. nitrobenzene, aniline, *p*-aminophenol and hydrogen). The available data is rather qualitative in nature. In spite of its importance in determination of reaction mechanism, adsorption of multicomponent (mixtures) systems has also not been studied. Further studies on these aspects would be most valuable to obtain basic understanding of adsorption characteristic as well as determination of adsorption rate and equilibrium parameters.

Table 1-5: Literature search on adsorption of nitrobenzene, aniline on activated carbon and other supports

Sr.	*Adsorbate*	*Adsorbent*	*Results/ Conclusion*	*Reference*
1	*ANI*	*Coal*	*Adsorption from aqueous solution, Aniline adsorption rate is slower for preoxidised than for the unoxidised coal, Oxidation reduces coal porosity.*	*[72b]*
2	*NBN*	*γ-Alumina, Fe powder*	*Comparison of alumina and Fe from n-hexane solution. On alumina, isotherms presented Langmuirian shape while on Fe powder was sigmoid with two platue regions.*	*[73]*
3	*NBN, ANI*	*Activated carbon*	*Adsorption investigated at different pH of solution Electrostatic and dispersive adsorbate/adsorbent interactions significantly affected the equilibrium uptake.*	*[74]*
4	*NBN*	*Activated carbon*	*Effect of surface area on adsorption capacity was investigated. Presence of carboxylic surface groups reduces adsorption of NBN and quinonic group enhances it.*	*[75]*
5	*NBN, ANI*	*Activated carbon*	*Comparison of adsorption isotherms for nitrobenzene, aniline. Adsorption trend NBN> aniline*	*[76]*
6	*NBN*	*Carbon fiber*	*Dynamic adsorption curves were created by static and dynamic adsorption method Adsorption capacity of carbon fibers was more and rate of adsorption was high at high temp.*	*[77]*
7	*NBN*	*Carbon*	*Presence of electron withdrawing functional groups increased activation energy and thus higher temperature is required for desorption*	*[78]*
8	*NBN*	*Activated carbon*	*Adsorption was investigated using gas chromatography technique by injecting aqueous solution. Hydrogen bonding and steric hindrance significantly influence the adsorption*	*[79]*
9	*NBN,*	*Activated carbon*	*Conc. dependence of surface diffusivity of NB/benzonitrile was measured at different temp. Isotherms obeyed the potential theory of adsorption and partially expressed by Freundlich eqn. Correlation was derived with the measured conc./temp. dependence of surface diffusivity.*	*[80]*
10	*NBN*	*Activated carbon*	*Effect of varying particle size & shape, pore structure Adsorption process involves transport from bulk liquid to outer particle surface, then to particle interior and the adsorption step.*	*[81]*

NBN= nitrobenzene; ANI= aniline

Sr.	Adsorbate	Adsorbent	Results/ Conclusion	Reference
11	ANI	Silica gel	Benzene as solvent at 308-323 K Heats of wetting of aniline. Monolayer adsorption is independent of temperature, temperature affects only the participation of surface OH groups in adsorption process. Thermodynamic parameters were evaluated.	[82]
12	ANI	Granular activated carbon	Linear correlation between adsorptive affinity and acidic properties was shown	[83]
13	ANI,	Montmorillonite	Adsorption from methanol, effect of pH of solution, Adsorption depends on basicity of solute, complexing ability, polarity and Lewis acidity of the cation (for ion exchanged montmorillonite)	[84]
14	NBN,	Carbon	Temperature range 298-318 K, Enthalpy, entropy and free energy of adsorption determined	[85]
15	NBN	Graphite	Adsorption in neutral or acidic media at 293, 308, 323 K was studied. Free energy, enthalpy and entropy of adsorption was determined	[86]
16	NBN, ANI	Silica gel	Adsorption from binary solution from n-heptane and hexane. Multiplayer adsorption of NBN from n-heptane was observed. Data was analyzed in terms of different adsorbate-adsorbent and adsorbate-adsorbate interactions.	[87]
17	NBN, ANI	CTMAB-Bentonite	From water, optimum conditions for water adsorption was investigated Order of removal of pollutants: nitrobenzene>aniline	[88]
18	NBN, ANI	Copper chromite	Adsorption was studied at 483-558 K and partial pressures 0-40 kPa by gas chromatographic pulse technique. Adsorption followed Freundlich adsorption isotherm. NBN was physically adsorbed whereas aniline was chemisorbed on the catalyst surface.	[89]

Table 1-6: Summary of literature on adsorption of hydrogen from solution on catalyst

Sr.	*System*	*Results/conclusions*	*Reference*
1	*H_2 on Pd/Al_2O_3*	*Slurry reactor, atm. Pressure, 278-308 K, cumene as solvent, poisoning effect with CS_2. Study by zero and first moment analysis.*	*[92]*
2	*H_2 on Pd/Al_2O_3*	*Determination of separate gas-liquid reaction rate constant and adsorption equilibrium constant for Pd/Al_2O_3 used for hydrogenation of methyl styrene reaction. H_2 adsorption using cumene as solvent, 291-308 K.*	*[93]*
3	*H_2 on Pd/Al_2O_3*	*Cumene as solvent, in slurry reactor. Effect of catalyst reduction temperature on K, k and surface rate coefficients; high temp. reduction reduces dispersion of Pd and caused reduction in K,k and surface rate coefficients*	*[94]*
4	*H_2 on Ir/C*	*H_2 adsorption heat measured using potentiodynamic method. Competing chemisorption of water and hydrogen on catalyst surface.*	*[95]*
5	*H_2 on Ni black*	*Measurement by microcalorimetric method Influence of water was studied, Heat of adsorption of hydrogen on Ni decreased due to chemisorbed water.*	*[96]*
6	*H_2 on Pt black*	*Adsorption isobar by Frontal Temperature Programmed Sorption technique, gas phase adsorption*	*[97]*
7	*H_2 on Pt black*	*Effect of method of preparation on adsorption capacity, dependence of heat of adsorption of H_2 on the degree of coverage on Pt catalyst is described*	*[98]*
8	*H_2 on Group VIII metals (Ni, Pt, Pd, Rh, Ir)*	*Studies made by adsorption calorimetry, thermal desorption, electron microscopy and electrochemical methods*	*[99]*
9	*H_2 on 20% Pd/Al_2O_3*	*Adsorption properties of catalysts were studied at 293-333 K in 0.1 N H_2SO_4 solution by a method of elec. Charging curves.*	*[100]*

1.5 Scope and objectives for present work

A detailed literature survey presented in this chapter on the catalytic synthesis of *p*-aminophenol revealed that the development of a process for direct hydrogenation of nitrobenzene to *p*-aminophenol is a very complex reaction and there is a wide scope for catalyst development, optimization of process conditions, product separation and purification. While, Pt based catalysts are mostly studied for this system, there is no comprehensive information available on the effect of various reaction parameters on the hydrogenation process, adsorption data and the kinetics. The literature data available on the hydrogenation of *p*-nitrophenol to *p*-aminophenol is also rather qualitative in nature. Further, the catalytic hydrogenation of *p*-nitrophenol to *p*-aminophenol is also not investigated in sufficient details with respect to the catalysis and reaction kinetics. In view of the commercial importance of the *p*-aminophenol, the following specific problems were chosen for the present study.

1. To study the hydrogenation of nitrobenzene to *p*-aminophenol in a batch slurry reactor with specific objective to screen the effect of various reaction parameters on the activity and selectivity of the catalyst system.
2. To investigate the kinetics of hydrogenation of nitrobenzene to *p*-aminophenol using Pt/C catalyst in a four phase (gas-liquid-liquid-solid) reaction system.
3. To study the liquid phase adsorption of nitrobenzene, aniline and hydrogen on activated carbon and Pt/C catalysts at different temperatures
4. To study the catalytic hydrogenation of *p*-nitrophenol to *p* -aminophenol with the specific aim to investigate the activity and selectivity under various reaction conditions.

5. To investigate the kinetics of Pt catalyzed hydrogenation of *p*-nitrophenol to *p*-aminophenol in a batch slurry reactor with a detailed analysis of mass transfer effects.

1.6 References

[1] (a) Mills, P. and Chaudhari, R. *Catal. Today 37,* 367, **1997**. (b) Mills, P.; Ramchandran, P. and Chaudhari, R. *Rev. Chem. Eng. 8,* 1, **1992**. (c) Chaudhari, R. and Mills, P. *La. Chim. Ind. 82*, 539, **2000**.

[2] (a) Sheldon, R. *Chem. Ind*. 903,**1992**. (b) Hagens, J. *Industrial Catalysis: A practical approach, Wiley*-VCH, Weinheim, **1999**.

[3] Westerterp, K.; van Gelder, K.; Janssen, H. and Oyevaar, M. *Chem. Eng. Sci. 43*, 229, **1988**.

[4] (a) Kosak, J. *Ann. N. Y. Acad. Sci. 172,* 175, **1980**. (b) Rode, C. and Chaudhari, R. *Ind. Eng. Chem. Res. 33,* 1645, **1994**.

[5] Chaudhari, R.; Parande, M.; Ramchandran, P. and Brahme, P. *ISCRE* – 8, Pergamon Press, UK, 205, **1984**.

[6] Chaudhari, R.; Parande, M.; Ramchandran, P.; Brahme, P.; Vadgaonkar, H. and Jagannathan, R. *AIChE. J. 31*, 1891, **1985**.

[7] Rajshekharam, M. and Chaudhari, R. *Chem. Eng. Sci. 51,* 1663, **1996**.

[8] Brahme, P. and Doraiswamy, L. *Ind. Eng. Chem. Proc. Des. Dev. 15*, 130, **1976**.

[9] Mathieu, C.; Dietrich, E.; Delmas H. and Jenck J. *Chem. Eng. Sci. 47,* 2289, **1992**.

[10] Stuber, F.; Benaissa, M. and Delmas H. *Catal. Today 24,* 95, **1995**.

[11] Fouilloux, P. *Stud. Surf. Sci. Catal. 59,* 245, **1988**.

[12] Valerius, G.; Zhu, X.; Hofmann, H; Amtz, D. and Hass, T. *Chem. Eng. Proc. 35*, 11, **1996**.

[13] Doval, J.; Lythgoe, B. and Todd, A. *J. Chem. Soc. Chem. Comm*. 967, **1948**.

[14] Loewe, H. and Forsch, A. *Enc. Chem. Tech. 15,* 757, **1981**.

[15] Asscher, M. *Rec. Trav. Chim. 68*, 774, **1949**.

[16] Fillion, B.; Morsi, B.; Heier, K. and Machado, M. *Ind. Eng. Chem. Res. 41*, 697, **2002.**

[17] Chaudhari, R.; Jaganathan, R.; Kolhe, D.; Emig, G. and Hofmann, H. *Chem. Eng. Sci. 41*, 3073, **1986**.

[18] Rajshekharam, M; Fouilloux, P.; Schweich, D.; Bergaut, I.; Delmas, H. and Chaudhari, R. *Catal. Today 48,* 83, **1999**.

[19] Bachamp, A. *Annales de Chimie* (Paris) *42,* 186, **1854**.

[20] (a) Dictionary of Organic Compounds, 6th edition, Chapman and Hall, Editors: Cadogan, J.; Ley, S., Pattenden, G.; Raphel, R. and Rees, C. 1, **1996**. (b) Laboratories Dela Grange, French Pat. M 940, **1961**. Chem. Abstr. 58:3354 h.

[21] (a) Mitchell, S.; Waring, R.; Ullamann's Encyclopedia of Industrial Chemistry, 5th edition, VCH, Weinheim, *A2*, 99, **1985**. (b) kroschwitz, J. (Ed.) Kirk-Othmer

Encyclopedia of Chemical Technology, 4 th edition, Wiley Interscience, Vol.2, 580, **1995**.

[22] Komiyama, T. and Kazuhiro, T. *JP Pat. 54036220*, **1979**.

[23] (a) Watabe, K.; Naganuma, Y.; Tokumoto, S. and Sugyama, E. *JP Pat. 03127761*, **1991** (b) Watabe, K.; Naganuma, Y.; Endo, Y. and Komyama, T. *JP Pat. 03127762*, **1991** (c) Watabe, K.; Naganuma, Y.; Sugyama, E. and Komyama, T. *JP Pat. 03127763*, **1991** (d) Watabe, Y.; Naganuma, Y.; Sugiyama, E. and Komiyama, T. *JP Pat. 03112946*, **1991** (e) Komiyama, T. and Terada, K. *JP Pat. 54036220*, **1979** (f) Bean, F. and Thomas, S. *US Pat. 2376112*, **1945**.

[24] (a) Lawson, D. and Satter, D. *US Pat. 3645864*, **1972** (b) Bean, F. and Donovan, T. *US Pat. 2376112,* **1945** (c) Piguet, A.; Steinbuch, E. and Stocker, R. *US Pat. 1239822*, **1917** (d) Harwood, W. *US Pat. 3338806*, **1967** (e) Winslow, W. and Heise, G. *US Pat. 2427433*, **1947** (f) Levi, M.; Pesheva, I. and Dolapchieva, M. *Electrochimiya 19*, 44, **1983**. (g) Udupa, H. *Indian Chem. Eng. 30*, 53, **1988** (h) Sokolovskii, V.; Belyaev, V. and Snytnikova, G. *React. Kinet. Catal. Lett. 22,* 127, **1983**.

[25] (a) Bamberger, E. *Ber. 27*, 1347, **1894** (b) Bamberger, E. *Ber. 27*, 1548, **1894** (c) Bamberger, E. *Ber. 33*, 3600, **1900**.

[26] (a) Shine, H. Aromatic Rearrangements, Elsevier, Amsterdam, pp 129, **1967** (b) March, J. Advanced Organic Chemistry: Reaction Mechanisms and Structures, Wiley Publications, 4th Edition, pp 674, **1991** (c) Sone, T.; Hamamoto, K.; Seiji, Y., Shinkai, S. and Manabe, O. *J. Chem. Soc. Perkin II*, 298, **1981** (d) Sone, T.; Hamamoto, K.; Seiji, Y.; Shinkai, S. and Manabe, O. *J.Chem. Soc. Perkin II,* 1596, **1981**.

[27] Bassford, H. *US Pat. 2132454*, **1938**.

[28] Bean, F. *US Pat. 2446519*, **1948**.

[29] Vogel, A. A Textbook of Practical Organic Chemistry, 4th edition, ELBS, Longman, London, pp 657, **1978**.

[30] Henke, C. and Vaughen, J. *US Pat. 2198249*, **1940**.

[31] Li, S.; Ximin, Z. and Baoqui, S. *CN Pat. 1087623*, **1992** (b) Shi, L.; Zhou, X. and Shi, B. *CN Pat. 1087623,* **1994**.

[32] Medcalf, E. *US Pat. 4051187*, **1977**.

[33] Juang, T.; Hwang, J., Ho, H. and Chen, C. *J. Chin. Chem. Soc. 35,*135, **1988**.

[34] Greco, N. *US Pat. 3953509*, **1976**.

[35] Spigler, L. and Woodbury, N. *GB Pat.713622*, **1954**.

[36] Spigler, L.and Woodbury, N. *US Pat. 2765342*, **1956**.

[37] Brown, B. and Fredrick, A. *US Pat. 3535382*, **1970**.

[38] Sathe, S. *US Pat. 4176138*, **1979**.

[39] Derrenbacker, E. *US Pat. 4307249*, **1981**.

[40] Lee, L.; Chen, M. and Yao, C. *US pat. 4885389*, **1989**.

[41] Benner, R. *US Pat. 3383416*, **1968**.

[42] Kosak, J. in Kosak, J. (Ed.) Catalytic Organic Reactions, Marcel Dekker, NY **1988**.

[43] (a) Rylander, P.; Karpenko, I. and Pond, G. *US Pat. 3694509*, **1972**. (b) Rylander, P.; Karpenko, I. and Pond, G. *US Pat. 3715397*, **1973**.

[44] (a) Rylander, P. Catalytic Hydrogenation in Organic Synthesis, Academic Press NY, **1979**. (b) Leludec, J. *Fr. Pat. 2186963*, **1975**.

[45] Karwa, S. and Rajadhyaksha, R. *Ind. Eng. Chem. Res*. 26, 1746, **1987**.

[46] Pernoud, L.; Candy, J.; Didillon, B.; Jacquot, R. and Basset, J. *Stud. Surf. Sci. Cat. 130,* 2057, **2000**.

[47] Dunn, T. *US Pat. 4264529*, **1981**.

[48] Caskey, D. and Chapman, D. *US Pat. 4571437*, **1986**.

[49] Gao, Y.; Wang, F.; Liao, S. and Yu, D. *React. Kinet. Catal. Lett. 64*, 351, **1998**.

[50] Ahn, W.; Min, K.; Chung, Y.; Rhee, H.; Joo, S. and Ryoo, R. *Stud. Surf. Sci. Catal.135*, 4710, **2001**.

[51] Dewal, U.; Mhasakar, R.; Joshi, J. and Sawant, S. *Ind. Chem. J.* 29, **1980**.

[52] Zoran, A.; Khodzhaev, O. and Sasson, Y. *Chem. Comm*. 2239, **1994**.

[53] Tamaoki, A.; Yamamoto, K. and Kuroda, K. *JP Pat. 54066632,* **1979**.

[54] Chan, X. and Liu, Y. *CN Pat. 85103667*, **1986**.

[55] Jacquot, R. and Mercier, C. *EP Appl. 536070*, **1993**.

[56] Sidheswaran, P.; Hrishnan, V. and Bhat, A. *Ind. J. Chem. 36*, 149, **1997**

[57] Booth, G. Ullamann's Encyclopedia of Industrial Chemistry, *A17*, VCH, Weinheim, pp 411, **1991**.

[58] (a) Skipka, G.; Alles, H.; Duerholz, F. and Lindner, O. *DE 2930754*, **1981** (b) Shah, J. and Mahajan, S. *Chem. Ind. Dev. Ann*. C19, **1977** (c) Lukashevich, V. *J. Gen. Chem., 7*, 2209, **1937** (d) Lukashevich, V. and Voroshilova, M. *Org. Chem, Ind. 4*, 253, **1937**.

[59] Holtzclaw, C. and Bryan, W. *US Pat. 3177256*, **1965.**

[60] (a) Freifelder, M. and Robinson, R. *US 3079435*, **1963**. (b) Malpani, P. and Chandalia, S. *Ind. Chem. J. 15,* **1973** (c) Fang, Y.; Zhang, W.; Liu, C. and Yang, J. *Xiandai Huagong, 20*, 37, **2000** (d) Zhang, W.; Fang, Y.; Lai, X.. and Cui, Y. *Huaxue Shijie, 41*, 321, **2000.**

[61] Ostrovskii, V.; Bat, I.; Ovichinnikov, P. and Belozerskaya, S. *SU Pat. 1006428*, **1983**.

[62] Masatomo, F.; Tsukamoto, K. and Isobe, K. *JP Pat. 53031632*, **1978**.

[63] (a) Yao, H. and Emmett, P. *J. Amer. Chem. Soc. 81,* 4125, **1959**. (b) Yao, H. and Emmett, P. *J. Amer. Chem. Soc. 83,* 796, **1961**. (c) Yao, H. and Emmett, P. *J. Amer. Chem. Soc. 84,* 1086, **1962**.

[64] Goswami, N.; Rahman, M.; Huque, M. and Qaisuddin, M. *J. Chem. Tech. Biotechnol. 34*, 195, **1984**.

[65] Henke, C. *US Pat. 2183019*, **1939**.

[66] (a) Gu, S. and Yao, K. *Daxue Huaxue 12,* 42, **1997** (b) Ruopp, D. and Thorn, M. *US Pat. 4264526*, **1981**.

[67] Spiegler, L. *US Pat. 2947781*, **1960**.

[68] Mukkanti, K.; Rao, Y. ; Subba, Y. and Choudary, B. *Tetrahedron Lett. 30,* 251, **1989**.

[69] (a) Ruthven, D. Principles of Adsorption and Adsorption Processes, Wiley Interscience, **1984** (b) Tamaru, K. Dynamic Heterogeneous Catalysis, Academic Press, **1978** (c) Hayward, D. and Trapnell, B. Chemisorption, 2nd edition, Butterworth, London, **1964**.

[70] (a) Langmuir, I., *J. Am. Chem. Soc. 37*, 1139, **1915** (b) Langmuir, I., *J. Am. Chem. Soc. 40*, 1361, **1918** (c) Langmuir, I., *Trans. Faraday Soc. 17,* 621, **1921**.

[71] (a) Freundlich, H. Colloid and Capillary Chemistry, London; Methuen, **1926** (b) Satterfield, C. Heterogeneous Catalysis in Industrial Practice, McGraw-Hill International Edn, 2nd Edn, **1993**.

[72] (a) Tamon, H.; Atsushi, M. Okazaki, M. *J. Colloid Interface Sci. 177*, 384 **1996** (b) Homenauth, O. and McBride, M. *Soil Sci. Soc. Am. J. 58*, 347, **1994** (c) Aranovich, G. and Donohue, M., *J. Colloid Interface Sci. 178*, 764, **1996**.

[73] Ardizzone, S.; Hoiland, H.; lagioni, C. and Sivieri, E. *J. Elctroana. Chem. 447*, 17, **1998**.

[74] Rodovic, L.; Silva, I.; Ume, J., Menenedez, C.; Leon, L. and Scaroni, A. *Carbon 37,* 1339, **1997**.

[75] Agrawal, P.; Kapoor, J.; Kapoor, S.; Bhalla, A. and Bansal, R. *Ind. J. Chem. Tech. 3*, 187, **1996**.

[76] Zhou, M.; Martin, G.; Taha, S. and Santanna, F. *Water Res. 32,* 1109, **1998**.

[77] Zhongqi; X. and Xiaohua, L. *Huazhong Ligong Daxue Xuebao 28,* 102, **2000**.

[78] Torrents, A.; Damera, R. and Hao, O. *J. Hazard. Mater. 54,* 141, **1997**.

[79] Al-Baharani, K. and Martin, R. *Water Res. 108*, 731, **1976**.

[80] Miyahara, M and Okazaki, M. *J. Chem. Eng. Jpn. 26*, 510, **1993**.

[81] van Lier, W. Act. Carbon…. Fascinating mater. Edited by: Capelle, A.; De Vooys, F. Norit: Amersfoort, Netherland, 129, **1983** (CA, 102:67820).

[82] Nasuto, R. and Derylo, A. *Pol. J. Chem. 54*, 1089, **1980**.

[83] Vincenzo, A.; Giuseppe, B.; Vito, B. and Lorenzo, L. *Thermochim. Acta. 36*, 107, **1980**.

[84] Cloos, P.; Moreale, A.; Broers, C. and Badot, C. *Clay Miner. 14*, 307, **1989**.

[85] Glushchenko, V. and Khabalov, V. *Zh. Fiz. Khim. 51*, 1414, **1977**.

[86] Avramenko, V.; Glushchenko, V. and Kozlov, S. *Khim. Khim. Tekhnol. 22*, 1246, **1979**.

[87] Goworek, J.; Oscik, J.and Kusak, R. *J. Colloid Interface Sci. 103*, 392, **1985**.

[88] Zhu, L.; Li, Y.; Chen, S.; Liu, W. and Bao, J. *Huanjing Huaxue 16*, 233, **1997**.

[89] Choudhary, V.; Sansare, S. and Thite, G. *J. Chem. Tech. Biotech.* 42, 249, **1988**.

[90] (a) Cusumano, J.; Dembinski, G. and Sinfelt, J. *J.Catal. 5,* 471, **1966** (b) Spendel, L. and Boudart, M. *J. Phys. Chem. 64,* 204, **1960** (c) Alder, S. and Kravney, J. *J. Phy. Chem. 64*, 208, **1960** (d) Gruber, H. *J. Phy. Chem. 66,* 48, **1963** (e) Kramer, R. and Andre, M. *J. Catal. 58*, 287, **1979**.

[91] Satoh, N.; Hayashi, J. and Hattori, H. *Appl. Catal. A, 202*, 207 **2000**.

[92] Chen, S.; Smith, J. and McCoy, B. *J. Catal. 102,* 365, **1986**.

[93] Ahn B., Smith J.and McCoy B. *AIChE. J. 32*, 4, 566, **1986.**

[94] Chen, S.; Smith, J. and McCoy, B. *Chem. Eng. Sci. 42*, 293, **1987**.

[95] Zakumbaeva, G. and Urumbaeva, S. *React. Kinet. Catal. Lett. 8,* 333, **1978**.

[96] Zakumbaeva, G.; Omashev, K. and Khan, C. *React. Kinet. Catal. Lett. 6,* 363, **1977**.

[97] Sun, Y.; Li, Y.; Songying, C. and Peng, S. *React. Kinet. Catal. Lett. 6*, 233, **1977**.

[98] Zakumbaeva, G.; Zararnia, N. and Kuidina, V. *Electrochimiya, 15,* 1144, **1979**.

[99] Zakumbaeva, G. *Geterog. Katal. 4th,* Pt., 1, 241, **1979**.

[100] Naidin, V.; Zakumbaeva, G. and Sokol'skii, D. *Zh. Fiz. Khim. 51*, 183, **1977.**

* * * * *

Chapter Two

Catalysis and Kinetics of Hydrogenation of Nitrobenzene to *p*-Aminophenol

2.1 Introduction

The catalytic hydrogenation of nitrobenzene using transition metal catalysts is an important example of the industrial process, which provides a cleaner alternative to the conventional reduction process for the synthesis of *p*-aminophenol and aniline. Currently, Mallinckrodt Inc. is operating a process for the synthesis of *p*-aminophenol by catalytic hydrogenation of nitrobenzene using a heterogeneous supported platinum catalyst in a four phase catalytic system [1]. As per the literature review given in Chapter I, most of the information on this reaction is patented and there are only a few published reports dealing with the fundamental aspects such as catalysis and reaction kinetics. Being a multiphase catalytic reaction, a systematic study of the effect of reaction and physicochemical parameters on the rate behavior and selectivity is most essential to optimize the process performance and generate knowledge base useful in the design and scale-up of reactors.

Several transition metal catalysts e.g. palladium, platinum, rhodium, molybdenum etc. have been reported in the prior literature for the hydrogenation of nitrobenzene to *p*-aminophenol [1-3]. Among these, platinum catalysts have been reported to exhibit considerably higher activity/selectivity and stability compared to others [3]. This reaction involves four phases: solid (catalyst), gas (hydrogen) and two immiscible liquid phases (aqueous sulfuric acid and nitrobenzene). The overall performance of such a multiphase catalytic reaction may depend on various engineering factors such as gas to liquid mass transfer, liquid-liquid mass transfer, liquid-solid mass transfer, intraparticle diffusion and intrinsic reaction kinetics etc. Thus, to analyze such a multiphase catalytic reaction from the reaction-engineering

point of view, it is important to understand the rate behavior and intrinsic kinetics of this reaction.

The first objective of this work was to investigate the effect of various reaction conditions on the activity / selectivity behavior of catalytic hydrogenation of nitrobenzene to *p*-aminophenol using supported metal catalysts. The second objective was to investigate the kinetics of this reaction and develop rate equations, which can be useful for the design purpose.

2.2 Experimental

2.2.1 Materials

Nitrobenzene, aniline and sulphuric acid (98%) was procured from SD Fine Chemicals Ltd. (India). 3%Pt/C and *p*-aminophenol were procured from Aldrich Chemicals (USA). 3% Rh/C catalyst was obtained from Degussa, Germany. HPLC grade acetonitrile and water were purchased from Merck Chemicals (India). Hydrogen gas (>99% purity) was purchased from Inox Gas Co. (India). Other supported metal catalysts like Ni/C [4], Pd/C [5], Ru/C [6], Pt/SiO_2 [7], Pt/Al_2O_3 [8] and bimetallic supported Ni-Pt [9] were prepared by literature methods.

The intermediate phenylhydroxylamine was synthesized by a literature procedure [10]. Typically, a mixture of ammonium chloride (5 gm), nitrobenzene (10 gm) and distilled water (160 ml) was stirred vigorously in a 250 ml capacity round bottom flask by means of a magnetic stirrer. To this mixture, zinc dust (12.4 gm) was added over a period of 15-20 minutes at room temperature. As the reduction progressed, the temperature of the reaction content increased to 60-65^{o}C. After all the zinc dust was added, stirring was continued for fifteen minutes After 15-20

minutes, the temperature of the mixture ceased to increase indicating that the reaction was complete. While still hot, the solution was filtered under suction in order to remove the zinc oxide. The oxide residue was washed with 20 ml of hot water. The filtrate was added to a saturated sodium chloride solution and then cooled to 0°C. The phenylhydroxylamine, which crystallized out as light yellow needles, was filtered and dried under suction. The yield of crude phenylhydroxylamine was 6 gm (65% yield). The melting point of purified phenylhydroxylamine was 80°C (literature reported = 80-81°C). Since, phenylhydroxylamine deteriorated on storage, it was always freshly prepared for use as a standard for HPLC analysis.

2.2.2 Experimental set-up

The hydrogenation experiments were carried out in a 300-cm^3 capacity high-pressure hastelloy (C-276) autoclave supplied by Parr Instruments Co., USA. The schematic of the reactor set-up is shown in Figure 2-1. The reactor was fitted with an internal cooling coil and a magnetically driven impeller with four-blade stirrer capable of operations upto 1500 rpm. The temperature of the liquid in the reactor was maintained at a desired level (with a precision of ± 1K) with the help of a PID controller, which provided alternate heating and cooling arrangement. The reactor was also equipped with an internal thermocouple and a digital pressure transducer (with a precision of ± 1 psig) for temperature and pressure monitoring, respectively. The relevant safety features like rupture disc and high temperature-pressure cut-off were also installed as a part of the reactor set-up.

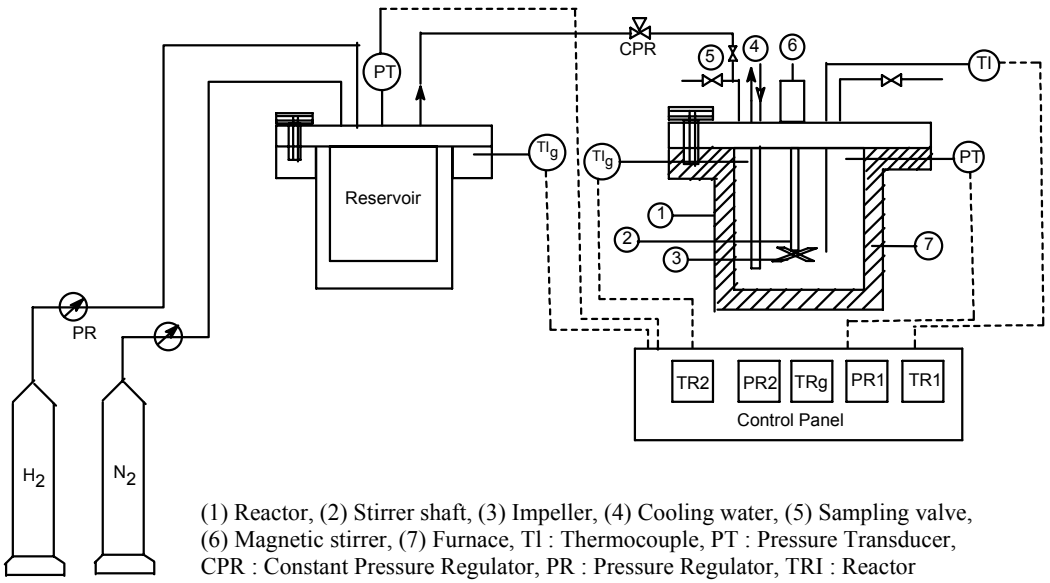

(1) Reactor, (2) Stirrer shaft, (3) Impeller, (4) Cooling water, (5) Sampling valve, (6) Magnetic stirrer, (7) Furnace, Tl : Thermocouple, PT : Pressure Transducer, CPR : Constant Pressure Regulator, PR : Pressure Regulator, TRI : Reactor Temperature Indicator, TRG : Gas Temperature Indicator, PRI : Reactor Pressure Indicator, PR2 : Reservior Pressure Indicator, TR2 : Reservior Temperature Indicator.

Figure 2-1: Schematic of the reactor set-up used for hydrogenation reactions

2.2.3 Analytical method

The reaction mixtures were analyzed for nitrobenzene, aniline, phenylhydroxylamine and *p*-aminophenol content using high performance liquid chromatography (HPLC). A Hewlett-Packard model 1050 liquid chromatograph equipped with the ultraviolet detector was employed. The analysis conditions were: column: lichrospher RP- 18 (250 × 4 mm); mobile phase: acetonitrile-water (30:70 v/v); flow rate: 0.8 ml/min; temp: 298 K, λ= 254 nm. A typical HPLC chart of reaction product mixture is shown in Figure 2-2.

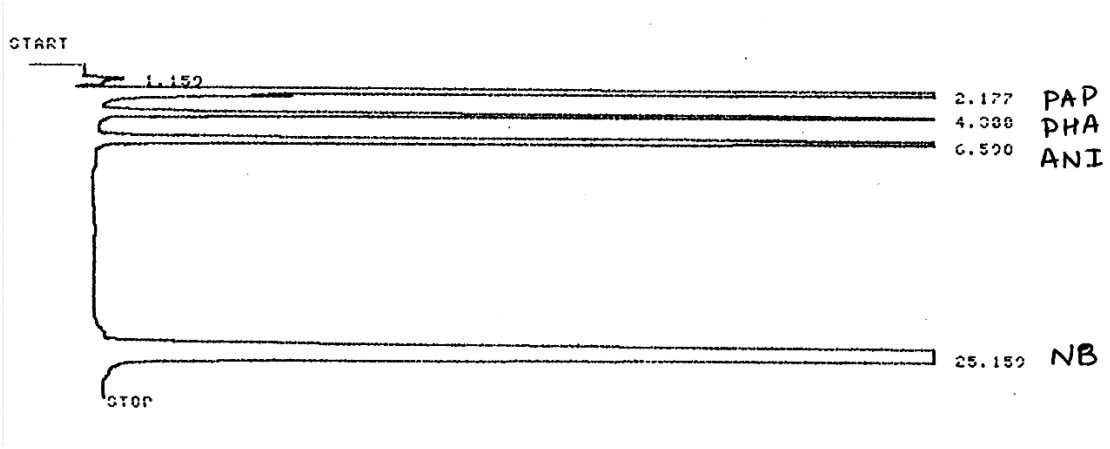

Figure 2-2: Typical HPLC chromatogram of reaction mixture
(PAP: *p*-aminophenol; PHA: phenylhydroxylamine; ANI: aniline and NB: nitrobenzne)

2.2.4 Experimental procedure

In a typical hydrogenation experiment, the autoclave was charged with nitrobenzene (23 gm, 1.869×10^{-4} kmol); 3% Pt/C (3.5×10^{-5} kg); 98 % sulfuric acid (6 ml) and water (67ml). The autoclave was then closed and the contents were first flushed with nitrogen and then with hydrogen for the removal of any dissolved air and oxygen. The reactor was then heated to a desired temperature under slow stirring. After the desired temperature was attained, hydrogen was introduced in the reactor and the stirring speed increased to 700 rpm. The reaction was continued at a constant pressure by supplying hydrogen from a reservoir vessel using a constant pressure regulator. The pressure drop in the reservoir vessel was measured as a function of time using a digital pressure transducer. After completion of the reaction, the reactor was cooled to room temperature and unreacted gas was vented off. The solid product mixture was diluted with distilled water and filtered to separate the

catalyst. To recover the *p*-aminophenol from the product mixture, the filtrate was treated with ammonia solution to neutralize the acid and to separate *p*-aminophenol. The solid obtained was filtered and washed with toluene, vacuum dried and weighed. The filtrate was extracted with toluene to separate aniline and unreacted nitrobenzene, if any. The aqueous and organic layers were analyzed for nitrobenzene, aniline, *p*-aminophenol and any other byproduct.

2.3 Results and Discussion

The catalytic hydrogenation of nitrobenzene to *p*-aminophenol is a two-step reaction. In the first step, nitrobenzene is hydrogenated to phenylhydroxylamine, which then undergoes a Bamberger rearrangement to *p*-aminophenol. Formation of aniline by further hydrogenation of phenylhydroxylamine is a major side reaction (Scheme 2-1). Thus, for the optimum yield of *p*-aminophenol, it is essential to achieve maximum yield of phenylhydroxylamine in the first step for rearrangement to *p*-aminophenol rather than further hydrogenation to aniline in the second step.

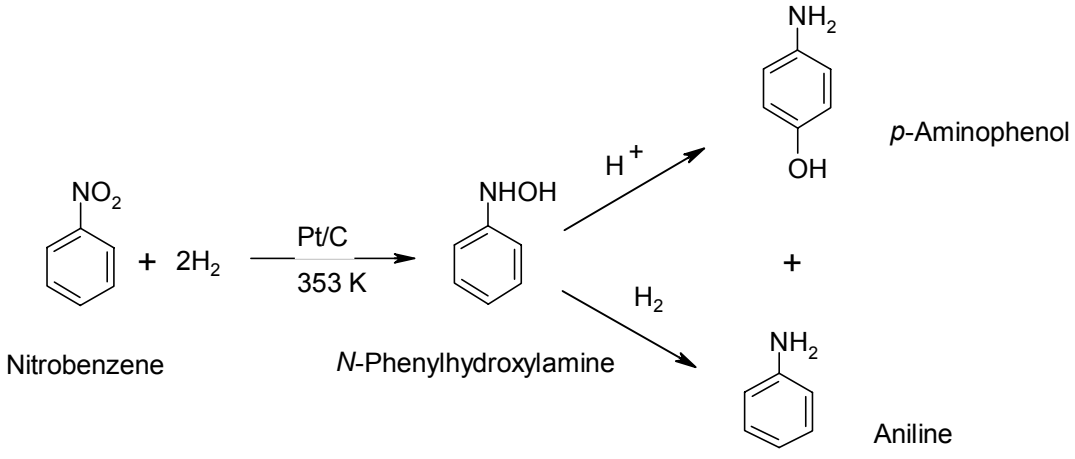

Scheme 2-1: Catalytic hydrogenation of nitrobenzene to *p*-aminophenol

In order to investigate the catalytic activity and selectivity of different catalysts and to understand the effect of various reaction parameters, several experiments were carried out at different initial conditions. The range of parameters varied for the study is given in Table 2-1. All reactions were carried out to complete conversion of nitrobenzene except those for kinetic studies. The reactions were followed by the hydrogen consumption-time data. In each experiment, a final reaction sample was also analyzed by HPLC to calculate the conversion of nitrobenzene and selectivity to *p*-aminophenol and aniline. The experimental results were expressed in terms of average catalytic activity and selectivity. The average catalytic activity (*N)* expressed as kmol/kg.hr, was defined as the amount of nitrobenzene consumed per unit weight of the catalyst per hour based on the time required to achieve more than 99% conversion of nitrobenzene. In a few initial experiments, the amount of hydrogen consumed was compared with the amount of *p*-aminophenol and aniline obtained to ascertain the material balance.

Table 2-1: Range of operating conditions

Parameter	***Range***
Catalyst loading, kg	$1.75 \times 10^{-5} – 7.0 \times 10^{-5}$
Nitrobenzene, kmol	0.934×10^{-4} - 3.74×10^{-4}
Hydrogen pressure, MPa	*0.68 - 6.80*
Sulfuric acid (98 %), ml	*3 - 12*
Temperature, K	*323 - 373*
Speed of agitation, rpm	*300 - 1000*

2.3.1 Catalyst screening experiments

The activity of various transition metal catalysts, consisting of supported Pt, Pd, Rh, Ru, Ni and Ni-Pt, Ni-Pd bimetallic compositions, for hydrogenation of nitrobenzene to *p*-aminophenol was investigated at 353 K and 2.72 MPa of hydrogen pressure and the results are presented in Table 2-2. The highest catalytic activity was observed for 3%Pt/C catalyst whereas 3 % Ru/C was almost inactive for this reaction (< 4% conversion of nitrobenzene in 6 hours). The 3% Pd/C catalyst favored aniline formation. The observed trend for the selectivity to *p*-aminophenol using different transition metal catalysts was similar to those reported previously by Juang et al. [3] who explained the highest activity of Pt catalysts on the basis of Chen's hypothesis [11], which suggested that, the affinity of oxygen atom for the catalyst plays an important role in selecting the pathway for catalytic hydrogenation of 2-hydroxycyclohexanone, catechol and 5-keto-*d*-gluconate. By the same reasoning Juang et al. [3] suggested that the affinity of oxygen atom of phenylhydroxylamine molecule for the catalyst could influence the catalytic reaction mechanism. Accordingly, if the oxygen atom has a lower affinity for the catalyst, more *p*-aminophenol is produced due to the greater tendency of phenylhydroxylamine to dissociate from the catalyst surface. Subsequently, a catalyst such as Pd with higher oxygen affinity favored formation of aniline over *p*-aminophenol because the intermediate phenylhydroxylamine remains attached to the catalyst surface long enough and results in further hydrogenation to aniline rather than being released into the solution and being rearranged to *p*-aminophenol [3]. Similarly, in case of Ru, the strong interaction between Ru and oxygen results in poisoning of the catalyst thereby retarding the hydrogenation of nitrobenzene. The effect of support on the catalytic activity of platinum catalysts was also investigated. Several platinum

metal catalysts on different supports were prepared and screened for their activity and selectivity in the hydrogenation of nitrobenzene to *p*-aminophenol (entry 1, 6 and 7; Table 2-2). The highest catalytic activity was observed for carbon supported Pt catalyst whereas the selectivity was nearly independent of the support nature.

Table 2-2: Effect of transition metal catalysts on the hydrogenation of nitrobenzene to *p*-aminophenol (PAP)

Entry	***Catalyst***	***Time***	***Conv.***	***Selectivity (%)***		***Activity, N***
		(min.)	***(%)***	***PAP***	***Aniline***	***(kmol/kg.hr)***
1	*3 % Pt/C*	*65*	*100*	*58*	*42*	*4.907*
2	*3 % Pd/C*	*110*	*100*	*24*	*76*	*2.899*
3	*3 % Rh/C*	*201*	*100*	*20*	*80*	*1.594*
4	*3 % Ru/C*	*300*	*4*	*0*	*100*	-
5	*3 % Ni/C*	*360*	*36*	*13*	*87*	*0.320*
6	*3 % Pt/SiO_2*	*70*	*100*	*57*	*43*	*4.557*
7	*3 % Pt/ Al_2O_3*	*88*	*100*	*60*	*40*	*3.625*
8	*10 % Ni/C*	*90*	*28*	*14*	*86*	*0.996*
9	*10 % Ni/SiO_2*	*90*	*32*	*11*	*89*	*1.103*
10	*10 % Ni/ZSM-5*	*90*	*45*	*45*	*55*	*1.602*
11	*10 % Ni-0.05 % Pt/ZSM-5*	*90*	*49*	*11*	*89*	*1.745*
12	*10 % Ni-0.1 % Pt/ZSM-5*	*90*	*42*	*25*	*75*	*1.495*
13	*10 % Ni-1 % Pt/ZSM-5*	*90*	*93*	*63*	*36*	*3.310*
14	*10 % Ni-1 % Pd/ZSM-5*	*90*	*30*	*20*	*79*	*1.068*

Reaction conditions: *Nitrobenzene: 1.869×10^{-4} kmol; catalyst: 3.5×10^{-5} kg; water: 67 ml; sulfuric acid (98%): 6ml; temperature: 353 K; H_2 pressure: 2.72 MPa; agitation: 700 rpm.*

It is interesting to note that the Ni catalysts were also active for this reaction, although their activity and selectivity was lower than the Pt catalyst. This is the first report on the nickel catalyzed hydrogenation of nitrobenzene to *p*-aminophenol. Since the nickel catalysts would be attractive from a commercial point of view due to

their low cost compared to platinum and palladium, few other Ni containing catalysts were also investigated for this reaction (Entry 8-14; Table 2-2). It was observed that 10% Ni/ZSM-5 had highest catalytic activity (1.602 kmol/kg.hr) and selectivity to *p*-aminophenol (45%) among the screened heterogeneous nickel catalysts. The activity of nickel catalysts could be further improved by addition of a second metal such as Pd or Pt (Entry 11-14; Table 2-2). Finally, the effect of Pt content on hydrogenation activity as well as selectivity to *p*-aminophenol was also investigated and the results are presented in Figure 2-3. The catalyst activity increased with increase in Pt content of catalyst. On the other hand, selectivity to *p*-aminophenol was maximum at 3% metal loading and lower on either decreasing or increasing the Pt content.

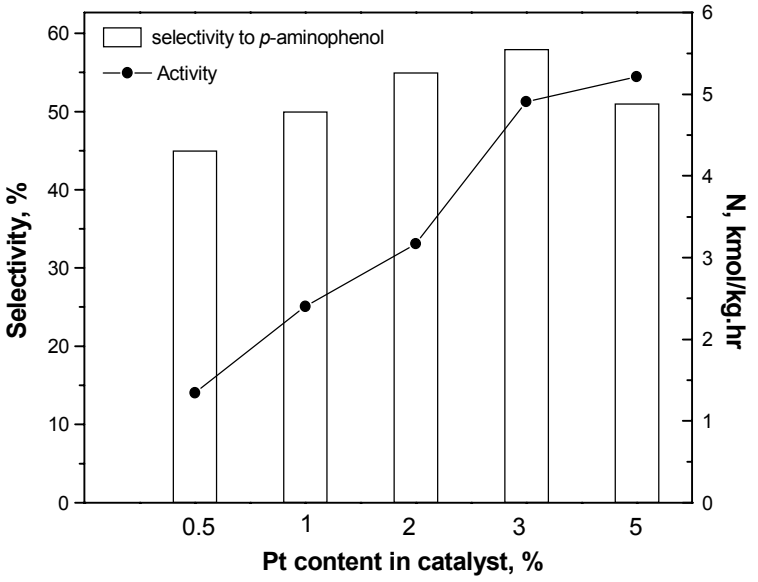

Figure 2-3: Effect of platinum content of catalyst on the catalytic activity and selectivity to *p*-aminophenol

Reaction conditions: *Nitrobenzene: 1.869×10^{-4} kmol; 3 % Pt/C: 3.5×10^{-5} kg; water: 67 ml; sulfuric acid (98%): 6 ml; temperature: 353K; H_2 pressure: 2.72 MPa; agitation: 700 rpm.*

2.3.2 Pt/C catalyst: Effect of reaction conditions

Since, the highest catalytic activity and selectivity to *p*-aminophenol was obtained for 3% Pt/C catalyst, further experiments were carried out using this catalyst to investigate the effect of various reaction parameters such as initial nitrobenzene loading, hydrogen pressure, sulfuric acid charged, temperature and speed of agitation on the catalyst activity and selectivity to *p*-aminophenol.

The effect of initial nitrobenzene charge on the initial hydrogenation rate, average catalytic activity and selectivity was investigated in the range of 0.548×10^{-4} to 3.74×10^{-4} kmol at 353 K and the results are presented in Table 2-3. The selectivity to *p*-aminophenol was found to remain almost constant (70.9 %) upto 0.934×10^{-4} kmol of nitrobenzene, beyond which it decreased drastically with increase in nitrobenzene charge (42 % at 3.74×10^{-4} kmol). The initial rate of hydrogenation was almost independent of nitrobenzene charge. It is important to note here that, as nitrobenzene is present as a separate immiscible phase and the products: aniline, *p*-aminophenol and phenylhydroxylamine, are instantaneously extracted in the aqueous sulfuric acid phase, the concentration of nitrobenzene in the organic phase remains nearly constant even with a change in the charge. Hence, the initial rate of hydrogenation remains independent of nitrobenzene charge. Another important issue here is, with increase in time and conversion of nitrobenzene, volume of organic phase decreases and hence the catalyst (which is essentially present in the organic phase as per visual observation) loading in the organic phase increases. This leads to a compensation effect on the rate of hydrogenation with change in time, hence, a nearly constant rate of hydrogenation is observed over most of the time duration.

Table 2-3: Effect of nitrobenzene loading on catalytic activity and selectivity to *p*-aminophenol.

***Nitrobenzene* × 10⁴**	**$R_A \times 10^3$**	***Selectivity (%)***		***N***
(kmol)	***(kmol/m³.s)***	***p-Aminophenol***	***Aniline***	***(kmol/kg.hr)***
0.548	*2.00*	*70.90*	*29.1*	*2.289*
0.934	*2.01*	*70.66*	*29.34*	*2.671*
1.869	*2.11*	*58.00*	*42.00*	*4.907*
3.252	*2.12*	*42.19*	*57.81*	*10.685*

Reaction conditions: *3% Pt/C: 3.5 × 10⁻⁵ kg; sulfuric acid (98%): 6 ml; temperature: 353 K; H_2 pressure: 2.72 MPa; agitation: 700 rpm.*

The effect of hydrogen partial pressure on the catalytic activity and selectivity was studied in the range of 0.68 - 6.80 MPa at 353 K, and the results are given in Table 2-4. The average catalytic activity increased with increase in hydrogen pressure. The maximum selectivity for *p*-aminophenol was observed at 2.72 MPa, which decreased on either increasing or lowering the hydrogen pressure. At higher hydrogen partial pressures, the selectivity to *p*-aminophenol decreased probably because the excess hydrogen concentration promotes the hydrogenation of phenylhydroxylamine to aniline.

Table 2-4: Effect of hydrogen pressure on catalytic activity and selectivity to *p*-aminophenol.

H_2 pressure	***Selectivity (%)***		***N***
(MPa)	***p-Aminophenol***	***Aniline***	***(kmol/kg.hr)***
0.68	*41.93*	*58.10*	*1.099*
2.72	*58.00*	*42.00*	*4.907*
4.76	*39.03*	*60.97*	*5.593*
6.80	*40.23*	*59.77*	*6.379*

Reaction conditions: *Nitrobenzene: 1.869 × 10⁻⁴ kmol; 3 % Pt/C: 3.5 ×10⁻⁵ kg; water: 67 ml; sulfuric acid (98%): 6 ml; temperature: 353 K; agitation: 700 rpm.*

The Bamberger rearrangement of the intermediate phenylhydroxylamine is a key step during the hydrogenation of nitrobenzene to *p*-aminophenol. Therefore, the effect of sulfuric acid (98%) amount was also investigated in a range of 3 - 12 ml keeping other reaction conditions constant. The average catalytic activity was found to decrease with increase in the amount of acid added (Figure 2-4). The selectivity to *p*-aminophenol increased with increase in acid concentration upto 6 ml, beyond which it remained almost constant. This may be due to the fact that the mobility of hydrogen ions is more at lower concentration [12]. The almost constant selectivity to *p*-aminophenol obtained at even higher acid concentrations may be due to the limiting availability of phenylhydroxylamine for rearrangement.

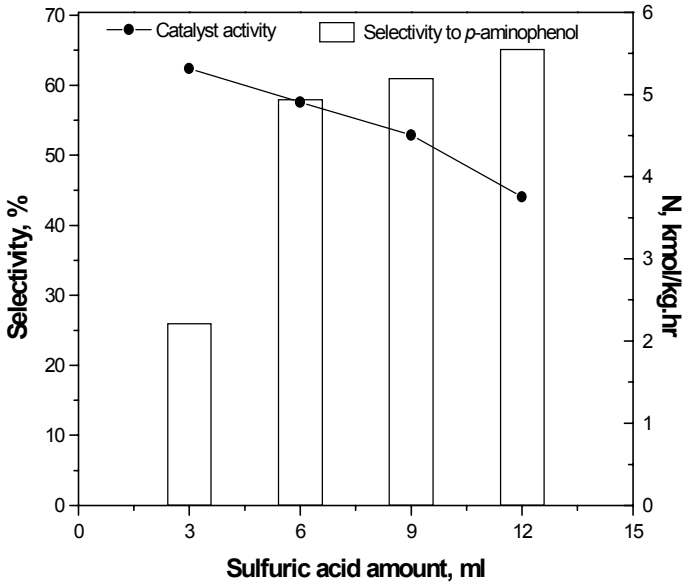

Figure 2-4: Effect of sulfuric acid amount on catalytic activity and selectivity to *p*-aminophenol.
Reaction conditions: *Nitrobenzene: 1.869×10^{-4} kmol; 3 % Pt/C: 3.5×10^{-5} kg; water: 67 ml; H_2 pressure: 2.72 MPa; temperature: 353 K; agitation: 700 rpm.*

The effect of speed of agitation on the catalyst activity and selectivity to *p*-aminophenol was also investigated in the range of 300 to 1000 rpm at 353 K and at hydrogen pressure of 2.72 MPa (Figure 2-5). The selectivity of *p*-aminophenol increased with increase in speed of agitation indicating that the phase transfer catalysis may be an important aspect, since the present system involves two immiscible liquids, nitrobenzene and water. The intermediate phenylhydroxylamine requires transfer to the aqueous layer by liquid-liquid mass transfer before its rearrangement. The catalyst activity was found to increase with increase in speed of agitation.

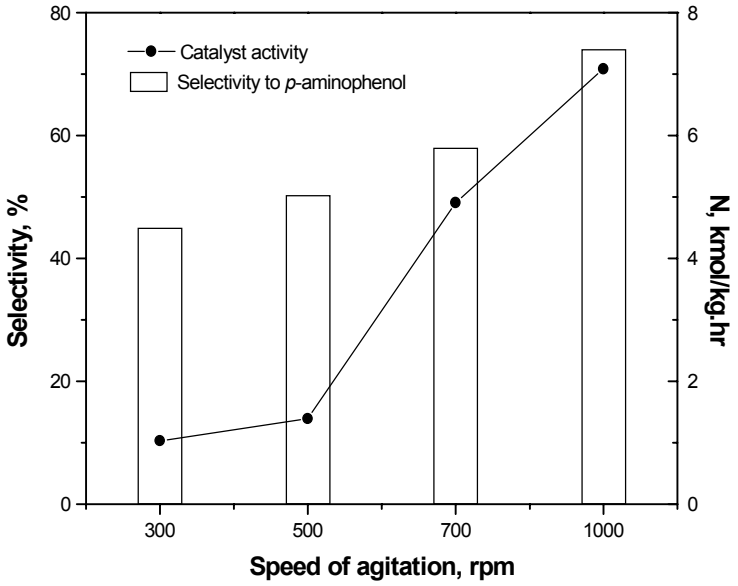

Figure 2-5: Effect of speed of agitation on the catalytic activity and selectivity to *p*-aminophenol at 353 K.
Reaction conditions: *Nitrobenzene: 1.86 × 10^{-4} kmol; 3% Pt/C: 3.5 × 10^{-5} kg; water: 67 ml; sulfuric acid (98%): 6 ml; temperature: 353 K; H_2 pressure: 2.72 MPa.*

The effect of temperature on the average catalytic activity and selectivity was investigated in the temperature range of 323-373 K at 2.72 MPa hydrogen pressure and the results are given in Table 2-5. The results indicate that the average catalytic

activity increased with temperature. The selectivity to *p*-aminophenol also increased with temperature from 40 % at 323 K to 58 % at 353K, and remained constant with further increase in temperature from 353 to 373 K.

Table 2-5: Effect of temperature on catalytic activity and selectivity to *p*-aminophenol

Temperature	***Selectivity (%)***		***N***
(K)	***p-Aminophenol***	***Aniline***	***(kmol/kg.hr)***
323	*39.21*	*60.79*	*1.491*
353	*58.00*	*42.00*	*4.907*
373	*59.10*	*40.90*	*9.165*

Reaction conditions: *Nitrobenzene: 1.86× 10^{-4} kmol; 3% Pt/C: 3.5× 10^{-5} kg; water: 67 ml; sulfuric acid (98 %): 6 ml; H_2 pressure: 2.72 MPa; agitation: 700 rpm.*

The reusability of 3% Pt/C catalyst was investigated by using the same catalyst for successive runs of hydrogenation of nitrobenzene to *p*-aminophenol. In these experiments, the reactor was cooled to 313 K, so that the reaction crude remained as a homogeneous mixture. The catalyst was allowed to settle down and supernant solution was taken out from the reactor. The reactor was then charged with fresh nitrobenzene and aqueous acid to carry out the recycle experiment. The catalyst recycle experiments were performed at 353 K and a hydrogen partial pressure of 2.72 MPa with 6 ml of 98% sulphuric acid (Figure 2-6). The catalyst was found to retain its activity even after four recycles without affecting the conversion of nitrobenzene, however, selectivity for *p*-aminophenol decreased by about 5-7%. This lowering of selectivity could be due to the formation of amine compounds in the reaction that may act as a poison [12]. The overall cumulative turn over number (TON) for the catalyst was found to be 1.38×10^5.

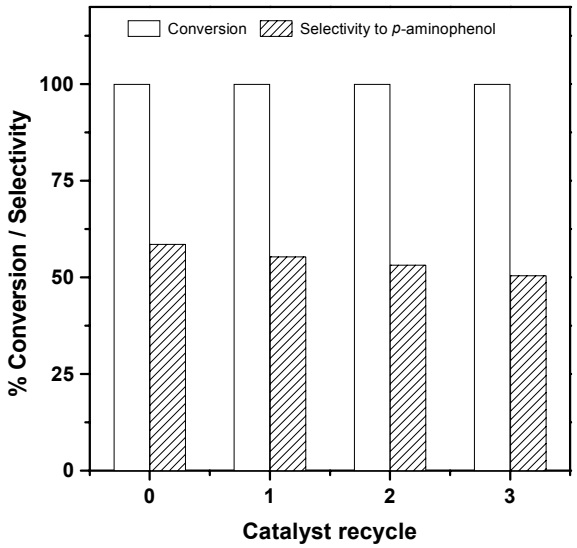

Figure 2-6: Catalyst recycle experiments.
Reaction conditions: *Nitrobenzene: 1.86 × 10^{-4} kmol; sulfuric acid (98%): 6ml; water: 67ml; temperature: 353K; H_2 pressure: 2.72 MPa; agitation: 700 rpm.*

2.3.3 Use of solid acids for Bamberger rearrangement

The rearrangement of phenylhydroxylamine to *p*-aminophenol (Bamberger rearrangement) is catalyzed by acid. A wide variety of acids have been reported in literature for this rearrangement but sulfuric acid is most effective acid [13]. Use of other acids such as hydrochloric acid or phosphoric acid resulted in poor yields of *p*-aminophenol (less than 7%) as compared to that obtained using sulfuric acid (57%)[13]. The main drawback of using strong mineral acid like sulfuric acid is the corrosion of the reactor material. Also, in large-scale production of bulk chemicals, neutralization and disposal of acid are economically and environmentally not desirable. The regeneration of the spent acid is expensive. In order to overcome the problems associated with the use of strong mineral acids, it would be attractive to explore the use of environmentally acceptable acid resources such as solid acids for this reaction. With such solid acid catalysts, corrosion problem can be eliminated and also separation and recycling of acid is easier. Regeneration of the solid acid

catalysts could be achieved by simple thermal/chemical treatments. In view of this, the efficiency of various solid acids such as ion exchange resin, acidic clay (montmorillonite), acid treated SiO_2 and acidic zeolites was investigated instead of sulfuric acid for the rearrangement of phenylhydroxylamine to *p*-aminophenol. The results presented in Table 2-6 indicate that cation exchange resins can efficiently catalyze the rearrangement of phenylhydroxylamine to *p*-aminophenol. In particular, the sulfonated polystyrene polymer (Indion 130) gave highest activity among the various solid acids used. The recyclability of cation exchange resin was also studied by using the same resin after recovery, with and without acid treatment for the successive runs. It was observed that the used resins had to be acid treated (to regenerate the acid site) for better reusability of the resin.

Table 2-6: Effect of solid acids on the selectivity to *p*-aminophenol by catalytic hydrogenation of nitrobenzene.

Solid acid	***pH***	***Selectivity (%)***		***N***
		p-Aminophenol	***Aniline***	***(kmol/kg.hr)***
Indion-130	*5.25*	*21*	*79*	*2.78*
Indion-130 (reused with acid treatment)	*5.32*	*20*	*80*	*2.66*
Indion-130 (reused without acid treatment)	*6.75*	*16*	*84*	*2.56*
Ion exchanged montmorillonite	*5.62*	*21*	*78*	*1.83*
Acid treated silica	*5.29*	*19*	*81*	*4.00*
Al_2O_3	*6.79*	*16*	*84*	*4.00*
Zeolite H-Y	*6.50*	*15*	*85*	*4.00*
β-Zeolite	*6.60*	*12*	*88*	*2.56*

Reaction conditions: *Nitrobenzene: 1.869×10^{-4} kmol; 3 5 Pt/C: 3.5×10^{-5} kg; water: 67 ml; solid acid: 6×10^{-3} kg; temperature: 353K; H_2 pressure: 2.72 MPa; agitation: 700 rpm.*

Though, the current level of selectivity obtained for *p*-aminophenol with solid acid catalysts are lower than sulfuric acid, they eliminate the corrosion problems. For a large aniline plant, the strategy of producing *p*-aminophenol as a co-product may provide an attractive process.

2.3.4 Kinetic studies

The catalytic hydrogenation of nitrobenzene to *p*-aminophenol involves initial reduction of nitrobenzene to intermediate phenylhydroxylamine, which undergoes *insitu* rearrangement to *p*-aminophenol in the presence of an acid. Formation of aniline via further hydrogenation of phenylhydroxylamine is the main competing side reaction. Thus, the catalytic conversion of nitrobenzene to *p*-aminophenol is an example of a multiphase (gas-liquid-liquid-solid) reaction system. The overall hydrogenation rate in this case may be influenced by transport effects such as gas-liquid, liquid-liquid and liquid-solid mass transfer. The complex hydrodynamics, distribution of catalyst in organic/aqueous phases and liquid-liquid dispersion would also affect the overall rate of such reactions.

In order to study the intrinsic kinetics of hydrogenation of nitrobenzene to *p*-aminophenol, a few initial hydrogenation experiments were carried out using 3% Pt/C catalyst. The main reaction products were *p*-aminophenol and aniline with 45-75 % selectivity to *p*-aminophenol depending on the reaction conditions. The presence of phenylhydroxylamine was not detected during analysis, indicating that it had only transient lifetime probably because the rearrangement of phenylhydroxylamine to *p*-aminophenol was an instantaneous reaction in the aqueous phase. The material balance of reactants and products, based on the amount of nitrobenzene and hydrogen consumed and amount of *p*-aminophenol and aniline formed were in agreement to the extent of 95-98% as per the reaction stoichiometry shown in Scheme 2-1. No hydrogenation was observed in the absence of a catalyst indicating the absence of any homogeneous side reactions. For kinetic study, experiments were carried out under differential, (<15 % conversion) as well as

integral conditions in which hydrogen consumption, concentration of *p*-aminophenol, aniline and nitrobenzene were measured.

2.3.4.1 Analysis of initial rate data

Analysis of the initial rate data is useful in understanding of the dependency of reaction rates on the individual parameters and also in the evaluation of significance of mass transfers effects. In each experiment for the kinetic study, the concentrations of aniline, *p*-aminophenol and nitrobenzene were determined after approximately 10-15% conversion of nitrobenzene (evaluated from the hydrogen consumption profiles as a function of time). The initial rates of formation of aniline (r_1) and *p*-aminophenol (r_2) and hydrogen consumption were calculated from the experiments carried out for low conversion level (less than 15% of nitrobenzene) at different sets of initial conditions. These results are given in Table 2-7.

It was visually observed that the catalyst remained in the organic phase (nitrobenzene) suggesting that the hydrogenation reaction takes place in the organic phase. Hence, the rate of reaction was expressed as kmol/ m^3 (organic phase)/ s and catalyst loading was expressed as kg/m^3 (organic phase). The effect of catalyst loading and hydrogen pressure on the initial rates was studied over a temperature range of 323 – 338 K.

Table 2-7: Initial rate data for hydrogenation of nitrobenzene to *p*-aminophenol and aniline

Temperature (K)	***H_2 Pressure (MPa)***	***3 % Pt/C (kg/m^3)***	***$r_1 \times 10^3$ ($kmol/m^3.s$)***	***$r_2 \times 10^3$ ($kmol/m^3.s$)***
323	*0.68*	*1.5*	*0.07*	*0.48*
	2.72	*1.5*	*0.29*	*1.46*
	4.76	*1.5*	*0.52*	*2.06*
	6.80	*1.5*	*0.69*	*2.46*
	2.72	*0.5*	*0.09*	*0.48*
	2.72	*1.0*	*0.19*	*0.97*
338	*0.68*	*1.5*	*0.15*	*0.92*
	2.72	*1.5*	*0.62*	*2.45*
	4.76	*1.5*	*1.10*	*3.21*
	6.80	*1.5*	*1.57*	*3.66*
	2.72	*0.5*	*0.20*	*0.87*
	2.72	*1.0*	*0.41*	*1.63*
353	*0.68*	*1.5*	*0.28*	*1.13*
	2.72	*1.5*	*1.08*	*2.53*
	4.76	*1.5*	*1.83*	*3.16*
	6.80	*1.5*	*2.69*	*3.27*
	2.72	*0.5*	*0.33*	*0.85*
	2.72	*1.0*	*0.71*	*1.69*

Note : r_1 and r_2 are expressed as kmol/m^3 (organic phase).s

In order to determine the significance of gas-liquid mass transfer resistance, the effect of agitation frequency on the rate of hydrogenation was studied in the range of 400-1000 rpm at 353 K. The initial hydrogenation rates were determined from the hydrogen consumption-time data. The results shown in Figure 2-7 indicate that the hydrogenation rate was independent of agitation frequency above 700 rpm at lower catalyst loading (1.5 kg/m^3), whereas for higher catalyst loading (3.5 kg/m^3) the rate of reaction was found to increase with increase in the speed of agitation. These results suggest that the data at lower catalyst loading (1.5 kg/m^3) were in the kinetic regime and therefore, further experiments were carried out at catalyst loadings in a range of 0.5-1.5 kg/m^3.

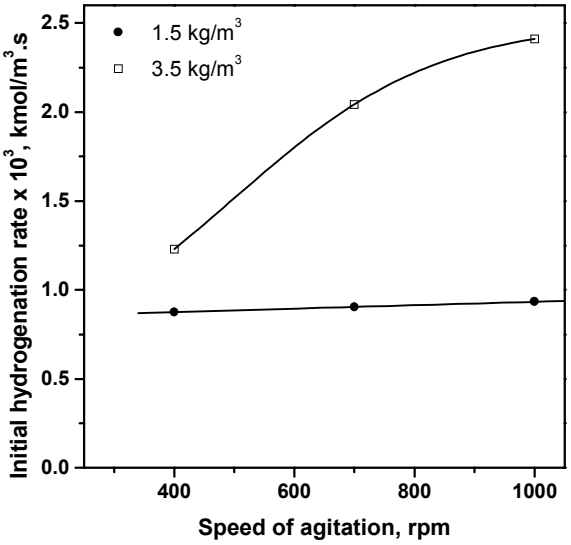

Figure 2-7: Effect of speed of agitation on initial rate of hydrogenation.
Reaction conditions: *Nitrobenzene: 9.34 × 10^{-5} kmol; sulfuric acid (98%): 3ml; water: 84 ml; H_2 pressure: 2.72 MPa; temperature: 353 K.*

The effect of catalyst loading on the initial rate of formation of aniline and *p*-aminophenol is shown in Figure 2-8 and 2-9 respectively. In both the cases, the rate of formation was found to increase linearly with the catalyst loading.

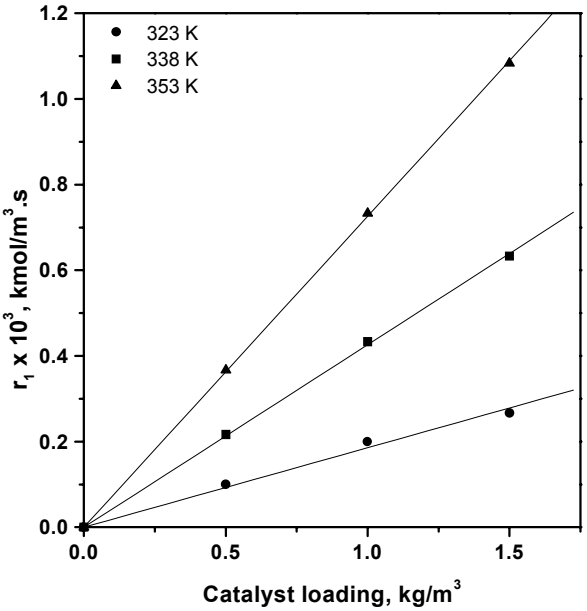

Figure 2-8: Effect of catalyst loading on initial rate of formation of aniline
Reaction conditions: *Nitrobenzene: 9.34 × 10^{-5} kmol; sulfuric acid (98%): 3 ml; water: 84ml; H_2 pressure: 2.72 MPa; agitation: 1000 rpm.*

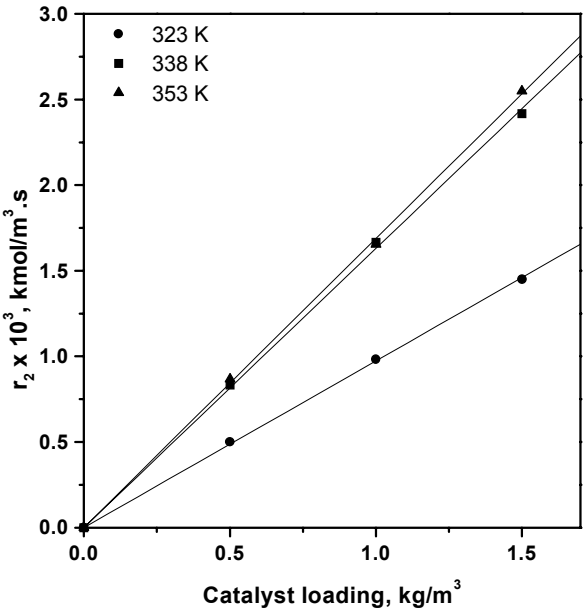

Figure 2-9: Effect of catalyst loading on initial rate of formation of *p*-aminophenol
Reaction conditions: *Nitrobenzene: 9.34 × 10^{-5} kmol; sulfuric acid (98%): 3 ml; water: 84ml; H_2 pressure: 2.72 MPa; agitation: 1000 rpm.*

The effect of hydrogen partial pressure on the initial rate of formation of aniline and *p*-aminophenol was investigated in a range of 0.68-6.8 MPa at various temperatures and the results are presented in Figure 2-10 and 2-11 respectively. The initial rate of formation of aniline increased linearly with hydrogen partial pressures at all temperatures. The initial rate of formation of *p*-aminophenol increased linearly with hydrogen partial pressure upto 4.08 MPa; beyond which it remained nearly constant at all temperatures. The effect of nitrobenzene loading was also investigated in the range of $9.34 \times 10^{-5} - 37.39 \times 10^{-5}$ kmol. The rate of hydrogenation was found to be independent of nitrobenzene charge under the experimental conditions.

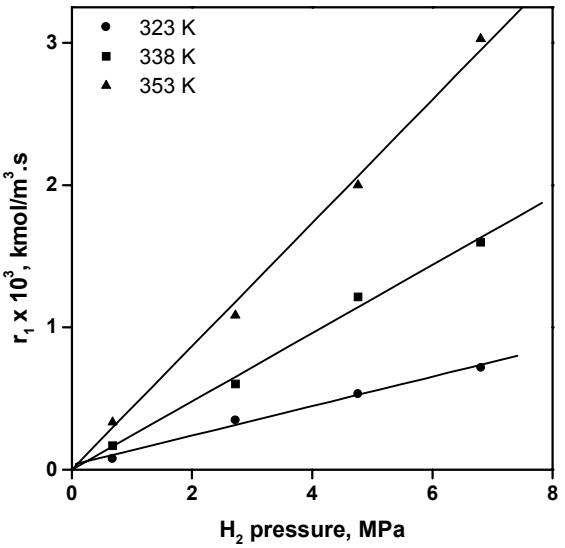

Figure 2-10: Effect of hydrogen partial pressure on initial rate of formation of aniline at different temperatures.
Reaction conditions: *Nitrobenzene: 9.34 × 10^{-5} kmol; 3 % Pt/C: 1.5 kg/m^3; sulfuric acid (98%): 3ml; water: 84 ml; agitation: 1000 rpm.*

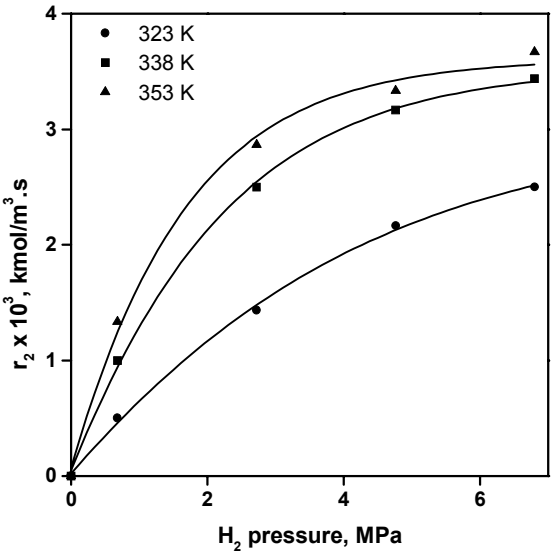

Figure 2-11: Effect of hydrogen partial pressure on initial rate of formation of *p*-aminophenol at different temperatures.
Reaction conditions: *Nitrobenzene: 9.34 × 10^{-5} kmol; 3 % Pt/C: 1.5 kg/m^3; sulfuric acid (98%): 3ml; water: 84 ml; agitation: 1000 rpm.*

The catalytic hydrogenation of nitrobenzene in the presence of an acid results in the formation of *p*-aminophenol and aniline (Scheme 2-1). The formation of aniline as well as *p*-aminophenol proceeds through the intermediate phenylhydroxylamine. Since, in most of the experiments, phenylhydroxylamine detected was negligibly small (less than 2 %) the stoichiometric reactions for the formation of aniline and *p*-aminophenol (considering hydrogen consumption) can be written as below.

$$B + 3A \rightarrow E + 2W \tag{2-1}$$

$$B + 2A \rightarrow P + W \tag{2-2}$$

where, A= hydrogen, B=nitrobenzene, E=aniline, P= *p*-aminophenol and W= water.

For hydrogenation of nitrobenzene to aniline the rate of hydrogenation using Pt catalyst has been reported to be zero order with respect to nitrobenzene concentration and first order with respect to hydrogen partial pressure [14]. Therefore, the rate equation for the formation of aniline from nitrobenzene was assumed to be

$$r_1 = wk_1 A_{NB} \tag{2-3}$$

Where r_1 is the rate of formation of aniline (kmol/m^3.s); w is the catalyst loading (kg/m^3) and, A_{NB} is the concentration of dissolved hydrogen in nitrobenzene (kmol/m^3). In accordance with the effect of nitrobenzene, catalyst loading and hydrogen pressure discussed above for the catalytic conversion of nitrobenzene to *p*-aminophenol, a single site Langmuir-Hinshelwood rate model was proposed for hydrogenation of nitrobenzene to *p*-aminophenol (equation 2-4).

$$r_2 = \frac{wk_2 A_{NB}}{1 + K_A A_{NB}} \tag{2-4}$$

Where r_2 is the rate of formation of *p*-aminophenol (kmol/m^3.s). Here it was assumed that the rearrangement of phenylhydroxylamine to *p*-aminophenol is fast compared to other steps. The value of kinetic constant, k_1, in equations (2-3) was calculated from the observed rate of formation of aniline. For the estimation of values of k_2 and K_A equation (2-4) was rearranged as

$$\frac{1}{r_2} = \frac{1}{wk_2 A_{NB}} + \frac{K_A}{wk_2} \tag{2-5}$$

A plot of $1/r_2$ versus $1/A_{NB}$ gives a straight line with slope equal to $1/wk_2$. Knowing the value of k_2, the value of K_A was calculated from the intercept of this graph (Figure 2-12). For this purpose, the values of r_1 and r_2 calculated were taken from Table 2-7. The value of A_{NB} (i.e. dissolved hydrogen concentration in nitrobenzene) was calculated at the given pressure using the literature solubility data [15]. The values of k_1, k_2 and K_A obtained at different temperatures are given in Table 2-8.

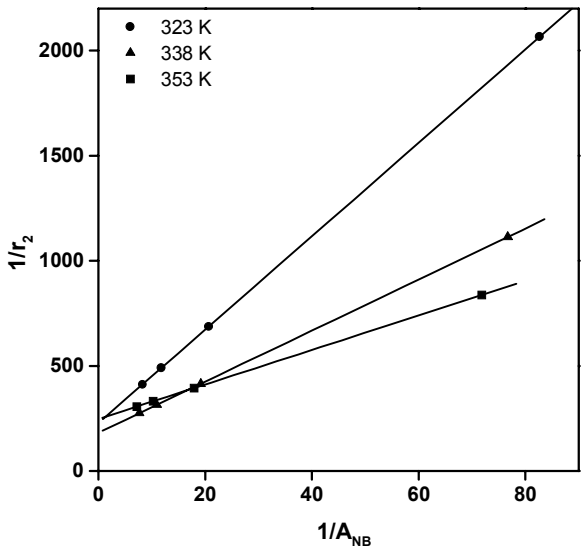

Figure 2-12: Plots of $1/r_2$ versus $1/A_{NB}$ according to equation 2-5 at different temperatures.

Table 2-8: Values of kinetic parameters at different temperatures

Temp. ***K***	$k_1 \times 10^3$ ***(kmol/kg/s)***	K_2 ***(m³/kg/s)***	K_A ***(m³/kmol)***
323	*3.90*	*0.030*	*10.23*
338	*7.82*	*0.054*	*14.95*
353	*12.51*	*0.081*	*30.06*

The comparison between experimental and predicted rates of formation of *p*-aminophenol and aniline using the above kinetic constants and rate equations (2-3) and (2-4) is given in Figure 2-13, which show a good agreement.

.

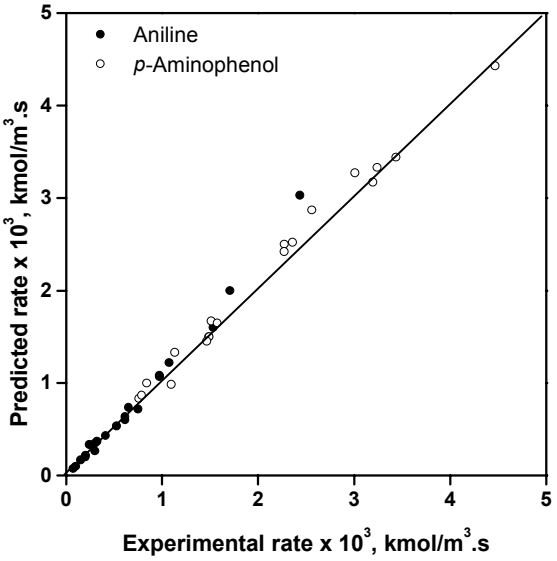

Figure 2-13: Experimental *vs* predicted rates of formation of aniline and *p*-aminophenol.

From the kinetic constants obtained by the method described above, the apparent energy of activation was calculated from the Arrhenius plots (Figure 2-14) to be 35.89 and 31.54 kJ/mole for hydrogenation of nitrobenzene to aniline and *p*-aminophenol respectively. The heat of adsorption was also determined from the graph of $ln\ K_A$ vs $1/T$ was 33 kJ/mole.

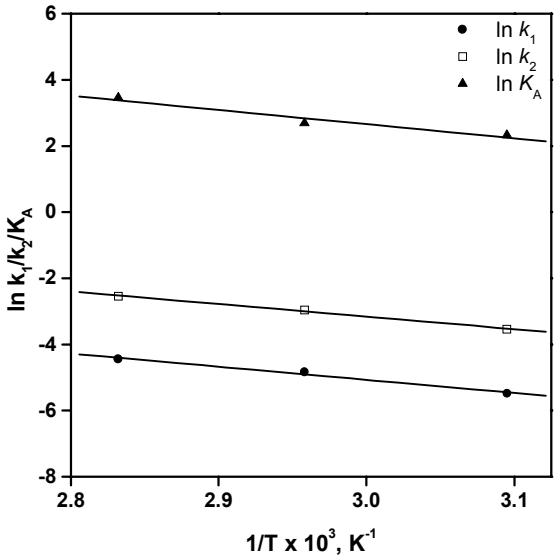

Figure 2-14: Arrhenius plots

2.3.4.2 Interpretation of integral batch reactor data

In order to further examine the suitability of the above rate equations (2-3 and 2-4) and estimated kinetic parameters for the hydrogenation of nitrobenzene to *p*-aminophenol under integral conditions, a batch reactor model was proposed. For this purpose, the following assumptions were made: (1) Hydrogen pressure is constant throughout the reaction time, (2) isothermal conditions prevail, and (3) aniline and *p*-aminophenol formed were immediately transferred to aqueous phase as their sulfate salts, therefore, the nitrobenzene concentration was essentially constant but the volume of nitrobenzene changes (decreases) with the progress of the reaction. This aspect has to be taken into account while proposing a batch reactor model. The volume of nitrobenzene at anytime in the reactor is given as

$$V = \frac{B_l M_w}{\rho_{NB}} \tag{2-5}$$

Where B_l is moles of nitrobenzene at the given instance, M_w and ρ_{NB} are the molecular weight and density of nitrobenzene respectively. The rate of change of nitrobenzene (kmol/s) in a reactor can be given as

$$\frac{dB_l}{dt} = -V(r_1 + r_2) \tag{2-6}$$

Substituting for the value of V from equation 2-5,

$$\frac{dB_l}{dt} = -\frac{B_l M_w}{\rho_{NB}}(r_1 + r_2) \tag{2-7}$$

The rate of formation of aniline can be given as

$$\frac{dE}{dt} = Vr_1 = \frac{B_l M_w}{\rho_{NB}} \times wk_1 A_{NB} \tag{2-8}$$

and, the rate of formation of *p*-aminophenol can be given as

$$\frac{dP}{dt} = Vr_2 = \frac{B_l M_w}{\rho_{NB}} \times \frac{wk_2 A_{NB}}{1 + K_A A_{NB}} \tag{2-9}$$

Equations 2-8 and 2-9 were solved using Runge-Kutta method with the initial conditions, at $t = 0$, $B_l = B_{l0}$ and $E_l = P_l = 0$ (where E_l = moles of aniline and P_l = moles of *p*-aminophenol). The total moles hydrogen consumed during the reaction can be calculated as:

$$H_2 consumed = 3E_l + 2P_l \tag{2-10}$$

Experiments were carried out at different initial conditions for more than 75 % conversion of nitrobenzene and the hydrogen consumption data were measured as function of time. The model predictions and experimental data at different temperatures, catalyst loading and hydrogen partial pressures are shown in Figure 2-15 to 2-17 respectively, which show excellent agreement. Thus, the rate parameters determined here represent the results obtained under both differential and integral conditions.

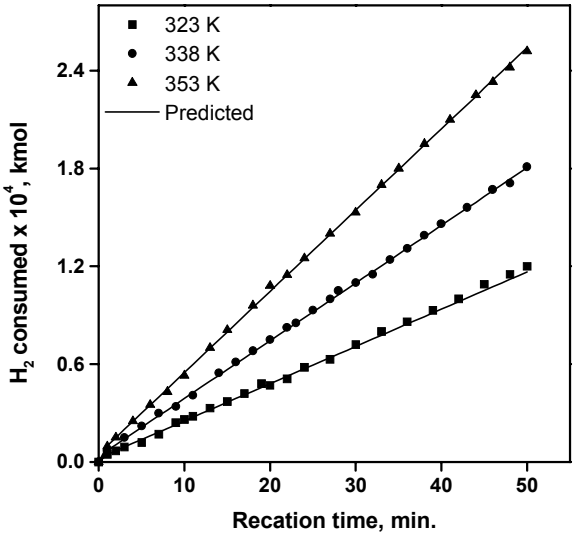

Figure 2-15: Comparison of experimental and predicted results for the hydrogen consumption-time data at different temperatures.
Reaction conditions: *Nitrobenzene: 9.34× 10^{-5} kmol; 3 % Pt/C: 1.5 kg/m^3; sulfuric acid: 3 ml; water: 84 ml; H_2 pressure: 2.72 MPa; agitation: 1000 rpm.*

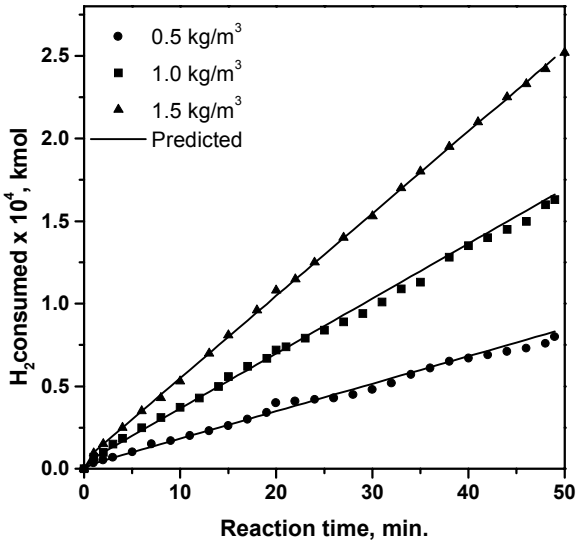

Figure 2-16: Comparison of experimental and predicted results for the hydrogen consumption-time data for different catalyst loadings at 353 K.
Reaction conditions: *Nitrobenzene: 9.34 x 10^{-5} kmol; sulfuric acid (98%): 3ml; water: 84 ml; temperature: 353 K; H_2 pressure: 2.72 MPa; agitation: 1000 rpm*

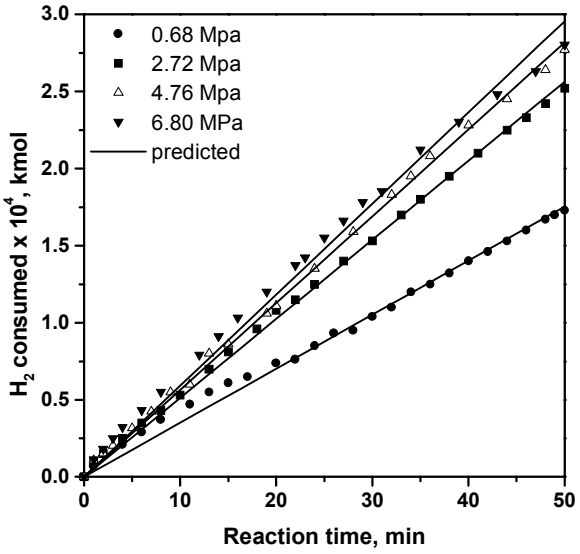

Figure 2-17: Comparison of experimental and predicted results for the hydrogen consumption-time data for different hydrogen partial pressures at 353 K.
Reaction conditions: *Nitrobenzene: 9.34 × 10^{-5} kmol; catalyst: 1.5 kg/m^3; acid: 3ml; water: 84 ml; temperature: 353 K; agitation: 1000 rpm*

2.4 Conclusions

The hydrogenation of nitrobenzene to *p*-aminophenol was investigated in presence of sulphuric acid in a batch slurry reactor. Aniline was obtained as a major by-product. The highest catalytic activity and selectivity was obtained for Pt/C catalyst. The effect of various parameters like nitrobenzene amount, hydrogen pressure, sulphuric acid amount, temperature and speed of agitation on average catalytic activity and selectivity to *p*-aminophenol was studied using 3% Pt/C catalyst. The average catalyst activity increased linearly with hydrogen pressure, whereas selectivity of *p*-aminophenol increased with increase in the hydrogen pressure up to 2.72 MPa and decreased with further increase in hydrogen pressure. The selectivity of *p*-aminophenol increased with acid amount upto 6ml, beyond which it was almost constant. The average catalyst activity and selectivity to *p*-aminophenol increased with increase in speed of agitation. The catalyst could be successfully used for three recycle experiments giving a cumulative TON of 1.38×10^5.

The kinetics of 3% Pt/C catalyzed hydrogenation of nitrobenzene to *p*-aminophenol was also investigated. The rate of formation of *p*-aminophenol showed zero order dependence with respect to nitrobenzene and first order dependence on hydrogen pressure at lower pressure tending to zero order at higher pressure above 4.76 MPa. On the basis of data obtained in the kinetic regime, a Langmuir-Hinshelwood type rate equation was proposed. The kinetic parameters were evaluated. From the temperature dependence of the kinetic constants, the activation energy was found to be 31.54 kJ/mole. A batch slurry reactor model based on the proposed rate equation and the estimated kinetic constants was found to represent the kinetics of the hydrogenation of nitrobenzene to *p*-aminophenol satisfactorily.

2.5 Notations

A_{NBl} Concentrations of hydrogen in nitrobenzene, kmol/m^3

B_l Moles of nitrobenzene

E_l Moles of aniline

k_1 Rate constant, m^2/kg.s

k_2 Rate constant, m^3/kg.s

K_A Adsorption constant, m^3/kmol

M_w Molecular weight of nitrobenzene

N Average catalytic activity, kmol/kg.hr

P_l Moles of *p*-aminophenol

r_1 Rate of formation of aniline, kmol/m^3.s

r_2 Rate of formation of *p*-aminophenol, kmol/m^3.s

R_A Overall rate of hydrogenation, kmol/m^3.s

V Volume of nitrobenzene, ml

w Catalyst loading, kg/m^3

ρ_{NB} Density of nitrobenzene

2.6 References

[1] (a) Sathe, S. *US Pat. 4176138*, **1979** (b) Derrenbacker, E. *US Pat. 4307249*, **1981** (c) Greco, N. *US Pat. 3953509*, **1976** (d) Benner, R. *US Pat. 3383416*, **1968** (e) Dunn, T. *US Pat.* 4264529, **1981**.

[2] Medcalf, E. *US Pat. 4051187*, **1977**.

[3] Juang, T.; Hwang, J., Ho, H. and Chen, C. *J. Chin. Chem. Soc. 35,*135, **1988**

[4] Roberts, J. Hydrogenation catalysts, Noyes Data Corporation, Park Ridge, NJ, USA, **1976**.

[5] Mozingo, R. Organic Synthesis Collective Volume 3, Ed. Horning, E. John Wiley, London, 685, **1955**.

[6] Suju, M., Ph.D.Thesis, University of Pune, India, **2001**.

[7] Imamura, S.; Higashihara, T.; Saito, Y.; Aratini, H.; kanai, H. and Tsuda, N. *Catal. Today 50,* 369, **1999**.

[8] Jackson, S.; Keegan, M.; McLellan, G.; Meheux, P.; Moyes, R.; Webb, G.; Wells, P.; Whyman, R. and Willis, J. *Stud. Surf. Sci. Catal. 63*, 135, **1991**.

[9] Rajshekharam, M., Ph.D.Thesis, University of Pune, India, **1997**.

[10] Kamm, O. Organic Synthesis Collective Volume 1, ed. Horning, E. John Wiley, London, 445, **1955**.

[11] (a) Chen, C.; Yamamoto, H. and Kwan, T. *Chem. Pharm. Bull. 17*, 2349, **1969**. (b) Chen, C.; Yamamoto, H. and Kwan, T. *Chem. Pharm. Bull. 18*, 1305, **1970** (c) Hwang, M.; Chen, S. and Chen, C. *J. Chin. Chem. Soc. 22*, 335, **1975**.

[12] Dewal, U.; Mhasakar, R.; Joshi, J. and Sawant, S. *Ind. Chem. J.* 29, **1980**.

[13] Henke, C. and Vaughen, J. *US Pat. 2198249*, **1940**.

[14] Li, C.; Chen, Y. and Wang, W. *Appl. Catal. A 119*, 185, **1994**.

[15] Radhakrishnan, K.; Ramchandran, P.; Brahme P. and Chaudhari R. *J. Chem. Eng. Data*, *28*, 1, **1983**.

* * * * *

Chapter Three

Adsorption Equilibrium Studies on Activated Carbon and Pt/C Catalysts Suspended in Liquid Phase

3.1 Introduction

Adsorption of a solute (reactant) from the liquid phase is an important step in the liquid-solid as well as gas-liquid-solid catalytic reactions. The nature of adsorption isotherms and the mechanism of adsorption play important roles in the activity and selectivity behavior of catalysts. Because of the participation of the surface, the explanation of reaction mechanism for heterogeneously catalyzed reactions is more difficult than for homogeneous catalytic reactions. In every heterogeneous catalytic reaction, the key steps involved are adsorption of reactants (or at least one of the reactants) on the surface of a solid catalyst, reaction between the adsorbed species to form the product and desorption of product from the solid catalyst surface to the bulk phase [1]. The overall rate of the catalytic process is controlled by one of these steps. In the development of appropriate kinetic model for any reaction, therefore, it is useful to have a quantitative knowledge of the adsorption equilibrium characteristics of various reaction components on the catalyst. Despite its importance in understanding the catalytic reaction mechanism and the kinetic modeling for a variety of industrially important reactions, adsorption from the liquid phase has not been studied extensively, compared to the adsorption from the vapor phase. Often, the adsorption equilibrium constants are determined indirectly by fitting the experimental rate data to a certain form of rate model. Only in rare cases the adsorption equilibrium parameters have been determined experimentally [2].

In this chapter, an attempt has been made to experimentally measure the adsorption equilibrium parameters for nitrobenzene, aniline and hydrogen on Pt/C catalyst and activated carbon from the liquid phase. A detailed literature review on the liquid phase adsorption of nitrobenzene, aniline and hydrogen is presented in Chapter I. From the literature reports, it was noted that the adsorption of

nitrobenzene and aniline has been investigated primarily in the context of wastewater treatment [3]. However, there is no report on the adsorption of nitrobenzene and aniline from solution on Pt/C catalyst. In the only significant report, Choudhary et al. [4] have investigated the vapor phase adsorption of nitrobenzene and aniline on copper chromite catalyst. The objective of this work was therefore, to investigate the adsorption of reactants/products involved in the catalytic hydrogenation of nitrobenzene to *p*-aminophenol namely nitrobenzene, aniline and hydrogen. Following specific objectives were set forth:

1. To study the adsorption of nitrobenzene, aniline and hydrogen in the slurries of activated carbon and Pt/C catalyst.
2. To study the adsorption of nitrobenzene and aniline from their binary mixtures on the catalyst.
3. To fit the experimental data to a suitable adsorption isotherm and evaluate the adsorption equilibrium constants and related thermodynamic quantities.

3.2 Experimental

3.2.1 Materials

Nitrobenzene, aniline and activated carbon were obtained from SD Fine Chemicals (India). HPLC grade methanol and water were purchased from Merck Chemicals (India). Hydrogen gas (>99 % purity) was supplied by Inox ltd. (India). Hexachloroplatinic acid was purchased from Arora Matthey Ltd. (India.).

3.2.2 Preparation of Pt/C Catalyst

3%Pt/C catalyst was prepared using a literature procedure [5]. The carbon support was activated by treating with 10 % HNO_3 for 6–8 hours, then washed with distilled water till free of acid and dried at 373 K overnight before use. 3 % Pt/C catalyst was prepared as follows: A solution of hexachloroplatinic acid in distilled water was obtained by warming hexachloroplatinic acid (0.796 gm) in distilled water (15 ml) for 10 min. This solution was added drop-wise to a stirred suspension of activated carbon (10 g) in distilled water (100 ml) in a 250 ml round bottom flask at room temperature and stirred for 1-2 hours until the supernant solution became colorless. The water was evaporated under vacuum to get the dried catalyst. The dried catalyst was calcined in furnace at 393 K and the reduction was carried out at 623 K for 2 h under a hydrogen flow of 30 ml/min. Since, a detailed adsorption study was carried out using 3% Pt/C catalyst, the catalyst was characterized for crystallite size, oxidation state of metal and other details as discussed below.

The XRD analysis of the catalyst sample was carried out using a Phillips model XRD 1730 using Ni filtered Cu-Kα radiation and a proportional counter detector at a scan rate of 4°/min. The average crystallite size of metallic Pt was calculated using the Scherrer equation [6]

$$L_{nm} = \frac{k\lambda}{\beta \cos\theta} \tag{3-1}$$

where, L_{nm} is the average crystallite size of the Pt present in nm, λ is the wavelength of CuKα radiation (0.1503 nm), k=0.9, Scherrer constant, θ is the Bragg angle of diffraction and β is the line broadening at half intensity. The average crystallite size of the 3% Pt/C catalyst was 18 nm. The XPS analysis was carried out on ESCA-3-MK (VG Scientific, UK) instrument using a MgKα radiation source. A C1s spectrum

with a binding energy value of 284.6 eV was used as reference. The XPS spectra of 3% Pt/C catalyst showed a peak at 71.4 eV binding energy, which indicated that Pt was completely reduced [7]. The various specifications of 3% Pt/C catalyst are given in Table 3-1.

Table 3-1: Specifications of activated carbon and 3 % Pt/C catalyst used in adsorption study.

Property	***Activated carbon***	***3 % Pt/C***
Surface area, m^2/kg	9.74×10^5	7.64×10^5
Porosity	5.5×10^{-1}	5.0×10^{-1}
Metal crystallite size, nm	--	*18*
Pore volume, m^3/kg	3.7×10^{-4}	2.63×10^{-4}

3.2.3 Experimental procedure

Nitrobenzene and aniline are sparingly soluble in water and therefore, the adsorption was investigated from their methanolic solutions. A schematic of the reactor setup used for adsorption measurement of nitrobenzene and aniline is shown in Figure 3-1. The adsorption vessel was provided with a Teflon stopper and reflux condenser to ensure that there was no loss of methanol during the experiment. In a typical adsorption experiment, 0.5 gm of 3% Pt/C catalyst was added to a glass reactor followed by the addition of known quantity of nitrobenzene in methanol. Initial sample (mixture of nitrobenzene and methanol) was taken before starting the experiment. The experiment was started by switching the stirrer on. Each experiment was carried out at a constant temperature and intermittent samples were taken out at certain time intervals and analyzed by Gas Chromatography.

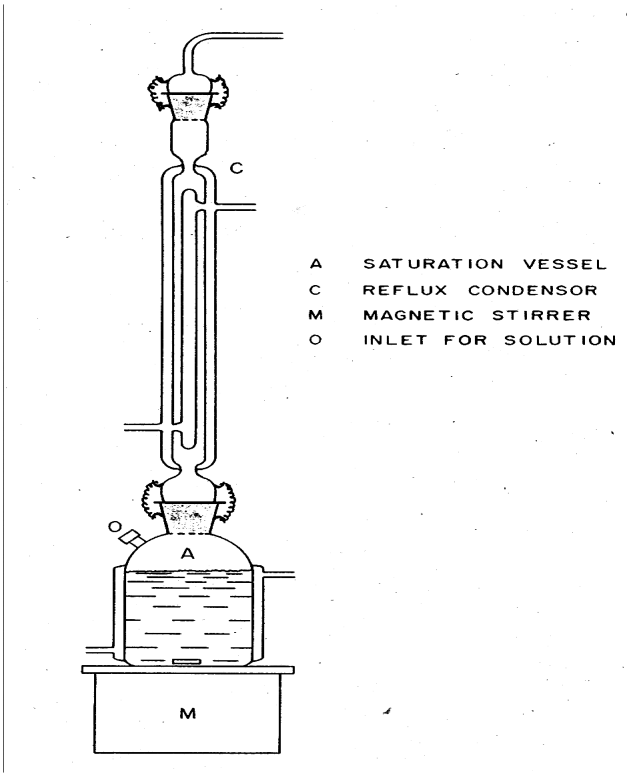

Figure 3-1. Schematic diagram of the experimental setup used for adsorption of nitrobenzene and aniline

A Varian gas chromatograph (model 5890) fitted with a thermal conductivity detector was used for this purpose. The analytical conditions were: column 10 % OV-17 (10 ft. length and 0.25 inch outer diameter); injector temperature: 423 K; detector temperature: 493 K; column temperature: 413 K; carrier gas (nitrogen) flow: 30 ml/min. The experiment was continued until analysis of two successive samples was constant, which confirmed the adsorption equilibrium stage. The quantity of adsorbed solute per unit weight of catalyst was calculated as follows:

$$q = \frac{V(C_o - C_e)}{w} \tag{3-2}$$

Where, q is adsorbed quantity of adsorbate, kmol/ kg of catalyst; V is volume of reaction solution, m^3; C_0 is initial concentration of adsorbate, kmol/m^3; C_e is equilibrium concentration of adsorbate, kmol/m^3 and w is weight of adsorbent taken, kg. A similar procedure was employed to study the binary adsorption of nitrobenzene and aniline from their methanolic solution.

Hydrogen adsorption experiments were carried out in a 50-cm^3 high-pressure reactor supplied by Parr Instruments Co. (U.S.A.). The schematic of reactor set-up was similar to that described in Chapter 2 (Figure 2-1). Prior to adsorption studies, the solubility of hydrogen in water at desired temperatures was measured experimentally by an absorption technique. In a typical adsorption experiment, the clean autoclave was charged with 30 cm^3 of distilled water and 1 gm of 3 % Pt/C catalyst. The reactor was flushed with high purity nitrogen and then heated to a desired temperature under slow stirring (200 rpm). After the temperature was equilibrated at the set point, hydrogen gas was introduced to the desired level and the contents were stirred vigorously (1000 rpm). The pressure drop in the autoclave was noted using a digital pressure transducer as a function of time. The stirring was continued for 30 min, at the end of which the absorption of the gas practically ceased. The difference in the initial and final pressures in the reactor correspond to the total amount of gas absorbed (i.e. solubility + adsorption). The amount of hydrogen adsorbed was calculated by subtracting the solubility at equilibrium pressure from the total absorption. Using the above method, adsorption of hydrogen on activated carbon and Pt/C catalysts in slurry (water) was studied at different temperatures (298-338 K) and partial pressures of hydrogen (0.68-5.44 MPa).

3.3 Results and discussion

The hydrogenation of nitrobenzene in presence of Pt/C catalyst and acid gives a mixture of aniline and *p*-aminophenol. The reaction is believed to proceed through the formation of phenylhydroxylamine as an intermediate (Scheme 2-1). The phenylhydroxylamine does not appear to be a major reaction component as it has only a transient lifetime. Also, the product *p*-aminophenol has limited solubility in methanol as well as water. Therefore, the adsorption of phenylhydroxylamine and *p*-aminophenol was not investigated. The results on the adsorption of other components namely, nitrobenzene, aniline and hydrogen are discussed below.

3.3.1 Adsorption of nitrobenzene and aniline

The single component adsorption of nitrobenzene and aniline on 3 % Pt/C catalyst was investigated from their methanolic solutions. The typical adsorption curves for nitrobenzene and aniline on 3 % Pt/C catalyst at 298 K are shown in Figure 3-2. The adsorption capacity of nitrobenzene was found to be higher than aniline on the same catalyst. The typical adsorption curves at different temperatures for nitrobenzene and aniline are shown in Figures 3-3 and 3-4 respectively. The adsorbed quantities of both, nitrobenzene and aniline, decreased with increase in temperature. Several adsorption experiments were conducted and in each case the adsorption dynamic curve was plotted and equilibrium adsorption quantity (q) was calculated.

The adsorption isotherms (plots of q versus C_e) for nitrobenzene and aniline at different temperatures are given in Figure 3-5 and 3-6 respectively. According to the classification of isotherms for adsorption from solutions suggested by Giles et al. [8], the isotherms of nitrobenzene and aniline on 3% Pt/C catalyst are similar to L_2 type, (i.e. normal or Langmuir isotherms, usually indicative of molecules adsorbed

flat on the surface or sometimes, of vertically oriented ions with particularly strong intermolecular attraction). The equilibrium adsorption quantities increased with the equilibrium solute concentration in solution initially but attain saturation at higher concentrations. The initial curvature shows that as more sites on the adsorbent surface are occupied or filled, it becomes increasingly difficult for the solute molecules to find a vacant site. This suggests that the adsorbed solute molecule is not vertically oriented and that there is no strong competition from the solvent [8].

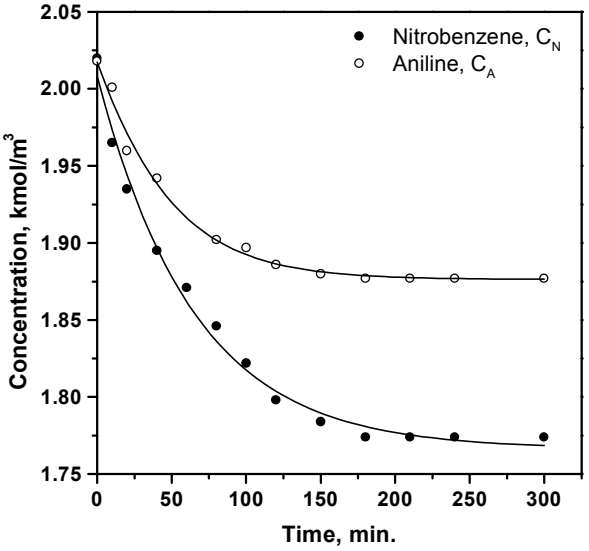

Figure 3-2: Typical dynamic curves for single component adsorption of nitrobenzene and aniline on 3% Pt/C catalyst at 298 K from methanolic solution.

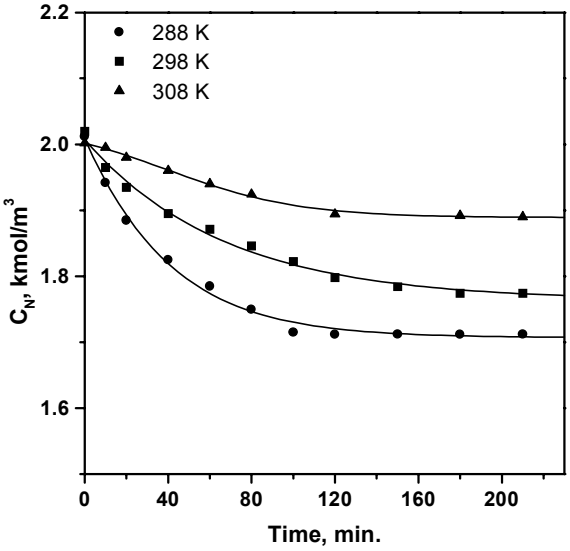

Figure 3-3: Dynamic curves for adsorption of nitrobenzene on 3% Pt/C catalyst at different temperatures from methanolic solution

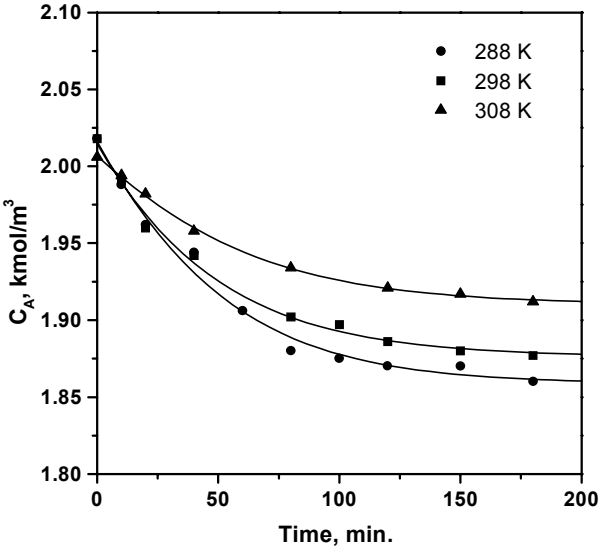

Figure 3-4: Dynamic curves for adsorption of aniline on 3% Pt/C catalyst at different temperatures from methanolic solution

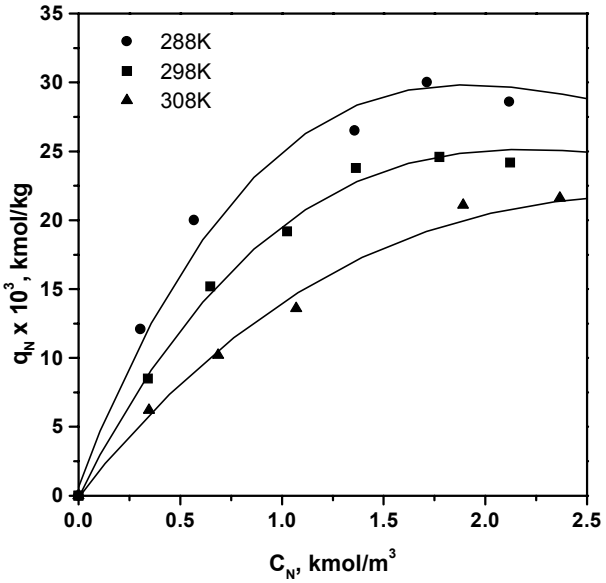

Figure 3-5: Adsorption isotherm of single component adsorption of nitrobenzene on 3% Pt/C catalyst at different temperatures

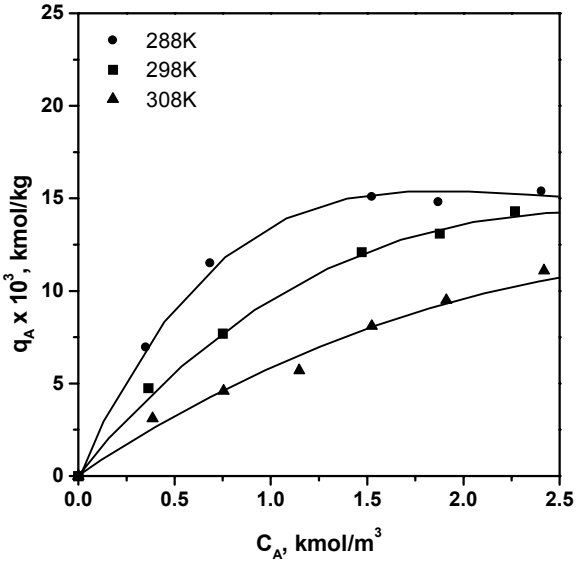

Figure 3-6: Adsorption isotherms of single component adsorption of aniline on 3 % Pt/C catalyst at different temperatures.

The adsorption equilibrium data obtained at various conditions indicated that the adsorption capacity of nitrobenzene was more than that of aniline on 3 % Pt/C catalyst at all the temperatures under investigation.

The adsorption of nitrobenzene and aniline on 3 % Pt/C catalyst was also compared with the data on activated carbon (Figure 3-7 and 3-8) at 298 K. It was observed that there was not much difference in the adsorption capacities of 3% Pt/C catalyst and activated carbon indicating that the adsorption in case of nitrobenzene and aniline could be physisorption. The adsorbed quantity, q, was slightly less for 3 % Pt/C catalyst as compared to activated carbon, which could probably be attributed to decrease in surface area of the catalyst.

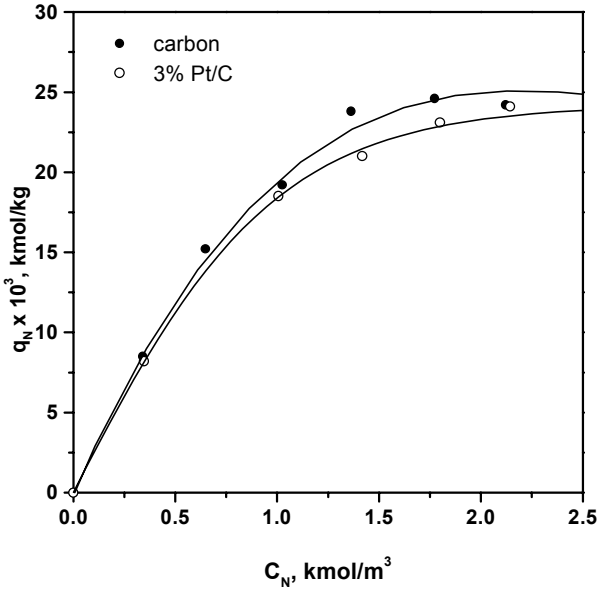

Figure 3-7: Comparison of adsorption of nitrobenzene on activated carbon and 3% Pt/C catalyst at 298K

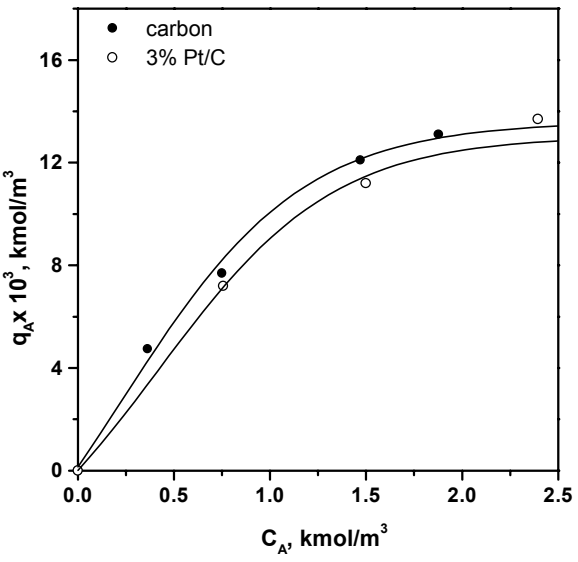

Figure 3-8: Comparison of adsorption of aniline on activated carbon and 3% Pt/C catalyst at 298K.

3.3.2 Fitting of nitrobenzene and aniline adsorption data

The general trends observed for adsorbed quantity (q) of adsorbate as a function of equilibrium concentration (C_e) for nitrobenzene and aniline on 3% Pt/C catalysts suggested that the Langmuir type equation might fit the adsorption data. The general form of Langmuir equation is:

$$q = q_m \frac{KC_e}{1 + KC_e} \tag{3-3}$$

Where, q is the amount adsorbed; q_m is the monolayer adsorption capacity of the adsorbent (carbon/catalyst); K is the adsorption equilibrium constant; and C_e is the equilibrium concentration of the adsorbate. Equation 3-3 can be rearranged as,

$$\frac{C_e}{q} = \frac{1}{q_m K} + \left(\frac{1}{q_m}\right) C_e \tag{3-4}$$

The C_e/q *vs* C_e plots according to the Langmuir equation for the adsorption of nitrobenzene and aniline at different temperatures shown in Figure 3-9 and 3-10 respectively, indicate a fairly good fit of the adsorption data to the Langmuir equation at all the temperatures. The values of the adsorption parameters (q_m and K) were calculated from the slope and intercepts and given in Table 3-2.

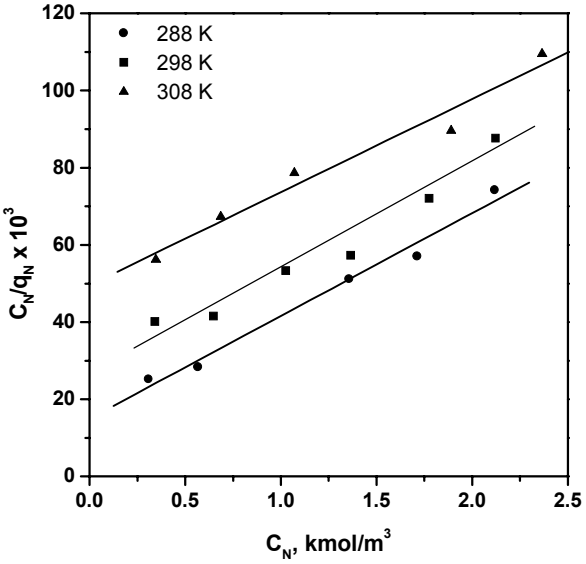

Figure 3-9: Langmuir plots (equation 3-4) for the adsorption of nitrobenzene on 3% Pt/C catalyst

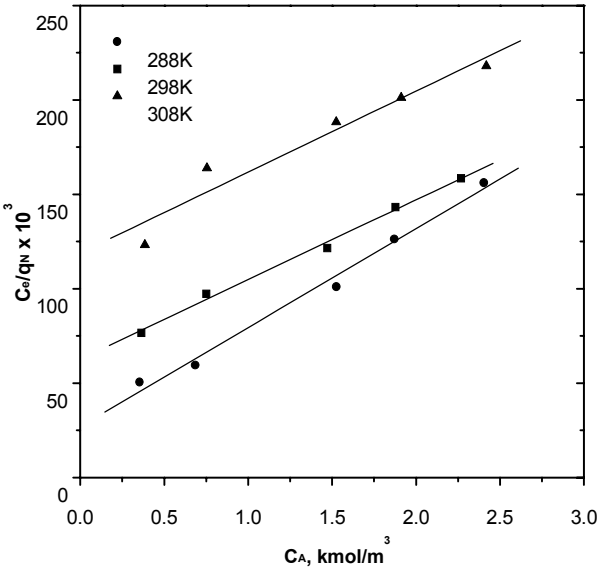

Figure 3-10: Langmuir plots (equation 3-4) for the adsorption of aniline on 3 % Pt/C catalyst

Table 3-2: Langmuir parameters (q_m and K) for the single component adsorption of nitrobenzene and aniline on 3% Pt/C catalyst at different temperatures

Adsorbate	***Temperature (K)***	***q_m (kmol/kg)***	***K (m^3/kmol)***
Nitrobenzene	*288*	*0.0375*	*1.785*
	298	*0.0376*	*1.005*
	308	*0.0414*	*0.487*
Aniline	*288*	*0.0221*	*1.100*
	298	*0.0236*	*0.674*
	308	*0.0308*	*0.233*

The value of q_m, adsorbed quantity for monolayer adsorption as per Langmuir theory was found to vary with temperature. The adsorption equilibrium constant (K) decreased with increase in temperature, which was also consistent with the Langmuir theory [9]. The heat of adsorption, ΔH_a, of nitrobenzene and aniline on 3% Pt/C catalyst can be obtained from the slope of plots of $ln\ K$ versus $1/T$ (Figure 3-11).

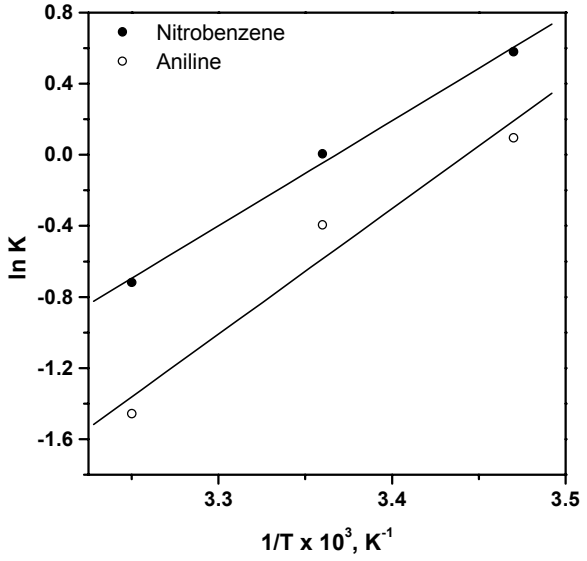

Figure 3-11: Temperature dependence of equilibrium adsorption constant for nitrobenzene and aniline on 3 % Pt/C catalyst from methanolic solution.

The heats of adsorption (ΔH_a) for nitrobenzene and aniline were found to be -49.06 and -58.618 kJ/mole respectively. These values indicate that the adsorption of nitrobenzene and aniline are exothermic processes. The above experimental data were also fitted to Freundlich adsorption isotherm, which has a general formula

$$q = kC^n \tag{3-5}$$

or

$$\log q = \log k + n \log C_e \tag{3-6}$$

The plots of *log q* versus *log* C_e (according to equation 3-6) are given in Figure 3-12. It can be seen that in case of nitrobenzene, the plots of *log q* versus *log* C_e are not linear suggesting that the adsorption data for nitrobenzene does not fit Freundlich adsorption isotherm. However, for aniline the plots of *log q* versus *log* C_e are nearly linear at 298 and 308 K (Figure 3-13).

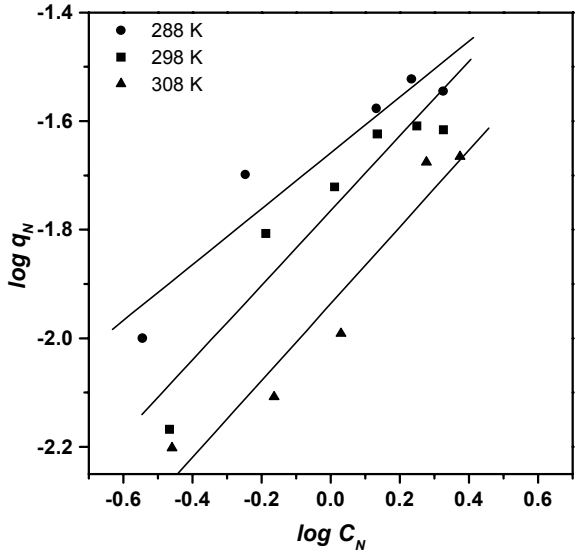

Figure 3-12: Freundlich plots (equation 3-6) for the adsorption of nitrobenzene from methanolic solution on 3 % Pt/C catalyst

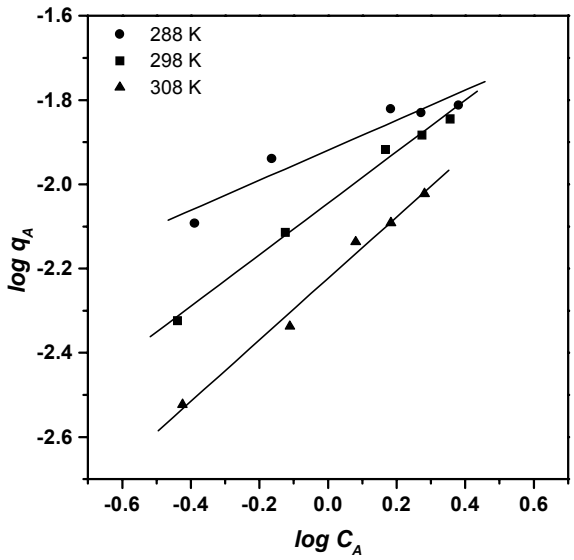

Figure 3-13: Freundlich plots (equation 3-6) for the adsorption of aniline from its methanolic solution on 3 % Pt/C catalyst

3.3.3 Binary adsorption of nitrobenzene and aniline

The binary adsorption of nitrobenzene and aniline from their methanolic mixtures was also investigated in a temperature range of 288-308 K. In each experiment, an equimolar mixture of nitrobenzene and aniline was used for adsorption studies and the results are given in Figure 3-14 and 3-15. For comparison, the adsorption data of the pure component is also given in these plots. Binary adsorption data are represented by dotted lines whereas solid lines represent pure component data. It can be seen that adsorption capacity of nitrobenzene decreases significantly because of the presence of aniline and vice versa.

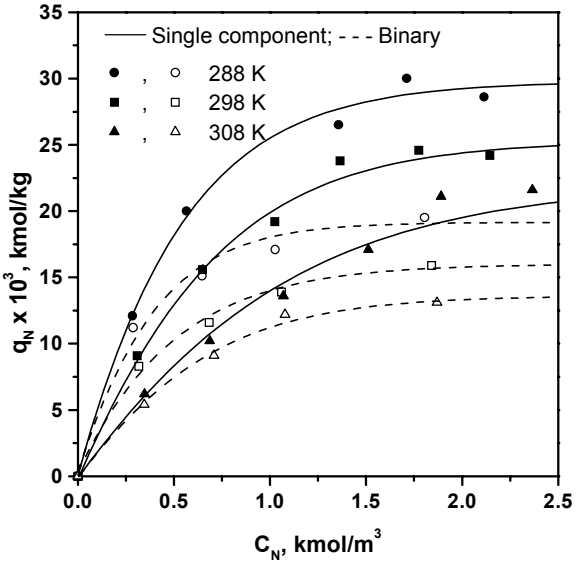

Figure 3-14: Adsorption isotherms for nitrobenzene from methanol in the presence of aniline on 3 % Pt/C catalyst at different temperatures (solid lines: pure component, dotted lines: binary adsorption).

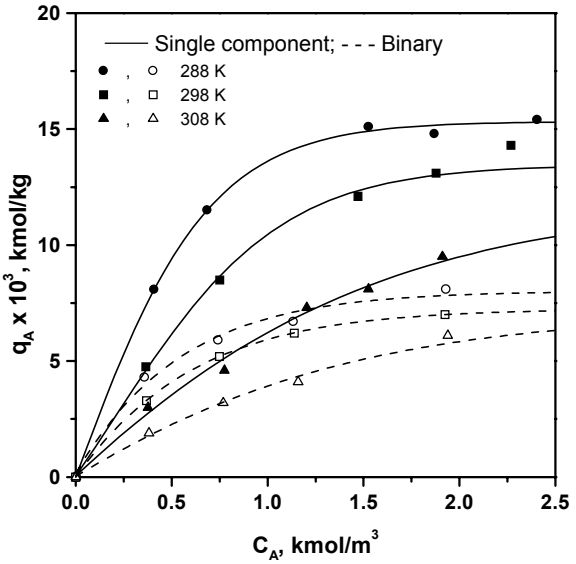

Figure 3-15: Adsorption isotherms for aniline from methanol in the presence of nitrobenzene on 3 % Pt/C catalyst at different temperatures (solid lines: pure component, dotted lines: binary adsorption).

It is interesting to note that the nature of adsorption isotherms for binary mixtures is similar to a pure component. Therefore, the adsorption data for binary mixtures may be fitted to an extended Langmuir equation (3-7) and (3-8) for nitrobenzene and aniline respectively.

For nitrobenzene

$$q_N = q_m\left[\frac{(K_N C_N)}{(1 + K_N C_N + K_A C_A)}\right] \tag{3-7}$$

For aniline

$$q_A = q_m\left[\frac{(K_A C_A)}{(1 + K_A C_A + K_N C_N)}\right] \tag{3-8}$$

Where, suffixes *N* and *A* represent nitrobenzene and aniline, respectively. According to Langmuir theory of adsorption, the adsorption equilibrium constant is expected to remain same for a component in pure as well as multicomponent system. Therefore, values of K_N and K_A obtained from single component adsorption for nitrobenzene and aniline, respectively, were used in equations 3-7 and 3-8. A comparison between the estimated and experimental q_N and q_A values shown in Figure 3-16 shows a good fit of the binary adsorption data according to the extended Langmuir equation 3-7 and 3-8. The results obtained for binary adsorption data can be interpreted on the basis of simple extension of Langmuir theory of adsorption to the case of adsorbate mixtures. The extended Langmuir equation for binary adsorption permits the adsorption of each component in the mixture to be calculated for any given equilibrium concentration without employment of constants other than those obtained from the isotherms of single component adsorptions. The equation 3-7 and

3-8 indicate that each component in the mixture should be adsorbed to a smaller extent than if it was present alone at the same equilibrium concentration.

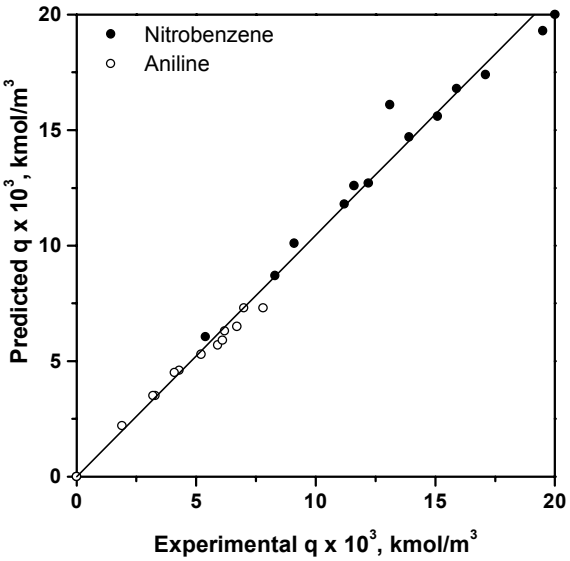

Figure 3-16: Comparison of the experimental and estimated (from equation 3-6 and 3-7) values of q_N and q_A for the binary adsorption of nitrobenzene and aniline on 3 % Pt/C catalyst.

3.3.4 Adsorption of hydrogen from liquid phase

The adsorption of hydrogen was also studied on 3 % Pt/C catalyst and activated carbon at different temperatures using water as solvent. The knowledge of solubility of hydrogen in water was essential for the calculation of adsorption capacity. Therefore, the solubility of hydrogen in water was determined experimentally by absorption technique. The difference between the total hydrogen intake and solubility gives total adsorbed quantity of hydrogen on the adsorbent (corrected to per kg of adsorbent).

Table 3-3: Experimental Henry's constant for hydrogen in water

Temperature (K)	***$H_e \times 10^3$ (kmol / m³. MPa)***
298	*7.13*
318	*7.10*
338	*6.24*

The plots of hydrogen uptake as a function of time at various hydrogen pressures on 3 % Pt/C catalyst at 298 K is shown in Figure 3-17. The equilibrium adsorption quantity of hydrogen (q) on 3 % Pt/C catalyst was determined from these curves at different temperatures. The plots of q versus A^* i.e. equilibrium liquid phase concentration of hydrogen (adsorption isotherm), is given in Figure 3-18.

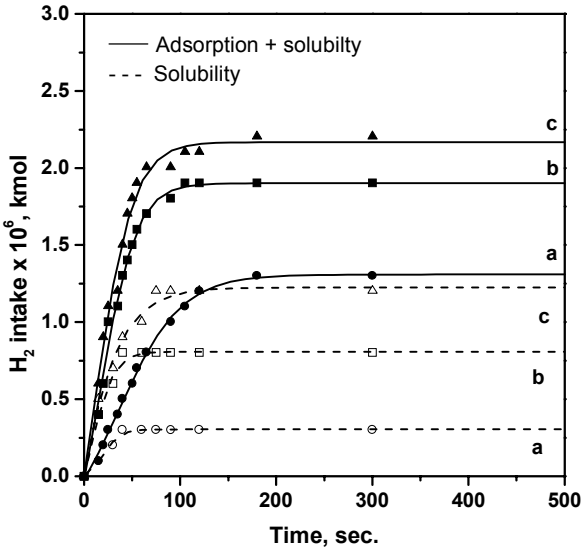

Figure 3-17: Hydrogen uptake as a function of time on 3% Pt/C catalyst at 298 K. initial pressure = (a) 1.64 MPa (b) 3.42 MPa; (c) 4.54 MPa. (Thick lines correspond to adsorption+ solubility; dotted lines represent solubility dynamics)

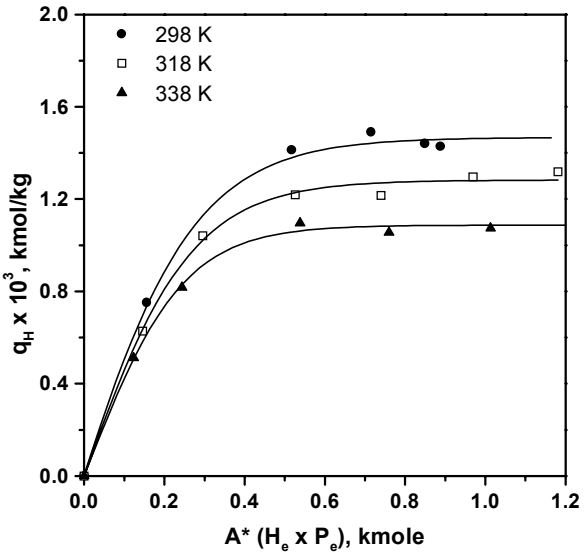

Figure 3-18: Adsorption isotherms for hydrogen on 3% Pt/C catalyst at different temperatures.

The general trends observed for adsorbed quantity of hydrogen versus equilibrium hydrogen concentration suggest a Langmuir type of adsorption. Therefore, the adsorption data for hydrogen adsorption on 3% Pt/C catalyst was fitted to a Langmuir type adsorption. The plots of $1/q$ versus $1/A^*$ for hydrogen on 3 % Pt/C catalyst at different temperatures are shown in Figure 3-19. These plots are linear, indicating a good fit of the adsorption data to the Langmuir equation at different temperatures. The values of q_m and K were calculated from the intercepts and slopes of these graphs, respectively and given in Table 3-4.

Table 3-4: Langmuir parameters (q_m and K) for hydrogen adsorption on 3% Pt/C catalyst at different temperatures.

Temperature, (K)	***$q_m \times 10^3$, (kmol / kg)***	***$K \times 10^{-6}$, (kg^{-1})***
298	*7.855*	*0.025*
318	*1.634*	*4.355*
338	*1.348*	*5.060*

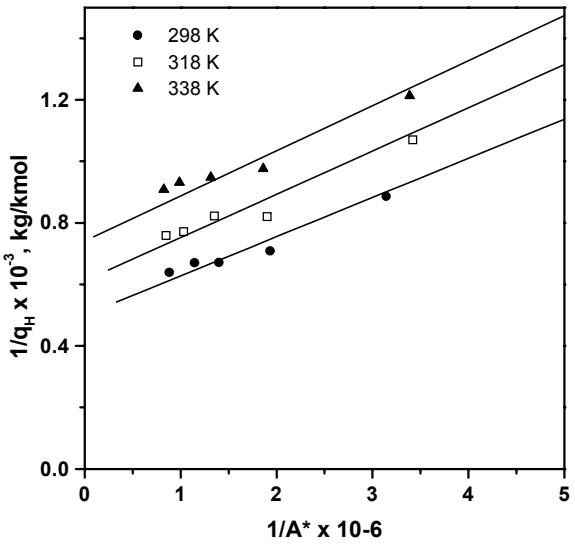

Figure 3-19: Langmuir plots (equation 3-5) for adsorption of hydrogen from water on 3% Pt/C catalyst.

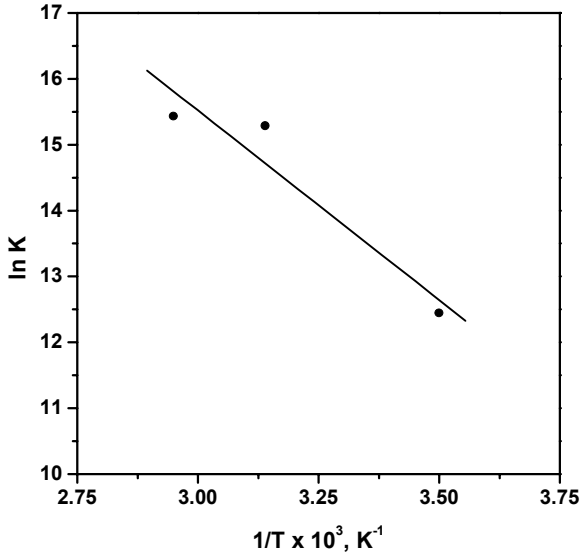

Figure 3-20: Temperature dependence of adsorption equilibrium constant for hydrogen adsorption on 3 % Pt/C catalyst from water.

The heat of adsorption (ΔH_a) calculated from the slope of $ln\ K$ versus $1/T$ plot (Figure 3-20) was 63.12 kJ/mole. The positive value of the heat of adsorption indicates a possibility of endothermic chemisorption. Such observation, though uncommon, has also been made earlier [10,11].

The reversibility of hydrogen adsorption was investigated at 298 K. In a typical experiment, the adsorption of hydrogen on 3% Pt/C catalyst was carried out at 298 K for 30 min. After the equilibrium was attained, the excess hydrogen was vented at the same temperature. The stirring was continued for further 30 min. to ensure that all the dissolved hydrogen was removed. Then fresh hydrogen was introduced in the reactor and the hydrogen intake was measured. It was observed that this time there was no adsorption of hydrogen on the catalyst. In order to further confirm whether the adsorption was reversibility, above experiment was repeated except that, after first adsorption experiment the catalyst was removed and refluxed in nitrogen atmosphere for 30 min. After that, the catalyst was again subjected to adsorption experiment to observe that the catalyst now adsorbed hydrogen almost equal to that in the fresh experiment. These experiments indicated that the hydrogen adsorption on 3% Pt/C catalyst was not physisorption but a chemisorption. The results of these experiments are given in Figure 3-21.

The adsorption of hydrogen on activated carbon from water was investigated at 298 K. It was observed that adsorption of hydrogen was very less as compared to 3 % Pt/C catalyst suggesting that hydrogen adsorption is specific in nature i.e. chemisorption (Figure 3-22).

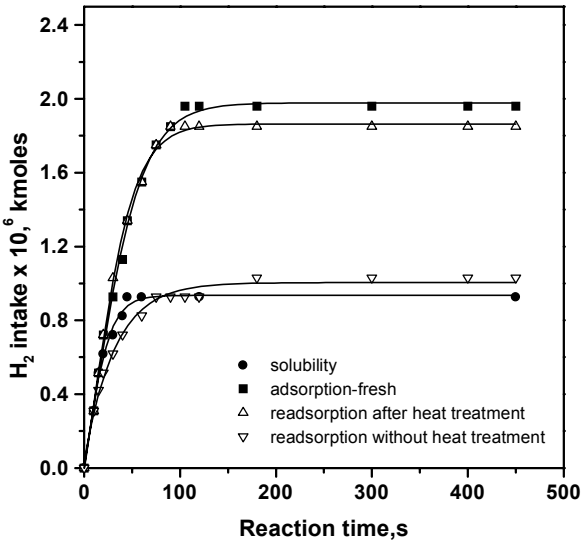

Figure 3-21: Reversibility of hydrogen adsorption on 3% Pt/C catalyst at 298 K

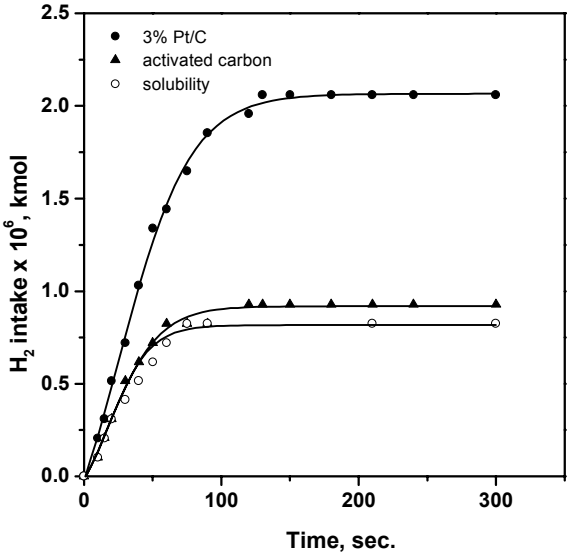

Figure 3-22: Comparison of hydrogen adsorption on activated carbon and 3% Pt/C catalyst from water at 298 K.

3.4 Conclusions

The liquid phase adsorption of nitrobenzene, aniline and hydrogen was investigated from the slurry of activated carbon and 3% Pt/C catalyst at different temperatures. The single component adsorption data for nitrobenzene, aniline and hydrogen fit the Langmuir adsorption isotherm. The adsorption of nitrobenzene and aniline from binary mixture also followed the extended Langmuir model. There was negligible difference in the adsorption capacity of activated carbon and 3% Pt/C catalyst in case of nitrobenzene and aniline suggesting that adsorption of nitrobenzene and aniline is physisorption. The heat of adsorption (ΔH_a) for nitrobenzene, aniline and hydrogen on 3 % Pt/C catalyst was calculated as -49.06, - 58.61 and 63.12 kJ/mole respectively. Liquid phase adsorption of hydrogen was carried out on 3% Pt/C catalyst and activated carbon at different temperatures. The adsorption of hydrogen was considerably more for 3% Pt/C catalyst compared to that for activated carbon.

3.5 Notations

C_0 Initial concentration of adsorbate, kmol/m^3

C_e Equilibrium concentration of adsorbate, kmol/m^3

C_A Equilibrium concentration of aniline, kmol/m^3

C_N Equilibrium concentration of nitrobenzene, kmol/m^3

K_A Adsorption equilibrium constant, m^3/kmol

q_A Adsorbed quantity of aniline, kmol/kg

q_N Adsorbed quantity of nitrobenzene, kmol/kg

q_m Monolayer adsorption capacity, kmol/kg

V Total volume of reaction mixture, m^3

w Adsorbent loading, kg

ΔH_a Heat of adsorption, kJ/mole

3.6 References

[1] Ramchandran, P.A. and Chaudhari, R.V., 'Three Phase Catalytic Reactors", Gorden and Breach Sci. Publishers, New York, **1983**.

[2] (a) Chen, S.; Smith, J. and McCoy, B. *J. Catal. 102,* 365, **1986** (b) Ahn B., Smith J.and McCoy B. *AIChE J. 32*, 566, **1986** (c) Chen, S.; Smith, J. and McCoy, B. *Chem. Eng. Sci. 42*, 293, **1987**.

[3] Sargeeva, T. *Electrokimiya*, *12*, 1383, **1976**. (b) Rodovic, L. *Carbon 35*, 1339, **1997** (c) Tororrenta, A. *J. Hazard. Mater*. *54*, 41, **1997**.

[4] Choudhary, V.; Sansare, S. and Thite, G. *J. Chem. Tech. Biotech. 42,* 249, **1988**.

[5] Macias Perez, M.; Martinez de Leces, C. and Solano, A. *Appl. Catal. A 151*, 461, **1997**.

[6] Robertson, S. and Anderson, R. *J. Catal. 33*, 286, **1971**.

[7] (a) Jia, C.; Jing, F.; Hu, W.; Huang, M. and Jiang, Y. *J. Mol. Catal. 91*, 139, **1994**. (b) Jackson, S.; Keegan, M.; McLellan, G.; Meheux, P.; Moyes, R.; Webb, G., Wells, P., Whyman, R. and Willis, J. *Stud. Surf. Sci. Catal. 63*, 135, **1991**.

[8] Giles, C.; MacEwan, T.; Nakhwa, S. and Smith, D. *J. Chem. Soc.* 3973, **1960**.

[9] Ruthven, D. Principles of Adsorption and Adsorption Processes, Wiley Interscience, **1984**.

[10] Chaudhari, R.; Parande, M., Pamchandran, P.; Brahme, P., Vadgaonkar, H. and Jaganathan, R. *AIChE J. 31*, 1891, **1985**.

[11] Broderick, D. and Gates, B. *AIChE J. 27*, 663, **1981**.

* * * * *

Chapter Four

Synthesis of *p*-Aminophenol by Catalytic Hydrogenation of *p*-Nitrophenol

4.1 Introduction

Synthesis of *p*-aminophenol by catalytic hydrogenation of nitrobenzene discussed earlier (Chapter 2) suffers from three major disadvantages: (a) formation of aniline as a side product, (b) use of highly corrosive reagents like sulfuric acid, and (c) difficulties in separation and purification of *p*-aminophenol from the reaction mass in pure form. The catalytic hydrogenation of *p*-nitrophenol is an alternative route for the synthesis of *p*-aminophenol, which obviates the above mentioned problems to some extent. The starting material for this route i.e. *p*-nitrophenol can be obtained either by hydrolysis of *p*-chloronitrobenzene or direct nitration of phenol. Conventionally, the reduction step is accomplished using Fe-acid reducing agent. The major disadvantage of the conventional process is that it uses large amounts of Fe and produces almost equivalent amount of Fe-FeO sludge, which poses serious waste disposal problems. The difficulties in the separation of pure *p*-aminophenol from the reaction mass containing Fe-FeO sludge is yet another drawback of the conventional process. A comprehensive literature review presented in Chapter 1 indicates that the transition metal catalyzed hydrogenation of *p*-nitrophenol can provide a cleaner route for the synthesis of *p*-aminophenol (Scheme 4-1). In general, several group VIII metal catalysts such as Pt, Pd and Ni etc. have been reported previously for the hydrogenation of *p*-nitrophenol [1-3]. Malpani et al. [4] have investigated the kinetics of Pd/C catalyzed hydrogenation of *p*-nitrophenol to *p*-aminophenol and found that the mass transfer of hydrogen from the gas phase to bulk liquid phase and then to the solid catalyst particle played an important role. Yao et al. [5] investigated the liquid phase hydrogenation of *p*-nitrophenol over colloidal Pd, Rh, Pt and Raney nickel catalysts. The rate of hydrogenation of nitrophenol using these catalysts was first order with respect to hydrogen. The rate

of hydrogenation was first order with respect to *p*-nitrophenol at lower catalyst concentration and zero order at higher catalyst loading. An empirical rate equation was also proposed to describe the hydrogenation rate behavior.

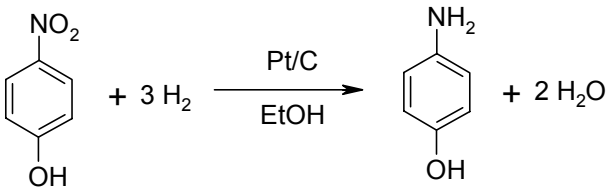

Scheme 4-1: Catalytic hydrogenation of *p*-nitrophenol to *p*-aminophenol

Considering the industrial importance of this reaction system, it would be worthwhile investigating catalysis and kinetics of this reaction in detail. Since, no comprehensive information was available in the literature on these aspects, the objective of this work was to first identify a suitable heterogeneous catalyst for the hydrogenation of *p*-nitrophenol to *p*-aminophenol giving high yields and undertake a detailed study on the effect of type and content of metal, catalyst support, solvent, hydrogen partial pressure and temperature on the initial rate of hydrogenation and average catalyst activity.

The second objective of this study was to investigate the intrinsic kinetics of catalytic hydrogenation of *p*-nitrophenol using 1%Pt/C catalyst with detailed analysis of mass transport effects at different temperatures and further develop a rate equation that could be useful for design of reactors.

4.2 Experimental

4.2.1 Materials

p-Nitrophenol was purchased from Loba Chemicals (India) Ltd. *p*-Aminophenol, 1% Pt/C, 1% Pd/C, 1% Rh/C, 1% Ru/C, 1% Pt/Al_2O_3 catalysts were purchased from Aldrich Chemicals, USA. Other supported catalysts (1% Pt/SiO_2, 1%Pt/HY, 1% Ni/C were prepared using standard literature procedures [6-8]. Hydrogen gas was supplied by Inox India Ltd. Solvents (ethanol, methanol, *n*-propanol and *n*-butanol) were obtained from SD Fine chemicals, Mumbai, and were freshly distilled before use. HPLC grade water and acetonitrile (Merck Chemicals, India) were used as received.

4.2.2 Experimental setup

The hydrogenation experiments were carried out in a 50-cm^3 capacity high-pressure slurry reactor (hastelloy C-276) supplied by Parr Instruments Co. USA. The reactor was provided with a magnetic stirrer to operate upto 1500 rpm. The reactor was maintained at a constant temperature with the help of a PID controller, which provided alternate heating and cooling. Temperature and pressure in the reactor were recorded using a digital display. The reactor was also equipped with relevant safety features like high temperature-pressure cut off and safety rupture disc. A schematic of the reactor set up is shown in Chapter II (Figure 2-1).

4.2.3 Analytical measurements

The analysis of all liquid samples was carried out using a Hewlett-Packard gas chromatograph model 6890 equipped with HP-1 capillary column (30 m length, 0.32 mm diameter) and flame ionization detector (FID). The analysis conditions were;

column temperature: 433 K, injection temperature: 523K; detector temperature (FID): 523 K; carrier gas (nitrogen) flow rate = 30 ml/min. The quantitative analytical procedure had relative accuracy within 2 %. Calibration factors were determined by using liquid standards having known compositions of *p*-nitrophenol and *p*-aminophenol**.** The water content in ethanol was measured by Karl-Fischer method.

4.2.4 Typical experimental procedure

In a typical hydrogenation experiment, 1% Pt/C (8mg, 0.266 kg/m^3), *p*-nitrophenol (2 gm, 0.4792 kmol/m^3) and 30 ml ethanol (90 %) were charged into a clean autoclave. The contents were flushed with nitrogen to ensure removal of traces of oxygen from the reactor. The reactor was then heated to 353 K under slow stirring (100 rpm) and the temperature was allowed to stabilize at the desired set point. Then, hydrogen gas was introduced to a desired level (2.72MPa) and the contents stirred vigorously (1000 rpm). The reactor was operated at a constant pressure throughout the reaction period by supplying hydrogen from a reservoir vessel using a constant pressure regulator. The pressure drop in the reservoir vessel was measured as a function of time using a digital pressure transducer. After completion of the reaction, the reactor was cooled and the excess gas was vented off. The product *p*-aminophenol was separated as a solid product in the autoclave due to its low solubility in the reaction medium at room temperature. The reaction mass was further diluted to 60 ml by acetonitrile and the resulting solution was analyzed on GC for *p*-nitrophenol and *p*-aminophenol content. The typical GC analysis charts are shown in Figure 4-1.

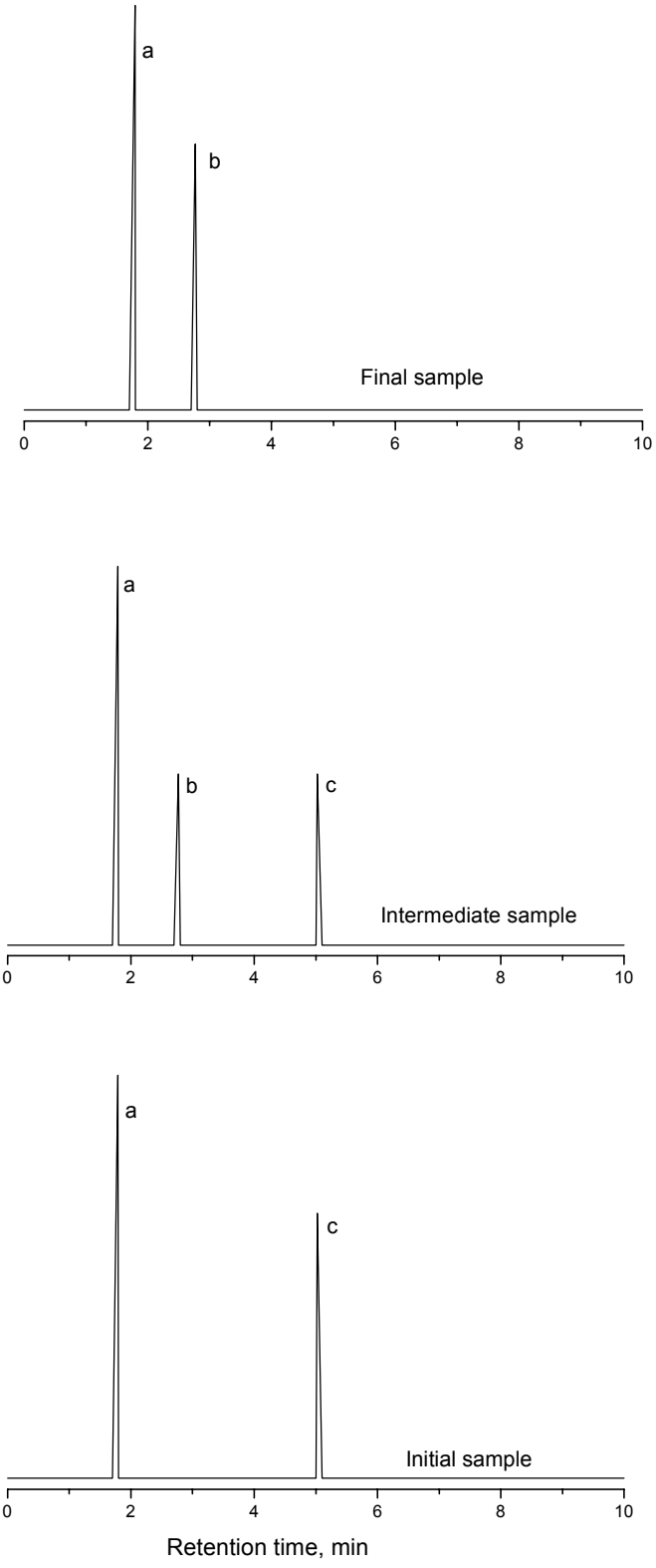

Figure 4-1: Representative gas chromatographic analysis charts
(a) Solvent (ethanol/acetonitrile), (b) p-Aminophenol, (c) p-Nitrophenol

4.3 Results and discussion

The hydrogenation of *p*-nitrophenol (Scheme 4-1) using 1% Pt/C catalyst was investigated in a batch slurry reactor in which concentration-time and hydrogen consumption data were obtained. The experimental results were expressed in terms of initial hydrogenation rate and average catalytic activity. The initial hydrogenation rate (R_A) was calculated from the hydrogen consumption-time data, essentially under low conversion conditions (<15 %). The average catalytic activity (N) expressed as kmol/kg.hr, was defined as the amount of *p*-nitrophenol consumed per unit weight of the catalyst per hour, based on the time required to achieve more than 99% conversion of *p*-nitrophenol. In a few initial experiments, the amount of hydrogen consumed was compared with the amount of *p*-nitrophenol consumed and *p*-aminophenol formed, which indicated almost 99% stoichiometric material balance without formation of any other side products in appreciable quantities. The typical concentration-time profiles for hydrogenation of *p*-nitrophenol to *p*-aminophenol are shown in Figure 4-2.

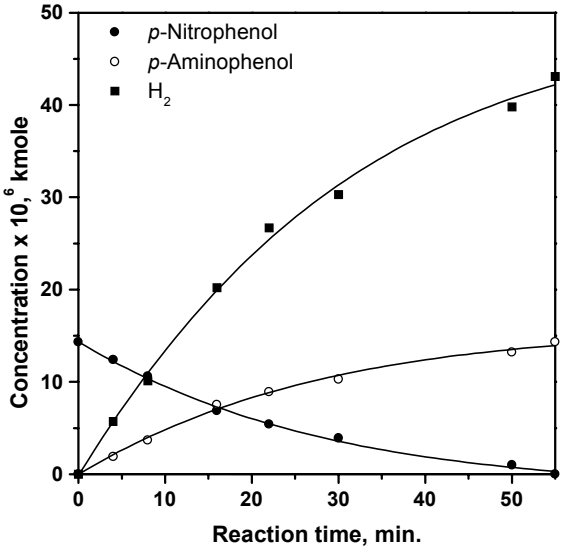

Figure 4-2: Typical concentration-time profile for hydrogenation of *p*-nitrophenol.
Reaction conditions: *p-Nitrophenol: 0.479 kmol/m³; catalyst (1% Pt/C): 0.266 kg/m³; ethanol (90%): 30× 10⁻⁶ m³; H₂ pressure: 2.72 MPa; temperature: 353 K; agitation: 1000 rpm.*

The effect of various reaction parameters was studied and the results are discussed below.

4.3.1 Catalyst selection

The activity of various supported transition metal catalysts for the hydrogenation of *p*-nitrophenol to *p*-aminophenol in ethanol (90%) solvent was investigated at 353 K and 2.72 MPa of hydrogen pressure and the results are presented in Table 4-1. The initial hydrogenation rate and catalytic activity for different transition metal catalysts followed the order Pt>Pd>Ni>Rh>Ru. Ruthenium showed least catalytic activity (only 10% conversion in 5 hours), whereas platinum had the highest activity. The typical hydrogen consumption profiles using different catalysts are compared in Figure 4-3.

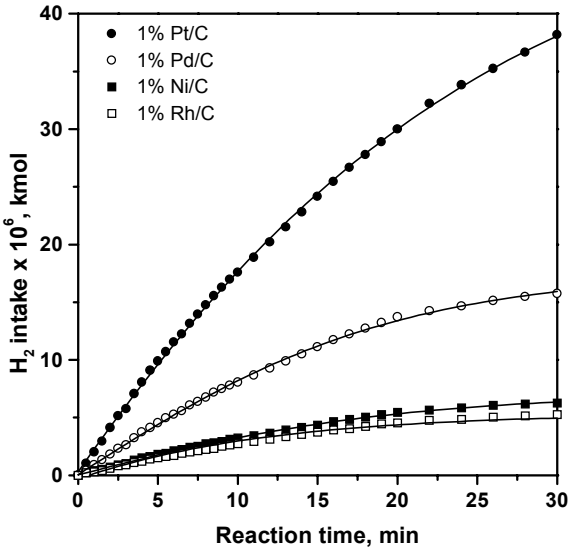

Figure 4-3: Effect of transition metal catalysts on the hydrogen consumption profiles.
Reaction conditions: *p-Nitrophenol: 0.479 kmol/m³; ethanol: 30×10⁻⁶m³; catalyst: 0.266 kg/m³; H₂ pressure: 2.72 MPa; temperature: 353 K; agitation: 1000 rpm.*

Table 4-1: Effect of transition metal catalyst on the initial rate of hydrogenation and catalytic activity of hydrogenation of *p*-nitrophenol to *p*-aminophenol

Sr.	***Catalyst***	$R_A \times 10^3$ ***(kmol/m³.s)***	***N (kmol/kg.hr)***
1	*1% Pt/C*	*1.096*	*1.960*
2	*1% Pd/C*	*0.501*	*0.595*
3	*1% Ni/C*	*0.199*	*0.446*
4	*1% Rh/C*	*0.166*	*0.380*
5	*1% Ru/C*	*0.016*	*0.034*

Reaction conditions: *p-Nitrophenol: 0.479 kmol/m³; ethanol (90%): 30×10⁻⁶m³; catalyst: 0.266 kg/m³; H_2 pressure: 2.72 MPa; temperature: 353 K; agitation: 1000 rpm.*

4.3.2 Effect of catalyst support

The effect of catalyst support on the activity of supported Pt catalysts (Table 4-2) indicated that the average catalytic activity of the carbon supported Pt catalyst was highest. The hydrogen consumption profiles for these experiments are compared in Figure 4-4.

Table 4-2: Effect of support on initial rate of hydrogenation and catalytic activity for hydrogenation of *p*-nitrophenol to *p*-aminophenol.

Sr. No.	***Catalyst***	$R_A \times 10^3$ ***(kmol/m³.s)***	***N (kmol/kg.hr)***
1	*1% Pt/C*	*1.096*	*1.960*
2	*1% Pt/Al_2O_3*	*0.333*	*0.812*
3	*1% Pt/SiO_2*	*0.109*	*0.185*
4	*1% Pt/HY*	*0.082*	*0.131*

Reaction conditions: *p-Nitrophenol: 0. 479 kmol/m³; ethanol (90%): 30×10⁻⁶m³; catalyst: 0.266 kg/m³; H_2 pressure: 2.72 MPa; temperature: 353 K; agitation: 1000 rpm.*

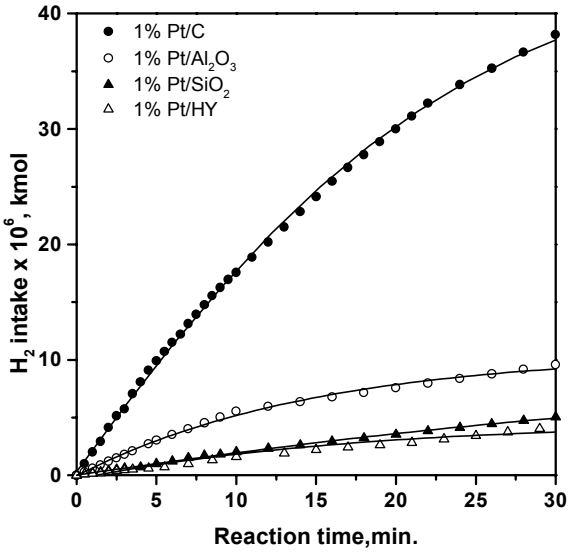

Figure4-4: Effect of catalyst support on hydrogen consumption profiles.
Reaction conditions: *p-Nitrophenol: 0.479 kmol/m³; ethanol (90%): 30×10⁻⁶m³; catalyst: 0.266 kg/m³; H₂ pressure: 2.72 MPa; temperature: 353 K; agitation: 1000 rpm.*

4.3.3 Effect of metal loading

The effect of metal content on the initial rate of hydrogenation for various Pt/C catalysts is shown in Table 4-3. The observed rates followed the expected trend with platinum content showing nearly a linear dependence. This also suggested that the observed hydrogenation rates correspond to the intrinsic rates of reaction because the rates are linearly dependent on the Pt metal loading. The hydrogen consumption profiles for Pt catalyst are shown in Figure 4-5. In all these cases, the selectivity of *p*-aminophenol also remained very high (> 99%).

Table 4-3: Effect of Pt content in Pt/C catalyst on initial rate of hydrogenation and catalytic activity for hydrogenation of *p*-nitrophenol.

Sr. No.	***Catalyst***	***$R_A \times 10^3$ (kmol/m³.s)***	***N (kmol/kg.hr)***
1	*0.5% Pt/C*	*0.524*	*1.347*
2	*1% Pt/C*	*1.096*	*1.960*
3	*2% Pt/C*	*2.034*	*2.412*
4	*3% Pt/C*	*2.895*	*3.017*

Reaction conditions: *p-Nitrophenol: 0.479 kmol/m³; ethanol: 30×10⁻⁶m³; catalyst: 0.266 kg/m³; H₂ pressure: 2.72 MPa; temperature: 353 K; agitation: 1000 rpm.*

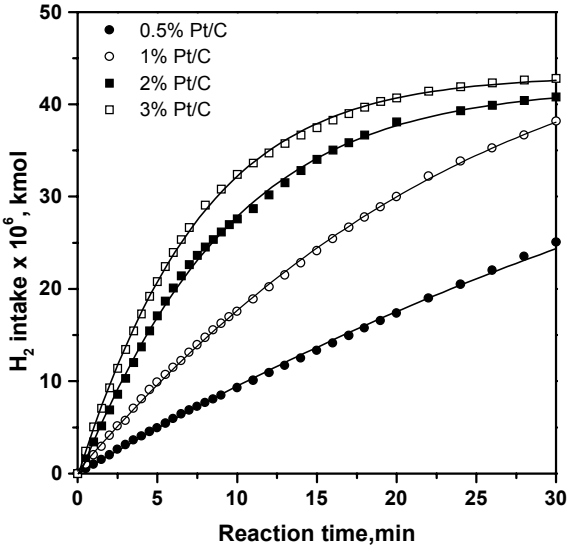

Figure 4-5: Effect of Pt content in Pt/C catalyst on the hydrogen consumption profiles.
Reaction conditions: *p-Nitrophenol: 0.479 kmol/m³; ethanol (90%): 30×10⁻⁶ m³; catalyst: 0.266 kg/m³; H₂ pressure: 2.72 MPa; temperature: 353 K; agitation 1000 rpm.*

4.3.1.4 Effect of solvent

The effect of solvents on the initial rate of hydrogenation and average catalytic activity was also investigated using 1% Pt/C catalyst at 353 K. The solvents used for this study included water, methanol, ethanol, *n*-propanol, *n*-butanol. The results are presented in Table 4.4. The average catalytic activity and initial rate of hydrogenation was highest in water as a solvent and lowest for *n*-butanol. It was observed that both, hydrogenation rate and catalytic activity increased with increase in polarity of the solvent. Such enhancement in the reaction rates and catalytic activity with increasing polarity has been observed earlier by Karwa et al. [9] for hydrogenation of nitrobenzene to aniline and was partly attributed to increase in the activity of nitro compounds in polar solvents. This conclusion was further supported by the effect of water content on the catalytic activity and the initial rate of hydrogenation, which increased with water content (Figure 4-6). All subsequent

kinetic experiments for the hydrogenation of *p*-nitrophenol to *p*-aminophenol were carried out using 90% ethanol as the solvent and 1% Pt/C catalyst.

Table 4-4: Effect of solvent on initial rate of hydrogenation and catalytic activity during hydrogenation of *p*-nitrophenol.

Sr.No.	***Solvent***	***Dielectric constant*** [a] ***(ε)***	$R_A \times 10^3$ ***(kmol/m³.s)***	***N (kmol/kg.hr)***
1	*Water*	*78.5*	*1.325*	*3.066*
2	*Methanol*	*32.6*	*1.170*	*2.160*
3	*Ethanol*	*24.3*	*1.096*	*1.960*
4	*n-Propanol*	*20.1*	*0.776*	*1.790*
5	*n-Butanol*	*17.80*	*0.406*	*0.342*

Reaction conditions: *p-Nitrophenol: 0.479 kmol/m³; solvent: 30×10⁻⁶ m³; 1%Pt/C: 0.266 kg/m³; H_2 pressure: 2.72 MPa; temperature: 353 K; agitation: 1000 rpm, a= from CRC Handbook.*

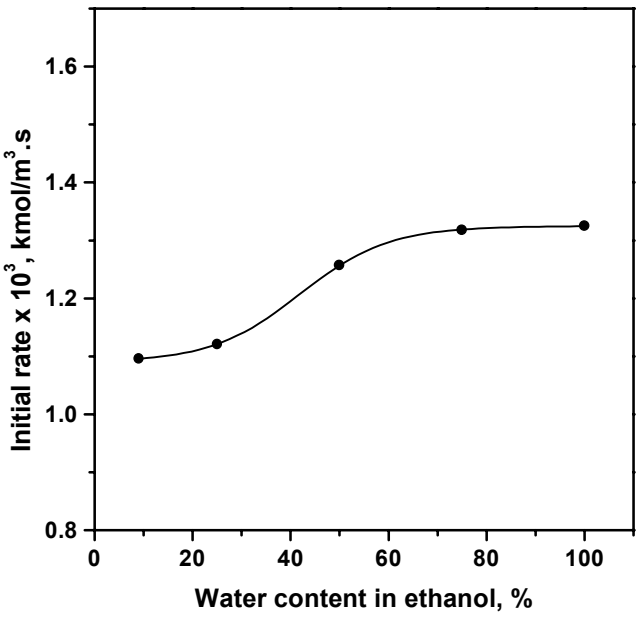

Figure 4.6: Effect of water content in ethanol on initial rate of hydrogenation and catalytic activity.
Reaction conditions: *p-Nitrophenol: 0.479 kmol/m³; ethanol: 30×10⁻⁶ m³; 1% Pt/C: 0.266 kg/m³; H_2 pressure: 2.72 MPa; temperature: 353 K; agitation: 1000 rpm.*

4.3.1.5 Effect of hydrogen pressure

The effect of hydrogen partial pressure on the initial rate of hydrogenation and average catalytic activity was also studied in the range of 1.36 to 6.80 MPa at 353 K, keeping all other parameters constant. The initial rate of hydrogenation increased with hydrogen pressure upto 4.08 MPa and thereafter it remained unchanged. The average catalytic activity also followed a similar trend. The results are presented in Figure 4-7. The typical hydrogen consumption-time profiles at various hydrogen partial pressures are shown in Figure 4-8.

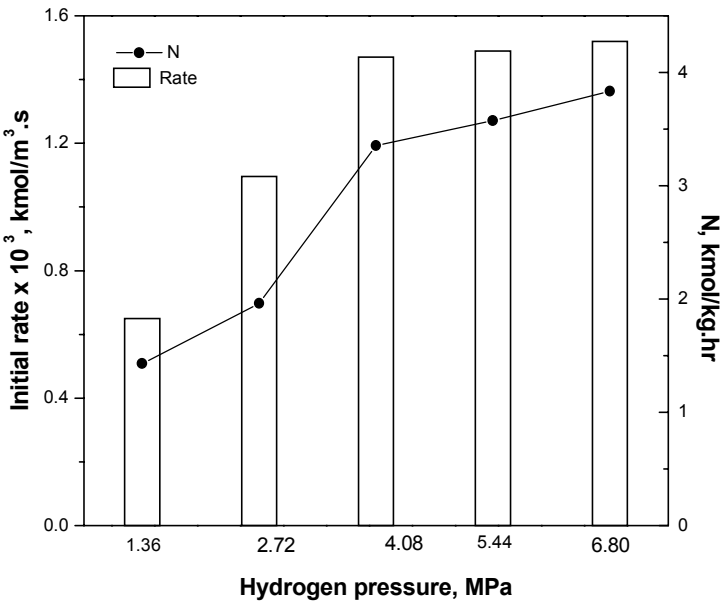

Figure 4-7: Effect of Hydrogen pressure on initial rate of hydrogenation and catalytic activity.
Reaction conditions: *p-Nitrophenol: 0.479 kmol/m³; 1% Pt/C: 0.266 kg/m³; temperature: 353 K; ethanol: 30×10⁻⁶m³; agitation: 1000 rpm.*

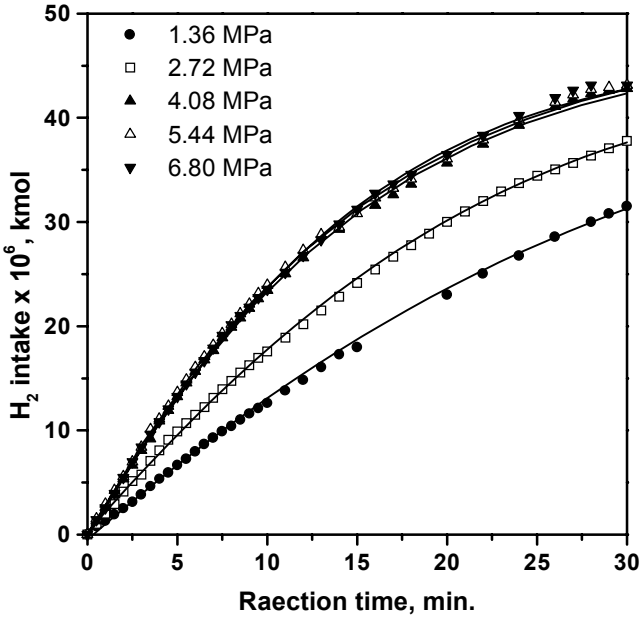

Figure 4-8: Effect of hydrogen partial pressure on hydrogen consumption profiles. ***Reaction conditions:*** *p-Nitrophenol: 0.479 kmol/m³; 1%Pt/C: 0.266 kg/m³; temperature: 353 K; ethanol, 30×10⁻⁶m³; agitation, 1000 rpm.*

4.3.1.6 Effect of substrate concentration

The effect of *p*-nitrophenol concentration on the initial rate of hydrogenation and activity of the catalyst was studied in the range of 0.119 to 0.958 kmol/m³ at 353 K. It was observed that the initial rate of hydrogenation increased with *p*-nitrophenol concentration upto 0.479 kmol/m³ beyond which it remained almost constant, as shown in Figure 4-9. The activity of the catalyst was found to increase with *p*-nitrophenol concentration. The hydrogen consumption-time profiles are presented in Figure 4-10.

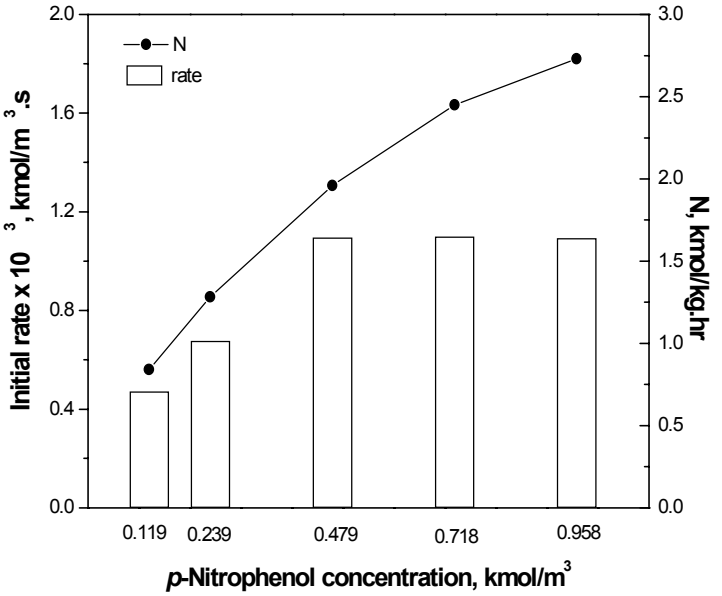

Figure 4-9: Effect of *p*-nitrophenol concentration on initial rate of hydrogenation and catalytic activity.
Reaction conditions: *1%Pt/C: 0.266 kg/m³; ethanol: 30×10⁻⁶ m³; H₂ pressure: 2.72 MPa; temperature: 353 K; agitation: 1000 rpm.*

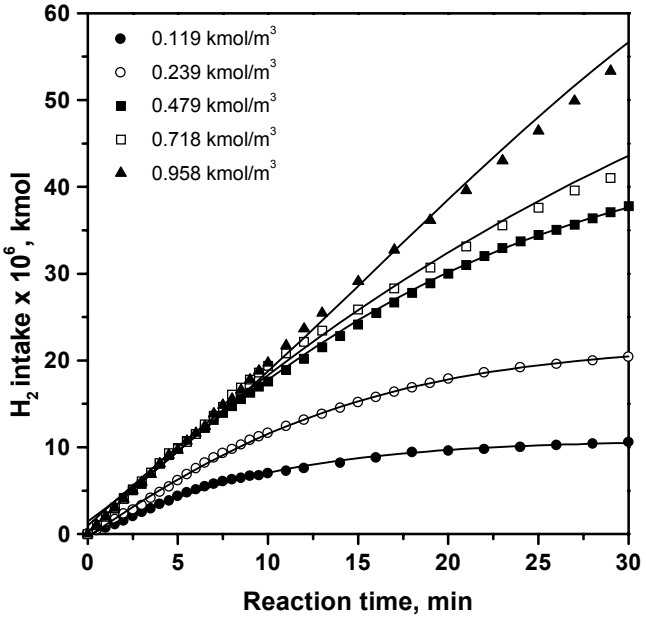

Figure 4-10: Effect of *p*-nitrophenol concentration on hydrogen consumption profiles.
Reaction conditions: *1%Pt/C: 0.266 kg/m³; ethanol: 30×10⁻⁶ m³; H₂ pressure: 2.72 MPa; temperature: 353 K; agitation: 1000 rpm.*

4.3.1.7 Effect of temperature

To study the effect of reaction temperature, the reactions were carried out in a temperature range of 308 K to 353 K at a hydrogen partial pressure of 2.72 MPa and 1000 rpm speed of agitation. The initial rate of hydrogenation as well as the average catalytic activity increased with temperature. The hydrogen consumption profiles at different temperatures are shown in Figure 4-11.

Table 4-5: Effect of temperature on initial rate of hydrogenation and average catalytic activity

Temperature (K)	***$R_A \times 10^3$ (kmol/m³.s)***	***N (kmol/kg.hr)***
308	*0.128*	*0.524*
323	*0.313*	*1.117*
338	*0.557*	*1.469*
353	*1.096*	*1.961*

Reaction conditions: *p-Nitrophenol: 0.479 kmol/m³; ethanol: 30×10⁻⁶m³; 1%Pt/C: 0.266 kg/m³; H_2 pressure: 2.72 MPa; agitation: 1000 rpm.*

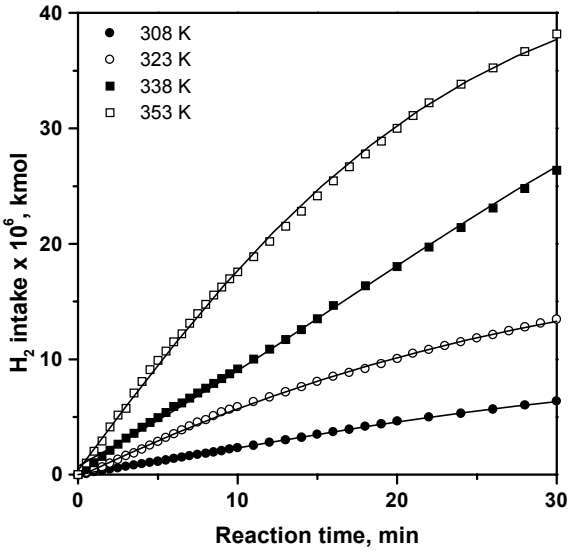

Figure 4-11: Effect of temperature on hydrogen consumption profiles
Reaction conditions: *p-Nitrophenol: 0.479 kmol/m³; ethanol: 30× 10⁻⁶m³; 1% Pt/C: 0.266 kg/m³; H_2 pressure: 2.72 MPa; agitation: 1000 rpm.*

4.3.2 Kinetic Studies

The preliminary experiments showed that with 1% Pt/C catalyst, initial hydrogenation of *p*-nitrophenol to *p*-aminophenol occurred selectively with material balance agreement more than 99 % (Figure 4-2). Therefore, for all kinetic runs, the rate measurements were followed by the observed hydrogen consumption-time data. It was also noted that no hydrogenation occurred in the absence of a catalyst, indicating the absence of any non-catalytic reaction. A few initial experiments were repeated to check the reproducibility, which indicated that reproducible results were obtained with an average error of less than 3%. The range of reaction conditions investigated is given in Table 4-6.

Table 4-6: Range of operating conditions

Parameters	***Range***
Temperature, K	*308 - 353*
Hydrogen pressure, MPa	*1.36 - 6.80*
Catalyst loading, kg/m³	*0.133 - 0.399*
p-Nitrophenol concentration, kmol/m³	*0.119 - 0.958*
Agitation speed, rpm	*600 - 1200*

4.3.8.1 Solubility measurement

The hydrogenation of *p*-nitrophenol is an example of a multiphase (gas-liquid-solid) catalytic reaction system and therefore, it was important to ensure that mass transfer effects were either eliminated or accounted for while determining the intrinsic reaction kinetics. In order to ascertain the importance of mass transfer effects, it was essential to know the solubility of hydrogen in aqueous ethanol. Since these data were not available in the literature for the required conditions, the

solubility was experimentally measured. The solubility of hydrogen in ethanol (90%) was measured using an absorption technique in a pressure autoclave. In a typical experiment for solubility measurement, a known volume of 90% ethanol (30 cm^3) was charged into the reactor and the contents were heated to a desired temperature. After the thermal equilibrium was attained, the void space above the liquid phase was pressurized with hydrogen to the required level ($P_{initial}$). The contents were then stirred vigorously till the gas-liquid equilibrium was established. To ensure the gas-liquid equilibrium, the contents were stirred till there was no further gas absorption. The final pressure in the reactor was recorded as P_{final}. The vapor pressure of the solvent was subtracted in calculating the $P_{initial}$ and P_{final} values. From the initial and final pressure readings the solubility of the gas was calculated as,

$$S = \frac{(P_{initial} - P_{final})V_G}{RTV_L} \tag{4.1}$$

Where, S is solubility of hydrogen, (kmol/m^3); $P_{initial}$ is initial pressure of hydrogen, (MPa); P_{final} is final pressure of hydrogen, (MPa); V_G is volume of gas, (m^3); V_L is volume of liquid, (m^3); R is Gas constant, (m^3. MPa $kmol^{-1}$. K^{-1}) and T is absolute temperature, (K).

For calculation of the solubility, it was assumed that under the equilibrium conditions, the volume expansion due to dissolved gas in the liquid phase was negligible. The solubility of hydrogen in ethanol (90%) was measured at different partial pressures of hydrogen and temperatures. The Henry's law constant H was calculated as,

$$H = \frac{S}{P_{final}} \tag{4.2}$$

The solubility data were determined in a temperature range of 308-353 K and the results are presented in Table 4-7.

Table 4-7: Solubility of hydrogen in ethanol (90%) at different temperatures

308 K		***323 K***		***338 K***		***353 K***	
P	***S×10²***	***P***	***S×10²***	***P***	***S×10²***	***P***	***S×10²***
1.447	*4.91*	*1.467*	*5.15*	*1.398*	*5.06*	*1.881*	*7.02*
2.687	*9.13*	*2.728*	*9.58*	*2.825*	*10.23*	*3.032*	*11.32*
3.445	*11.71*	*3.376*	*11.85*	*3.500*	*12.68*	*3.576*	*13.35*
4.272	*14.52*	*4.293*	*15.07*	*4.217*	*15.28*	*4.238*	*15.82*
6.050	*20.56*	*6.140*	*21.56*	*5.630*	*20.40*	*6.126*	*22.87*
7.028	*23.89*	*6.815*	*23.93*	*6.904*	*25.02*	*7.104*	*26.53*

P = hydrogen pressure, MPa and S = solubility, kmol/m³

The solubility of hydrogen was found to increase with hydrogen partial pressure at all the temperatures. The linear dependence of solubility on the partial pressure was in accordance with the Henry's law. The values of Henrys constant calculated from the above data using equation 4.2 are given in Table 4-8.

Table 4-8: Henry's constant for hydrogen in ethanol (90%)

Temperature, K	***H×10², kmol/m³.MPa***
308	*3.399*
323	*3.511*
338	*3.624*
353	*3.734*

4.3.8.2 Analysis of initial rate data

Analysis of initial rate data provides a first approach for understanding the dependency of the reaction rate on individual parameters and also in the evaluation of significance of mass transfer effects. As mentioned earlier, the initial rates were calculated from the slope of the hydrogen consumption *vs* time plots during the initial period of reaction such that the conversion of *p*-nitrophenol was less than 10-15 % and differential conditions prevailed. The effect of catalyst loading, speed of agitation, hydrogen partial pressure and *p*-nitrophenol concentration was studied in a temperature range of 308-353 K. The effect of catalyst loading on the initial rate at different temperatures is shown in Figure 4.12. The rate was found to vary linearly with catalyst loading at all temperatures indicating that gas-liquid mass transfer resistance may not be significant under the prevailing reaction conditions.

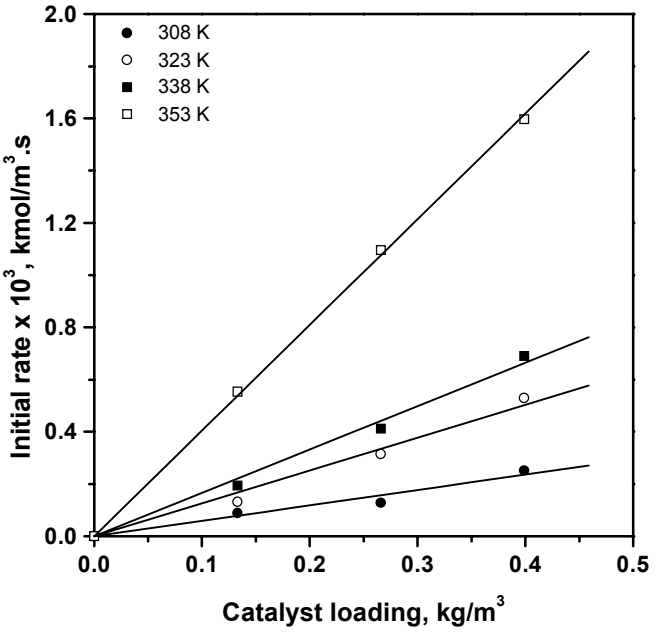

Figure 4-12: Effect of catalyst loading on initial rate of hydrogenation.
Reaction conditions: *p-Nitrophenol: 0.479 kmol/m³; ethanol (90%): 30×10⁻⁶ m³; pressure: 2.72 MPa.; agitation: 1000 rpm.*

To further confirm the significance of gas-liquid mass transfer resistance, the effect of agitation frequency on the rate of hydrogenation was studied. The results presented in Figure 4-13 at different temperatures, clearly indicated that the hydrogenation rate was independent of agitation frequency above 700 rpm and hence, the reaction could be assumed to operate in the kinetic regime.

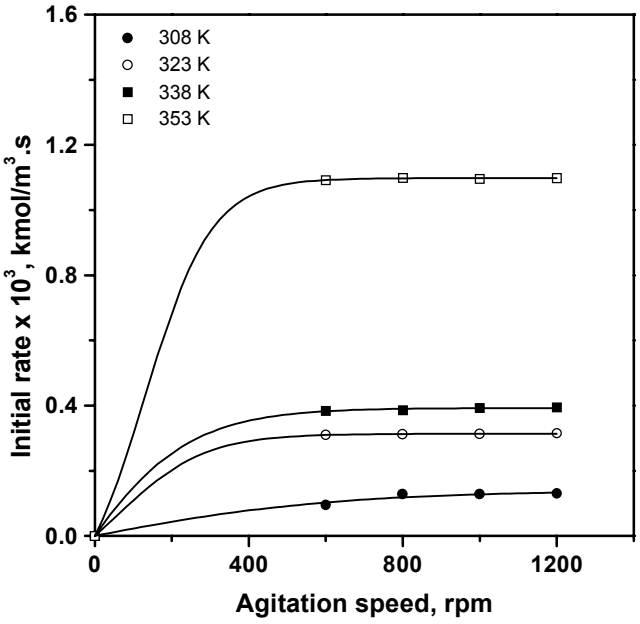

Figure 4-13: Effect of agitation frequency on initial rate of hydrogenation.
Reaction conditions: *p-Nitrophenol: 0.479 kmol/m³; ethanol: 30×10⁻⁶m³; 1% Pt/C: 0.266 kg/m³; pressure: 2.72 MPa.*

The effect of hydrogen partial pressure on the initial rate of hydrogenation was investigated at different temperatures and the results are presented in Figure 4-14. The initial rate of hydrogenation increased linearly with hydrogen partial pressure upto 4.08 MPa, but further increase in hydrogen pressure did not affect the hydrogenation rate very significantly at all the temperatures. The initial rate dependence on the partial pressure of hydrogen suggests that the surface reaction may be rate-controlling [10].

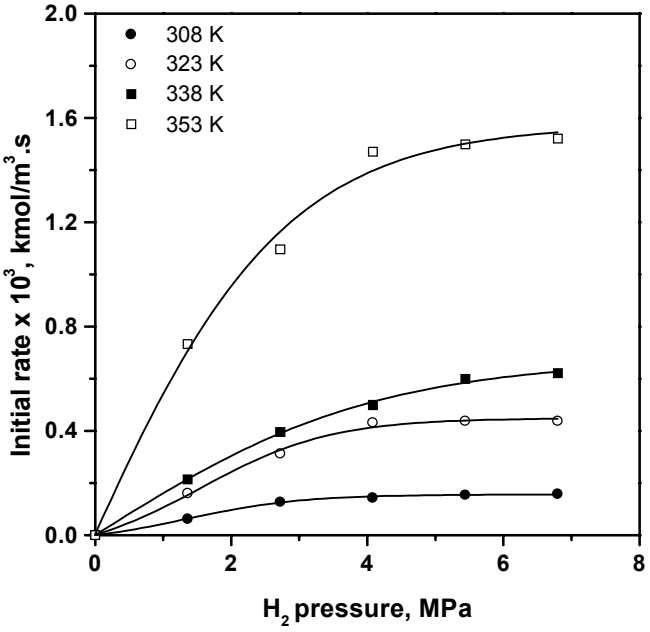

Figure 4-14: Effect of hydrogen pressure on initial rate of hydrogenation.
Reaction conditions: *p-Nitrophenol: 0.479 kmol/m³; ethanol: 30×10⁻⁶m³; 1% Pt/C: 0.266 kg/m³; agitation: 1000 rpm.*

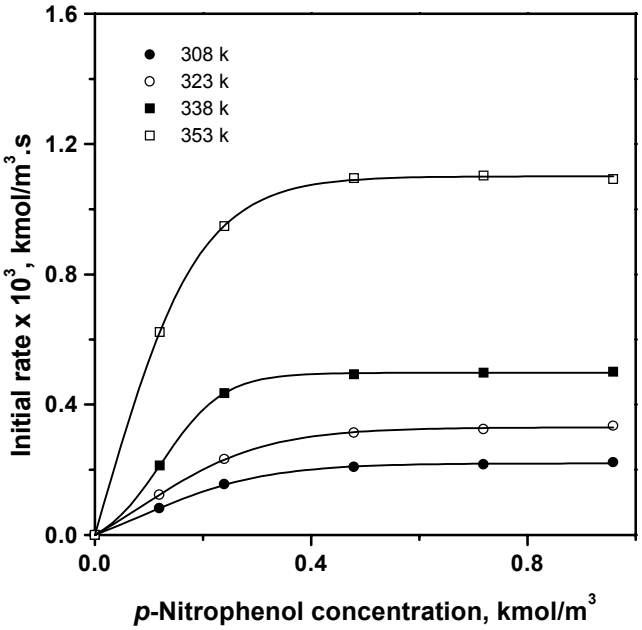

Figure 4-15: Effect of *p*-nitrophenol concentration on initial rate of hydrogenation.
Reaction conditions: *1% Pt/C: 0.266 kg/m³; ethanol: 30×10⁻⁶m³; pressure: 2.72 MPa; agitation: 1000 rpm.*

The effect of *p*-nitrophenol concentration on the initial rate of reaction was also investigated at different temperatures and the results are given in Figure 4-15. The hydrogenation rate showed a first order dependence at lower concentrations of *p*-nitrophenol beyond which, it was independent of initial concentration of *p*-nitrophenol.

4.3.8.3 Analysis of mass transfer effects

For the purpose of kinetic study, it was important to ensure that the rate data were obtained under kinetically controlled regime. In a three-phase slurry reactor, gas-liquid, liquid-solid and intraparticle diffusion resistances are likely to exist. In order to analyze the contribution of these mass transfer steps, quantitative criteria suggested by Ramchandran and Chaudhari [11] were used. Thus, the factors, α_1, α_2, and ϕ_{exp}. which represent the ratios of the observed rate of reaction to the maximum possible rates of gas-liquid, liquid–solid and intraparticle mass transfer rates, respectively were calculated from the initial rate data for all temperatures. The gas to liquid mass transfer can be considered unimportant if

$$\alpha_1 = \frac{R_A}{k_L a_B A^*} < 0.1 \tag{4.3}$$

Where, R_A is rate of hydrogenation, (kmol/m^3.s); k_L is gas-liquid mass transfer coefficient, (m/s); a_B is effective gas-liquid interfacial area, (m^2/m^3) and A^* is dissolved concentration of hydrogen, (kmol/m^3).

The solubility of hydrogen in the reaction medium determined experimentally (Table 4-7) was used in the calculation of α_1 value. The values of $k_L a_B$ can be calculated using the correlations described in the literature. However, in this work, $k_L a_B$ values were experimentally determined using the dynamic absorption method

[11]. This procedure was similar to that used for the solubility determination except that the dynamics of the gas-liquid equilibrium was studied as a function of time at a preset agitation frequency (1000 rpm), at a given pressure (2.72 MPa) and temperature. The concentration of dissolved hydrogen in the liquid phase (A_L) was measured as a function of time. The concentration change in the liquid was correlated to the mass transfer coefficient as:

$$k_L a_B = -\frac{1}{t}\ln\left[1 - \frac{A_L}{A^*}\right] \tag{4.4}$$

Thus, a semi log plot of (1-A_L/A^*) versus t gives a slope equal to - $k_L a_B$. The values of $k_L a_B$ obtained thus at different temperatures are given in Table 4-9. The liquid-solid mass transfer resistances can be considered negligible, if

$$\alpha_2 = \frac{R_A}{k_S a_P A^*} < 0.1 \tag{4.5}$$

Where, k_s is liquid-solid mass transfer coefficient, (m/s); a_P is effective liquid-solid interfacial area per unit volume of slurry (m^2/m^3). The effective liquid-solid interfacial area a_P can be calculated using following equation.

$$a_P = \frac{6w}{\rho_P d_P} \tag{4.6}$$

Where, w is catalyst loading, (kg/m^3); ρ_P is particle density, (kg/m^3); d_p is particle diameter, (m).

The liquid-solid mass transfer coefficient (k_s) was calculated using a correlation proposed by Sano et al. [12]:

$$\frac{k_S a_P}{DF_C} = 2 + 0.4\left[\frac{ed_P^4\rho_L^3}{\mu_L^3}\right]^{0.25}\left[\frac{\mu_L}{\rho_L D}\right]^{0.33} \tag{4.7}$$

Where, d_P is average diameter of the catalyst particle, (m); D is diffusion coefficient of hydrogen in liquid phase, (m^2/s); F_C is shape factor of the catalyst; e is energy supplied to the liquid per unit mass, (m^2/s^3); ρ_L is density of the liquid, (kg/m^3); μ_L is viscosity of the liquid (cp).

The density and viscosity of solvent was taken from literature report [21]. The energy supplied to the liquid per unit mass, e, in the above equation was calculated as [13]:

$$e = \frac{N_P N^3 d_I^5 \Psi}{\rho_L V_L} \tag{4.8}$$

where, N_P is power number; N is agitation speed (Hz); d_I is diameter of the agitator (m); ρ_L = density of the liquid, (kg/m^3); V_L is volume of the liquid, (m^3)

Here, Ψ is a correction factor for the presence of gas bubbles and is given by the correlation proposed by Calderbank [13]:

$$\Psi = 1.0 - 1.26\left[\frac{Q_G}{Nd_l^3}\right] \qquad \text{for} \qquad \frac{Q_G}{Nd_l^3} < 3.5 \times 10^{-2} \tag{4.9}$$

and

$$\Psi = 0.62 - 1.85\left[\frac{Q_G}{Nd_l^3}\right] \qquad \text{for} \qquad \frac{Q_G}{Nd_l^3} > 3.5 \times 10^{-2} \tag{4.10}$$

where, Q_G is the volumetric flow rate of gas, m^3/s. Since, a batch autoclave was used in this work, gas was not continuously bubbled, but was supplied as per the consumption to maintain a constant pressure. Therefore in the above calculations, Q_G, the volumetric flow rate of the gas was calculated as,

$$Q_G = R_{\max} \times V_L \times V_m \tag{4.11}$$

where, R_{max} is maximum rate of hydrogenation, $kmol/m^3.s$ and V_m is molar gas volume, $m^3/kmol$. For actual calculations, Q_G, was taken as 20% excess of that calculated by the above equation. The values of $k_l a_B$ and k_s were calculated as described above and are presented in Table 4-9.

Table 4-9: Gas-liquid and liquid-solid mass transfer coefficients at different temperatures

Temperature, K	***$K_L a_B$, s^{-1}***	***k_s, m/s***
308	*0.145*	*0.134*
323	*0.167*	*0.175*
338	*0.188*	*0.216*
353	*0.210*	*0.257*

The significance of intraparticle diffusion can be evaluated using the criteria based on experimental Thiele parameter (ϕ_{exp}) defined as [14];

$$\Phi_{\exp} = \frac{d_P}{6}\left[\frac{\rho_P R_A}{D_e w A_S}\right]^{0.5} \tag{4.12}$$

The intraparticle diffusion resistance can be assumed to be negligible for $\phi_{exp} < 0.2$. The effective diffusivity, D_e required in equation 4-12 was calculated as:

$$D_e = \frac{D\varepsilon}{\tau} \tag{4.13}$$

where, D is diffusion coefficient, m^2/s; ε is porosity of the catalyst and τ is tortuosity factor.

The molecular diffusion coefficients were calculated from Wilke-Chang equation [15], and the tortuosity factor was assumed as 3.0, the average value observed for carbon particles [16]. The diffusivity data are presented in Table 4-10. The value of A_S, the surface concentration of dissolved hydrogen was considered to be equal to A^* (calculated as= $P_{eq} \times H$), since external mass transfer resistances were found to be negligible.

Table 4-10: Diffusivity data of hydrogen in ethanol

Temperature (K)	***Molecular diffusivity ($D \times 10^9$ m^2/s)***	***Effective diffusivity ($D_e \times 10^9$ m^2/s)***
308	*3.337*	*0.556*
323	*4.907*	*0.817*
338	*6.903*	*1.150*
353	*9.457*	*1.570*

The calculated values of factors α_1, α_2, and $\phi_{exp.}$, were less than 0.1, 0.1 and 0.2 respectively for all the rate data and hence the gas-liquid, liquid-solid and intraparticle mass transfer resistances can be assumed to be negligible.

4.3.8.4 Kinetic modeling

The rate data obtained were fitted to different rate equations based on langmuir-Hinshelwood (L-H) or Eley-Rideal type models given in Table 4-11. In order to estimate the kinetic constants, the individual rate equation was subjected to a non-linear regression analysis using an optimization routine based on Marquard's method [17]. The objective function was chosen as follows:

$$\Phi = \sum_{i=1}^{n} (r_{exp} - r_{mod})_i^2 \qquad (4.14)$$

Where, r_{exp} is observed rate of hydrogenation and r_{mod} is predicted rate of hydrogenation.

The non-linear regression analysis was performed to estimate the kinetic constants such that the objective function ϕ has the minimum value. The values of the kinetic constants obtained using optimization program for different models are given in Tables 4-11. Since the magnitude of ϕ for all the models was more or less the same, model discrimination was necessary. The analysis of the experimental data was performed purely on the mathematical basis and therefore it did not account for the thermodynamic significance of the kinetic constants. Thus, according to the thermodynamic criteria suggested by Kittrel [18], the values for the kinetic constants have to satisfy certain conditions, which are derived from the thermodynamic considerations.

Table 4-11: Rate equations used and parameters obtained

Model	*Rate equation*	*Temperature (K)*	k_1 *(m³/kg)(m³/kmol.s)*	K_A *(m³/kmol)*	K_B *(m³/kmol)*	ϕ_{min}
I	$R_A = \frac{wk_1AB}{(1+k_AA)(1+k_BB)}$	*308*	2.026×10^{-2}	*5.741*	*4.262*	2.367×10^{-9}
		323	3.086×10^{-2}	*6.232*	*4.394*	6.970×10^{-9}
		338	4.501×10^{-2}	*4.487*	*6.166*	1.250×10^{-9}
		353	17.09×10^{-2}	*7.249*	*7.476*	5.117×10^{-8}
II	$R_A = \frac{wk_1AB}{(1+k_AA+K_BB)}$	*308*	*3.0901*	2.606×10^{3}	9.837×10^{2}	2.385×10^{-9}
		323	*4.8422*	2.843×10^{3}	1.077×10^{3}	7.374×10^{-9}
		338	*14.774*	5.453×10^{3}	2.824×10^{3}	1.763×10^{-9}
		353	*64.484*	1.029×10^{4}	4.321×10^{3}	1.008×10^{-7}
III	$R_A = \frac{wk_1AB}{(1+k_AA+K_BB)^2}$	*308*	1.927×10^{-2}	*3.890*	*1.489*	1.625×10^{-9}
		323	3.048×10^{-2}	*4.166*	*1.623*	4.339×10^{-9}
		338	3.771×10^{-2}	*3.396*	*1.704*	2.106×10^{-9}
		353	15.88×10^{-2}	*5.529*	*2.300*	2.824×10^{-8}

A= Liquid phase concentration of hydrogen (kmol/m^3); B= Liquid phase concentration of *p*-nitrophenol (kmol/m^3);

These constraints are

Rule 1: $k > 0$ (k should be a positive value)

Rule 2: $E_a > 0$ (energy of activation should be positive)

All models had positive values for kinetic parameters and therefore individual models cannot be discriminated using this criterion. A closer look at the Table 4-11 indicates that the kinetic constants for models I and III did not follow a general trend (either decreasing or increasing) with temperature and therefore can be rejected, whereas Model II satisfied all the constraints. The activation energy calculated using the Arrhenius plots (Figure 4-16) for various kinetics constants (model II) is given in Table 4-12.

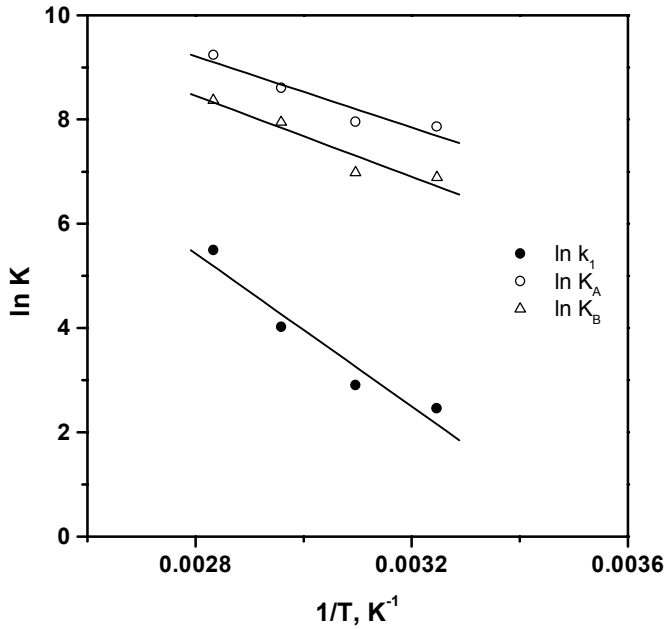

Figure 4-16: Temperature dependence of rate and adsorption equilibrium constants for model-II

Table 4-12: Activation energies and heats of adsorption calculated for Model – II.

Parameter	***E (kJ/mol)***
k_1	*60.980*
K_A	*28.402*
K_B	*32.312*

In order to assess the adequacy of the rate model II and accuracy of the kinetic constants, the results of the fittings were analyzed using the statistical criteria suggested by Kittrel [18] and Froment and Bischoff [19]. Thus, the models were further subjected for the residual analysis in which a relative residual (RR) defined as [20];

$$RR = \frac{r_{\exp} - r_{\mathrm{mod}}}{r_{\exp}} \tag{4.15}$$

were plotted as a function of hydrogen partial pressure and *p*-nitrophenol concentration. The relative residuals are normally distributed with almost zero means and exhibited no trend as a function of any independent variable. A further comparison of experimental and predicted rate data using model II is shown in Figure 4-19. From these observations, model II is recommended for the intrinsic kinetics of hydrogenation of *p*-nitrophenol to *p*-aminophenol with Pt/C catalyst,

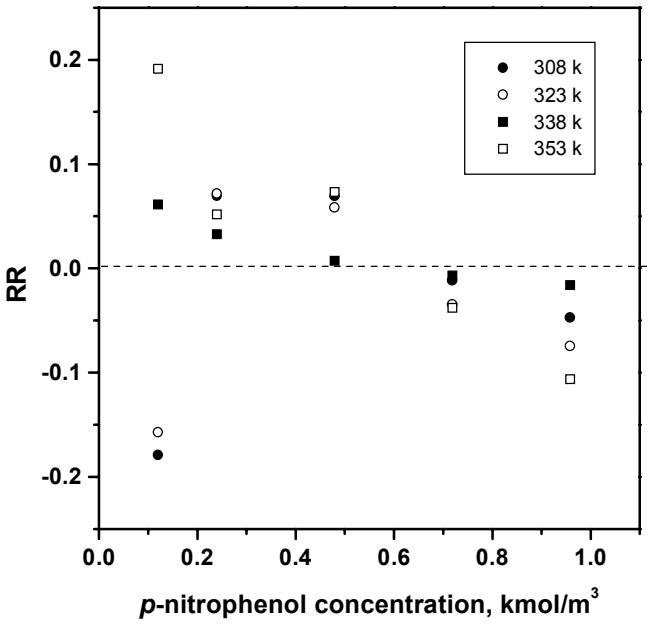

Figure 4-17: Residual plots for *p*-nitrophenol concentration

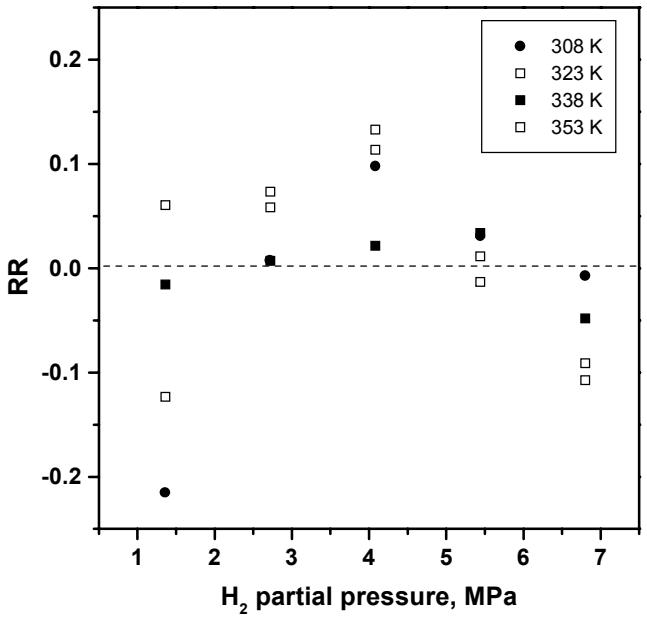

Figure 4-18: Residual plots for hydrogen partial pressure

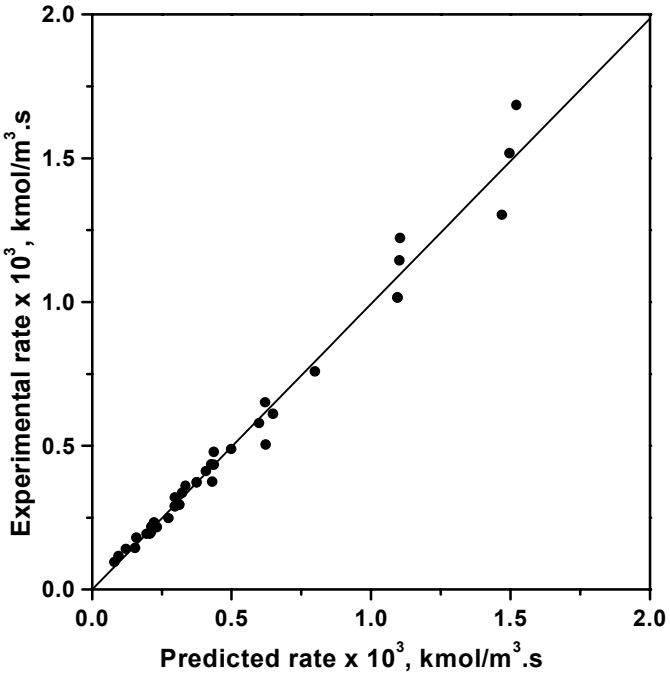

Figure 4-19: Comparison of experimental and predicted results
(•) Experimental, (—) Predicted

4.4 Conclusions

The hydrogenation of *p*-nitrophenol to *p*-aminophenol using 1% Pt/C catalyst was studied in a laboratory scale slurry reactor. Various supported transition metal catalysts were screened and it was observed that Pt/C catalyst had higher catalytic activity compared to supported Pd, Ni or Rh. Ru catalyst was found to be inactive for this reaction. Both the initial rates of hydrogenation and average catalytic activity increased with increasing polarity of the solvent. The addition of water resulted in increase in the catalytic activity as well as initial rate of hydrogenation. The kinetics of hydrogenation of *p*-nitrophenol to *p*-aminophenol was investigated using 1% Pt/C catalyst in a temperature range of 308-353 K, hydrogen pressure between 1.33–6.80 MPa, catalyst loading between 0.133-0.399 kg/m^3, initial *p*-nitrophenol concentration between 0.119-0.958 kmol/m^3 and agitator speed between 600-1200 rpm. Analysis of initial rates of hydrogenation showed that gas-liquid, liquid-solid and intraparticle mass-transfer resistances were not significant under the prevailing reaction conditions. The rates were first order at lower hydrogen pressures and independent beyond 4.08 MPa. Similarly, the initial rates were first order below *p*-nitrophenol concentration of 0.239 kmol/m^3, beyond which it was independent of *p*-nitrophenol concentration. For kinetic modeling, Langmuir-Hinshelwood and several empirical models were examined and the following rate equation was proposed:

$$R_A = \frac{wk_1AB}{(1 + k_AA + K_BB)}$$

The apparent energy of activation was found to be 60.98 KJ/mol.

4.5 Notations

a_B Effective gas-liquid interfacial area, m^2/m^3.

a_P Effective liquid-solid interfacial area per unit volume of slurry, m^2/m^3.

A^* Dissolved concentration of Hydrogen, $kmol/m^3$.

d_i Diameter of the agitator, m.

d_P Particle diameter, m.

D Diffusion coefficient for hydrogen in liquid phase, m^2/s.

D_e Effective diffusivity of hydrogen in liquid phase, m^2/s.

e Energy supplied to the liquid per unit mass, m^2/s^3.

F_c Shape factor of the catalyst.

k_1 Kinetic constant, $(m^3/kg)(m^3/kmol.s)$.

k_L Gas-liquid mass transfer coefficient, m/s.

k_s Liquid-mass transfer coefficient, m/s.

K_A Adsorption equilibrium constant for hydrogen, $m^3/kmol$.

K_B Adsorption equilibrium constant for p-nitrophenol, $m^3/kmol$.

N Agitation speed, Hz.

N_P Power number.

Q_G Volumetric flow rate of gas, m^3/s.

r_{exp} Observed rate of hydrogenation, $kmol/m^3.s$.

r_{mod} Predicted rate of hydrogenation, $kmol/m^3.s$.

R_A Rate of hydrogenation, $kmol/m^3.s$.

R_{max} Maximum rate of hydrogenation, $kmol/m^3.s$.

V_L Volume of the liquid, m^3.

V_m Molar gas volume, $m^3/kmol$.

w Catalyst loading, kg/m^3.

Greek Letters

ε Porosity of the catalyst.

τ Tortuosity factor.

ρ_L Density of the liquid, kg/m^3.

ρ_p Particle density, kg/m^3.

μ_L Viscosity of the liquid, cp.

4.6 References

[1] Spiegler, L. and Woodbury, N. *US Pat. 2947781*, **1960**.

[2] (a) Friefelder, M. and Robinson, R. *US Pat. 3079435* **1963** (b) Kratky, V.; Kralik M.; Hronec, M. and Zecca, M. *Stud. Surf. Sci & Catal. 130C*, 2321, **2000**.

[3] Henke, C. *US Pat. 2183019,* **1939**. (b) Sidheshwaran, P.; Krishnan, V and Bhat, A. *Indian J. Chem. A, 36*, 149, **1997**.

[4] Malpani, P. and Chandalia, S. *Ind. Chem. J.* 15, **1973**.

[5] (a) Yao, H. and Emmett, P. *J. Am. Chem. Soc. 84,* 1086, **1961** (b) Yao, H. and Emmett, P. *J. Am. Chem. Soc*. 81, 125 **1959** (c) Yao, H. and Emmett, P. *J. Am. Chem. Soc., 83,* 796, **1960**.

[6] Sen, B. and Vannice, M. *J.Catal. 52,* 133, **1988**.

[7] Laurent, D. and Klaus, K. *J. Mol. Catal. A, 142*, 275, **1999**.

[8] Roberts, J. Hydrogenation Catalysts, Noyes Data Corporation, Park Ridge, NJ, USA, **1976**.

[9] Rajadhyaksha, R. and Karwa S. *Chem. Eng. Sci. 41*, 1765, **1986**.

[10] Kapteijn, F.; Moulijn, J.; van Santen R. and Wever, R. *Stud. Surf. Sci. & Catal*, *123,* 91, **1999**.

[11] Ramchandran, P. and Chaudhari, R. 'Three Phase Catalytic Reactors", Gorden and Breach Sci. Publishers, New York, **1983**.

[12] Sano, Y.; Yamaguchi, N. and Adachi, T. *J. Chem. Eng. Jpn. 1*, 255, **1974**.

[13] Calderbank, P. *Trans. Instn. Chem. Engrs. 36*, 443, **1958**.

[14] Satterfield, C. Mass Transfer in Heterogeneous Catalysis, MIT Press, Cambridge, **1970**.

[15] Wilke, C. and Chang, P. *AIChE J. 1*, 264, **1955**.

[16] Komiyama, H. and Smith, J. *AIChE J. 21*, 670, **1975**

[17] Marquardt, D. *J. Soc. Ind. Appl. Math. 2*, 431, **1963**.

[18] Kittrell, J. *Adv. Chem. Engg. 8*, 97, **1970**.

[19] Froment, G. and Bischoff, K. *Chemical Reactor Analysis and Design*, Second Edn. John Wiley and Sons, New York, pp 84-101, **1990**.

[20] Trambouze, P. Chemical Reactor Tech. Edn. Paris, **1988**.

[21] Perry, R., Perry's Chemical Engineers Handbook, 6th edition, McGraw Hill, **1984**.

* * * * *

Chapter Five

Summary and Future Scope

The main objective of this thesis was to investigate the catalytic hydrogenation of nitrobenzene and *p*-nitrophenol for the preparation of *p*-aminophenol and the fundamental issues such as adsorption and reaction kinetics relevant to these processes. A summary of important conclusions, primarily based on the results presented in this thesis, and the scope of future work in the field of synthesis of *p*-aminophenol by catalytic hydrogenation route are summarized in this note.

The most significant impact of the work presented in this thesis is the utility of the catalytic hydrogenation as the clean and environmentally acceptable route for the synthesis of *p*-aminophenol, an important intermediate for several drug formulations. Though, only a couple of examples are illustrated in this thesis, the impact of the present study is much wider since, the catalytic hydrogenation and hydrogenation of nitro compounds in particular have wide ranging applications in fine chemicals, pharmaceuticals as well as bulk commodity chemicals.

The catalytic hydrogenation of nitrobenzene to *p*-aminophenol in a four-phase system is a unique example of a multiphase catalytic reaction system, in which the intermediate (phenylhydroxylamine) formed in the organic phase is first transferred to the immiscible aqueous acidic phase where it undergoes a acid catalyzed rearrangement to give the desired final product (*p*-aminophenol). While this route has been shown to be feasible with reasonably high selectivity to the *p*-aminophenol, there are several issues, which need further investigations. This system involves four different phases namely hydrogen as a gas phase, Pt/C catalyst as a solid phase, nitrobenzene as an organic phase and aqueous sulfuric acid as the second immiscible liquid phase. Such a complex system poses a serious challenge in operation on a commercial scale, as numerous uncertainties in scale-up of such multiphase system are likely to exist.

As a first step, a detailed investigation on the effect of various reaction parameters such as catalyst type, nitrobenzene loading, hydrogen pressure, speed of agitation and reaction temperature on the activity and selectivity to *p*-aminophenol was undertaken. It was observed that under optimum reaction conditions, *p*-aminophenol could be obtained with selectivity as high as 74%. One of the significant conclusions of this study was the use of a nickel catalyst for the catalytic hydrogenation of nitrobenzene to *p*-aminophenol. Although, selectivity obtained to *p*-aminophenol using nickel catalysts was lower compared to platinum catalysts, the considerably lower cost of nickel catalyst can be advantageous from commercial point of view. Yet another important conclusion of this work is the successful application of solid acids as replacement for sulfuric acid in this reaction. Again, though the selectivity to *p*-aminophenol is low in the case of solid acids compared to sulfuric acid, use of solid acids obviated the corrosion problems associated with the strong mineral acids and the unwanted salt formation.

Because of the complexities of the reaction system, a simplified approach to kinetic modeling of catalytic hydrogenation of nitrobenzene to *p*-aminophenol was considered in this thesis. A single site Langmuir-Hinshelwood type model was found to fit the kinetic data satisfactorily. However, more detailed analysis of a rigorous mathematical model for interphase mass transfer with catalytic reaction is necessary to develop deeper understanding about the design and scale-up aspects.

Like in any heterogeneous catalytic reaction, the adsorption characteristics of various reaction components on the catalyst surface would also have a significant impact on the overall performance of the catalyst as well as the rate of reaction. Therefore, detailed investigations of adsorption of nitrobenzene, aniline and

hydrogen on Pt/C catalyst was also undertaken. The significant conclusions of this study are as follows.

1. Adsorption capacity of nitrobenzene is more than aniline on 3% Pt/C catalyst in a temperature range of 288-308 K, from their methanolic solution.
2. There was negligible difference in the adsorption capacity of nitrobenzene and aniline on activated carbon and 3% Pt/C catalyst suggesting that the adsorption of nitrobenzene and aniline may be physical adsorption.
3. The adsorption data showed a good fit to the Langmuir adsorption isotherm. Binary adsorption of nitrobenzene and aniline could also be fitted to the extended Langmuir equation.
4. Adsorption of hydrogen from aqueous slurry of the catalyst (3% Pt/C) also followed Langmuir adsorption isotherm. The hydrogen adsorption was significantly more on 3% Pt/C catalyst than activated carbon suggesting that it is a case of chemisorption.

The important drawbacks of the synthesis of *p*-aminophenol by the catalytic hydrogenation of nitrobenzene include the use of highly corrosive mineral acids and the quantitative formation of aniline. Therefore, as an alternative, the catalytic hydrogenation of *p*-nitrophenol to *p*-aminophenol was also investigated. It was observed that highest catalytic activity was obtained using Pt/C catalyst. Therefore, a detailed investigation of the effect of various reaction parameters on the hydrogenation rate and average catalytic activity was undertaken to select the optimum reaction conditions. Further, a detailed kinetic study of hydrogenation of *p*-nitrophenol to *p*-aminophenol was performed to propose a rate equation to represent the kinetic data satisfactorily.

To summarize, the work presented in this thesis has allowed better understanding of some of the fundamental issues on reaction kinetics and engineering aspects of the two important catalytic hydrogenation reaction systems namely, hydrogenation of nitrobenzene to *p*-aminophenol and hydrogenation of *p*-nitrophenol to *p*-aminophenol. Considering the complexities involved in the four-phase reaction system, it is strongly recommended that further work on mass transfer and hydrodynamics of gas-liquid-liquid-solid system should be undertaken. This will be extremely useful for design and scale-up of such systems.

* * * * *

List of Publications

1. Synthesis of *p*-Aminophenol by Catalytic Hydrogenation of Nitrobenzene
   C. V. Rode, **M. J. Vaidya** and R. V. Chaudhari
   Organic Process Research and Development, 3, 465-470, **1999**.

2. Hydrogenation of nitrobenzene to *p*-aminophenol in a four-phase reactor: reaction kinetics and mass transfer effects
   C. V. Rode, **M. J. Vaidya,** R. Jaganathan and R. V. Chaudhari
   Chem. Eng. Sci., 56, 1299, **2001**

List of Patents

1. Single step process for the preparation of *p*-aminophenol
   R.V. Chaudhari, S.S. Divekar, **M. J. Vaidya** and C.V. Rode.
   US Pat. 6028227; 2000

2. Single step hydrogenation of nitrobenzene to *p*-aminophenol
   C. V. Rode, **M. J. Vaidya** and R. V. Chaudhari
   US Pat. 6403833; 2002